DESIGN OF DIMENSIONALLY-STABLE LAMINATED COMPOSITES SUBJECTED TO HYGRO-THERMO-MECHANICAL LOADING BY STOCHASTIC OPTIMIZATION METHODS

A Thesis Submitted to
the Graduate School of Engineering and Sciences of
İzmir Institute of Technology
in Partial Fulfillment of the Requirements for the Degree of

DOCTOR OF PHILOSOPHY

in Mechanical Engineering

by
Levent AYDIN

November 2011
İZMİR

We approve the thesis of **Levent AYDIN**

Assist.Prof.Dr. H. Seçil ARTEM
Supervisor

Prof.Dr. Metin TANOĞLU
Committee Member

Prof.Dr. Ramazan KARAKUZU
Committee Member

Assoc.Prof.Dr. Bülent YARDIMOĞLU
Committee Member

Assoc.Prof.Dr. Alper TAŞDEMİRCİ
Committee Member

2 November 2011

Prof.Dr. Metin TANOĞLU
Head of the Department of
Mechanical Engineering

Prof.Dr. R. Tuğrul SENGER
Dean of the Graduate School of
Engineering and Sciences

ACKNOWLEDGMENTS

I would like to express my gratitude to my advisor, Assist. Prof. Dr. H. Seçil Artem for her guidance, support, encouragement, and inspiration during the course of my Ph.D. studies. Her patience and kindness are greatly appreciated. I have been fortunate to have Dr. Artem as my advisor and I consider it an honor working with her.

I would like to thank also my committee members: Prof. Dr. Metin Tanoğlu, Prof. Dr. Ramazan Karakuzu, Assoc. Prof. Dr. Alper Taşdemirci and Assoc.Prof. Dr. Bülent Yardımoğlu for their invaluable comments and suggestion, which made my dissertation a better work.

Finally, I thank the İzmir Institute of Technology Science Research Foundation for providing financial assistance for this project.

ABSTRACT

DESIGN OF DIMENSIONALLY-STABLE LAMINATED COMPOSITES SUBJECTED TO HYGRO-THERMO-MECHANICAL LOADING BY STOCHASTIC OPTIMIZATION METHODS

The materials used in aerospace structures such as antenna, satellites and missiles should have such features as low density, high stiffness, low coefficients of thermal and moisture expansions simultaneously. Fiber reinforced polymer composite materials can satisfy these requirements with an appropriate stacking sequence using optimization methods and hence dimensionally stable composites are obtained. In this thesis, two different materials carbon/epoxy and E-glass/epoxy composites are considered. Both materials have been used for optimization, stress and failure analysis. However, only for E-glass/epoxy, experimental studies have been performed including determination of stiffness, strength characteristics, Poisson's ratio, fiber volume fraction, glass transition temperature (Tg) and coefficient of thermal expansion (CTE). The objective of optimization part is to design the stacking sequence of the carbon/epoxy and E-glass/epoxy laminated composites having low CTE and high elastic moduli. In design process, multi-objective genetic algorithm optimization of the carbon/epoxy composite plates are verified by single-objective optimization approach by using the Genetic Algorithm (GA), Generalized Pattern Search (GPS) and Simulated Annealing (SA) algorithms. MATLAB Optimization Toolbox is used to obtain Pareto-optimal designs and global optimum points for different model problems. Stress and strain distributions are presented through the thickness of the laminates subjected to mechanical, thermal, and hygral loadings. Stress analysis results showed that effect of mechanical loads dominate to hygral and thermal loads. All the stochastic search methods carried out in the present thesis have produced almost the same results with different stacking sequences.

ÖZET

STOKASTİK OPTİMİZASYON METOTLARI İLE HİGRO-TERMO-MEKANİK YÜKLEMEYE MARUZ BOYUTSAL KARARLI TABAKALI KOMPOZİTLERİN TASARIMI

Son yıllarda havacılık ve uzay sektöründe meydana gelen gelişmeler, yeni ve alternatif malzemeler kullanımı ihtiyacını da beraberinde getirmiştir. Bu sebeple ilgili alanda kullanılacak olan malzemelerden beklenen düşük yoğunluk, yüksek rijitlik, düşük termal ve nemsel genleşme katsayıları gibi özellikler, fiber katkılı, tabakalı kompozit malzemelerin, ağırlıklarının minimize edilmesi, açı dizilimlerinin ve rijitliklerinin optimize edilmesi yoluyla karşılanabilmiştir. Bu tezde E-glas/epoksi ve karbon/epoksi tabakalı kompozit malzemeler boyutsal kararlı hale getirilmeye çalışılmıştır. Boyutsal kararlı malzemelerin en belirgin özelliği termal ve nemsel değişimler gibi bazı çevresel etkilere maruz bırakıldıklarında bile boyutsal ve geometrik yapılarında meydana gelen değişimlerin çok küçük olmasıdır. Bu çalışmada, karbon/epoksi ve E-glas/epoksi kompozit malzemelerin her ikisi de optimizasyon, gerilme ve kırılma analizlerinde kullanılırken, rijitlik ve mukavemet karakteristiklerinin tanımlanması, termal genleşme katsayılarının ölçülmesi ve camsı geçiş sıcaklıklarının belirlenmesi gibi deneysel çalışmalarda sadece E-glass/epoksi kompozit göz önüne alınmıştır. Tezin optimizasyon kısmının amacı, fiber açı dizilimlerinin düşük termal genleşme katsayısı ve yüksek elastiklik modüllerini sağlayacak şekilde optimize edilmesidir. Tasarım kısmında, çok amaçlı genetik algoritma optimizasyon yöntemi kullanılmış ve matematiksel olarak doğrulamak için aynı problemler bir de tek amaçlı genetik algoritma (GA), genelleştirilmiş patern araması (GPSA) ve benzetimli tavlama (SA) algoritması yöntemleriyle de çözülmüştür. Tezin optimizasyon bölümü MATLAB *Optimization Toolbox* isimli özel bir araç kutusu yardımıyla yapılmıştır. Sonuç bölümünde, tabakalar boyunca gerilme ve gerinme dağılımları mekanik, termal ve higral yüklerin etkileri de gösterilerek verilmiştir. Bu tezde, kullanılan farklı optimizayon yöntemlerine rağmen birbirine çok yakın sonuçlar elde edilmiş, bu da kullanılacak optimizasyon yönteminin seçiminin stokastik olmak şartıyla benzer problemler için çok kritik olmadığını göstermiştir.

TABLE OF CONTENTS

LIST OF FIGURES

LIST OF TABLES

Table **Page**

CHAPTER 1

INTRODUCTION

1.1. Literature Survey

Laminated composites are widely used in aerospace, marine, automotive and other branches of engineering applications due to their inherent tailorability. The materials used in aerospace structures like antenna, satellites and missiles should have such features as low density, high stiffness, low coefficients of thermal and moisture expansions (Mangalgiri, 1999). Carbon fiber-reinforced polymer composite materials can satisfy these requirements with an appropriate stacking sequence (Le Rich & Gaudin, 1998). In order to obtain optimum design of laminated composite materials with such a stacking sequence, it is necessary to perform some of the optimization methods. Design and optimization of the laminated composite materials are one of the most interesting subjects of engineering because of the fact that traditional optimization techniques may not be applied to composites or may be used only in limited cases. A detailed discussion of various optimization methods and algorithms can be found in Rao (2009) for general application and in Gurdal et al. (1999) for composite design problems. Due to the complexity of the composite design and optimization problems, the use of stochastic optimization methods such as genetic algorithm, particle swarm optimizer, tabu search, simulated annealing algorithm, and ant colony optimization are appropriate. There are a few papers considering comparison of stochastic search algorithms in structural mechanics (Hasancebi et al., 2010; Manoharan, 1999) and review of optimization methods in composites (Ghiasi et al., 2009; Ghiasi et al., 2010). Optimization of laminated composite materials for only some specific problems have been studied by many researchers using multi-objective or single-objective approaches. However, Costa et al. (2004) have considered both of multi-objective and single-objective.

Genetic Algorithm is the most frequently used optimization method for composite design problems when compared to other stochastic search techniques (Fares et al., 2005). A methodology for the multi-objective optimization of laminated

composite materials has been proposed by Pelletier and Vel (2006). A multi-objective Genetic Algorithm has been used to obtain Pareto-optimal designs for the model problems. They have found that nonlinearities in the shape of the Pareto- optimal front enables to perform trade-off studies when choosing a particular design. Aydin and Artem (2009a) have considered multi-objective optimal design of the laminated composites using genetic algorithms. MATLAB Genetic Algorithm and Direct Search Toolbox is used to obtain Pareto-optimal design for three different model problems. The objectives of the problems are to maximize the Young's moduli and minimize the coefficient of thermal expansion (CTE) simultaneously for 8 and 16 layered carbon/epoxy composites. They have found that (i) mechanical loads dominate thermal effect, (ii) maximization of elastic modulus E_x and minimization of α_x produces lower strain values in x direction in all considered problems for given loading and environmental conditions. Apalak et al. (2008) have studied layer optimization for maximum fundamental frequency of laminated composite plates by means of genetic algorithm. They used an artificial neural network model in order to reduce the time searching for the optimal lay-up sequence**.** They have found that the natural frequencies of the composite square and rectangular plates are increased with increasing layer number. The problem for adjustment of residual stresses in unsymmetric composites has been studied by Hufenbach et al. (2001). The new laminate design method has been verified by experiments and numerical calculations on unsymmetric glass and carbon fiber-reinforced plastics. The method has been applied to the design of multi-layered curved hybrid structures. They have shown that the new optimization procedures ensure an efficient design of multi-layered and hybrid composites and the adjustment of the curvature to the technical demands. Park et al. (2008) have suggested new approaches to reduce the number of fitness function evaluations in genetic algorithms (GAs) applied to multidisciplinary optimization of composite laminates. The numerical efficiency of the present method has been validated by the sample problem of weight minimization of composite laminated plate under multiple design constraints. Their proposed methodology has been demonstrated to be numerically efficient in the multidisciplinary optimization of composite laminates. The layup of the maximum strength of laminated composites with free edges under extension, bending, and twisting loads have been optimized by Genetic Algorithm in the study of Cho and Rhee (2004). Inter-laminar and in-plane stresses, have been considered in estimating the strength of laminates. In the

formulation, a GA repair strategy has been adopted in order to satisfy given constraints. It has been demonstrated that GA with repair strategy works well in handling constraints in the layup optimizations of composite laminates. GA with multiple elitism has been able to find more solutions near the global optimum

Another stochastic optimization method used in composite design is Simulated Annealing (SA). A constant thickness optimization of laminated composite has been presented by Deng et al. (2005). In this paper, the edging stress of a composite plate has been taken into account as objective function for the SA algorithms. An efficient use of SA in the optimum stacking sequence of a composite laminate plate has been accomplished. The results of a simulation experiment have indicated that the proposed scheme provides much better solutions than the other two approaches with regard to computation time and optimality. The optimization of laminated and sandwich plates with respect to buckling load and thickness has been performed by Di Sciuva et al. (2003). Genetic Algorithm and Simulated Annealing methods have been employed and algorithms have provided almost the same results. It is also found that the SA is less time-consuming, therefore it appears to be more suitable for those problems that have complex numerical models. In the study carried out by Erdal and Sonmez (2005), they have attempted to develop a procedure that can locate global optimum designs of composite laminates with minimum liability to buckling for a very large design space. They have adopted an improved version of SA for buckling optimization of composites. Reliability of the algorithm has been investigated in different load ratios.

Generalized pattern search algorithm (GPSA) is a mostly local search method and the use of the algorithm in composite optimization is very few. GPSA has been used for optimal stacking sequence of a 64-layer composite plate made of graphite epoxy by Karakaya and Soykasap (2009). The optimization implementation has been done using MATLAB Genetic Algorithm and Direct Search Toolbox. They have concluded that the Genetic Algorithm is expensive but more effective in finding distinct global optima than generalized pattern search algorithm.

Since moisture and temperature lead to some changes on mechanical properties of the polymer matrix composites, dimensional changes induced by moisture and temperature are a significant feature in design of the composites (Kollar & Springer 2003). Therefore, some researchers have considered investigation of moisture and temperature effects on composite materials. For example, Le Rich and Gaudin (1998) have taken into account of the dimensional stability concept which is crucial feature of

space structures. Main objective of their study is to design the composite laminates as space materials considering thermal, hygral and mechanical constraints. They showed that substantial reductions of plate bending due to manufacturing inaccuracies can be obtained through stacking sequence optimization. Aydin and Artem (2010) have considered eight-layered carbon/epoxy symmetric and balanced laminated composites satisfying the conditions, low coefficient of thermal expansion on longitudinal and high elastic moduli on longitudinal and/or transverse directions. In design process, the problems are firstly formulated as multi-objective optimization problems. An alternative single-objective formulations including the nonlinear constraints are utilized for verification of the multi-objective approach. Regarding mechanical analysis, shear and normal stress distributions of the optimized composite plate are presented and the results show that mechanical loads dominate thermal and hygral loads. A theoretical investigation of the effects of hygrothermal residual stresses on the optimum design of laminated composites have been presented by Khalil et al. (2001). Angle-ply, cross-ply and quasi-isotropic laminates have been considered. These laminates are subjected to different mechanical, thermal and hygroscopic loading conditions. The results of the study show that the quasi-isotropic laminate is less sensitive to residual stresses and the glass/epoxy and Kevlar/epoxy composites are more affected by the absorption of moisture. Diaconu and Sekine (2003) have investigated the flexural characteristics and layup optimization for minimizing the deflection of laminated composite plates in environmental conditions of temperature and moisture. They have concluded that the maximum deflection can be reduced by optimized non-symmetric layup in the presence of in-plane thermal stresses. Fares et al. (2005) have examined minimization of the thermal post-buckling dynamic response and maximization of the buckling temperature level of composite plates subjected to thermal distribution. Design variables of the optimization problem are the thickness of layers and the fiber orientation angles. Shear deformation theory has been used in formulation of the design and control objectives. The results of the optimization studies have indicated that the optimum values of the fiber orientation angles may change throughout the post-buckling range. The selection of orientation angles as design variables is more effective than the optimization over the layer thickness. Thermal buckling optimization of laminated composite plates subject to a temperature rise is presented by Spallino and Thierauf (2000). The design and optimization problem have been formulated under strain and ply contiguity constraints and solved by using a guided random-search method. In their study, two different cases

have been considered and the results showed that essential contribution can be provided by the multi-objective optimization by evolution strategy coupled with game theory. In the study by Aydin and Artem (2009b), 8 layered symmetric and balanced carbon fiber-reinforced epoxy matrix composite plate design and optimization have been examined. Laminates are subjected to mechanical, thermal and hygral loads. Objective of the first problem is to maximize Young's modulus E_x and minimize the coefficient of thermal expansion α_x of the composite, simultaneously. The aim for the second problem is to maximize Young's moduli E_x and E_y while minimizing the coefficient of thermal expansion α_x. The authors have concluded from the analysis that mechanical load is very effective compared to hygral and thermal loads for normal stress σ_x; however, thermal load are dominated for σ_y.

Additionally, several techniques have been reported in the literature for the optimization of laminated composite materials for different applications of engineering such as determination of fundamental frequency, characteristic of wings, etc. A method of analysis determining the free vibration frequencies of cylindrically curved laminated panels under general edge conditions has been presented by Narita and Robinson (2006). The purpose of the study is to determine the optimum fiber orientation angles for the maximum fundamental frequency. The accuracy of the analysis and the layerwise optimization approach have been demonstrated in many numerical examples. It is also numerically showed that the optimum fundamental frequencies are higher than curved panels with any of typical lay-ups. In the paper by Farshi and Herasati (2006), a method about weight optimization of multilayer fiber composite plates subjected to the lateral loadings have been proposed. The solution of the optimization problem is based on a two stage strategy:(i) only the fiber orientation angles for the layers are treated as variables, (ii)only the layer thicknesses are design variables. If the thickness of the new layer of the composite approaches zero, the algorithm stops. Kameyama and Fukunaga (2007) has investigated the flutter and divergence characteristics of laminated composite plate wings. In order to analyze effect of layup configuration, the flutter and divergence characteristics have been drawn on the lamination parameter plane. The effectiveness of aeroelastic tailoring have been also presented through the design and optimization results. A general and developed approach procedure for composite optimal design, under the parameters weight, stiffness and strength has been studied by Bruyneel

(2006). The formulation of optimization problem considers a direct parameterization of the composite laminates in terms of the design variables. A non-homogeneous composite membrane design problem as well as an industrial test case have been presented as numerical examples. A new concept of a layerwise optimization approach for laminated composites is proposed by Narita (2003). The aim of the study is to optimize vibration behavior for the maximum natural frequency. Design variables are taken into account as fiber orientation angles. As examples, a Ritz method is utilized so as to calculate the natural frequencies of laminated plates under the combination of the edge conditions. The higher frequencies have been obtained than the reference values. It is hoped that the layerwise optimization approach can be extended to the composite structural design. A method for minimum thickness laminated composite is introduced by Farshi and Rabiei (2007). They have used a layerwise optimization approach under natural frequency limitations. The accuracies of the algorithm has been checked by comparison the results with similar examples.

1.2. Research Significance

Dimensionally stable structures with low mass play a very important role in the success of spacecraft mission, design of satellite structures and usage of other types of space equipments. In the development of alternative laminated composite plates, satisfying the conditions significantly lower weight, lower coefficient of thermal and moisture expansions, higher elastic moduli, and effect of environmental conditions such as moisture and temperature have to be considered for a wide range of space applications. Hence, so as to accomplish these purposes, structural optimization has become a more important step in designing these types of engineering structures and has been studied for minimum weight or maximum strength by many researchers.

Composite materials have been used: (i) to obtain light weight materials and (ii) to improve the static and dynamic rigidity of space structures. With the development of computer technology, it is now possible to identify under/over-stressed areas leading to optimization approach by designers (Siarajan & Nair, 2011). The main parameters relevant to thermal stability and mass of the composite structures are ply material, number of layers and the fiber orientation angles of the laminae. Introducing a mathematical model and analyzing it for different designs and design variables are

essential steps in order to accomplish an optimum design. In order to achieve this goal, it is necessary to utilize mathematical optimization tools along with mechanical analyses for the structural design (Siarajan & Nair, 2011). Coefficient of thermal expansion (CTE) of a composite is very important material parameter to be able to achieve design of dimensionally stable space structures. The linear CTE of a resin matrix composite is mostly influenced by the ply orientation angles and ply order of the laminated composite. Therefore, using fiber orientation angles as design variables are appropriate in design and optimization of composite materials for practical structures used in space (Daniel & Ishai, 1994). In Table 1.1, different design objectives of some engineering structures made up of composite materials have been listed. It can be seen form the table, for space applications such as antennae, satellite and solar reflectors, dimensional stability is crucial feature and obtaining lower coefficient of thermal and moisture expansion with higher stiffness should be taken into consideration.

Table 1.1. Different design objectives of engineering applications using composite materials (Source: Daniel & Ishai, 1994)

Design Objective	**Requirements**	**Materials**	**Applications**
Stiffness	• Small Deflection • High Buckling Load • High flexural rigidity • Low Weight	Carbon fiber Composite Kevlar fiber composite Boron fiber composite	Underground Vessels Sporting Goods Underwater Vessels
Strength	• High Load Capacity • Low Weight • High Inter-laminar Strength	Carbon fiber Composite Kevlar fiber composite S-Glass fiber composite	Joints Trusses Pressure Vessels
Dynamic Control and Stability	• Long Fatigue Life • High Resonance Frequency	Carbon, graphite fibers Thermoplastic Matrices	Engine Components Rotor blades Flywheels
Dimensional Stability	• Low coefficient of thermal and moisture expansion • High Stiffness (Ex, Ey)	Carbon fiber Composite Kevlar fiber composite Graphite fiber composite	Space Antennae Satellites Solar Reflectors
Damage Tolerance	• High impact resistance • High fracture toughness • Energy absorbent interlayers	Tough epoxy matrix Thermoplastic matrices	Ballistic Armor Impact Resistant Structures

1.3. Motivation, Objectives and Originality

After the literature survey, it is obvious that, the dimensional changes and weight are of considerable significance where extreme precision is required such as in some antennae panels and in some satellite structures. In order to improve hygrothermal performance of the materials or structures at a lower cost, rapid development of convenient products and new process technologies are important. Some of these developments can be achieved by developing new process technologies. Therefore, in future, composite structures used in aerospace applications can be expected to be optimized according to parameters such as strength, stiffness, and mass (Mangalgiri, 1999).

The objectives of the thesis can be listed as follows

1) To design the stacking sequence of the 4, 8, 12 and 16 layered carbon/epoxy and E-glass/epoxy laminated composites satisfying the conditions low coefficients of thermal and moisture expansion with high elastic moduli. Therefore, alternative dimensionally stable materials would be developed for space applications.

2) To incorporate in MATLAB Optimization Toolbox solvers *gamultiobj, ga, patternsearch* and *simulannealbnd* for composite design and optimization problems.

3) To capture the fundamental understanding of the effect of plies number to stacking sequences design for the carbon/epoxy and E-glass/epoxy laminated composites.

4) Determination and comparison of failure loads of optimized carbon/epoxy and E-glass/epoxy laminated composites by using Failure theories Tsai-Hill, Tsai-Wu, Hoffman and Hashin-Rotem including thermal and moisture effects.

5) Comparison of the stacking sequences optimizations of carbon/epoxy and E-glass/epoxy laminated composites.

6)Comparison of the single-objective and multi-objective optimization approaches for carbon/epoxy laminated composites.

7) Comparison of Stochastic Search algorithms: Genetic Algorithm, Simulated Annealing and Generalized Pattern Search for carbon/epoxy laminated composites subjected to mechanical thermal and hygral loadings.

8) To see the effects of combination of mechanical, thermal and hygral loads to normal and shear stress distributions of the optimized carbon/epoxy composites

9) Determination of basic mechanical and physical properties of E-glass/epoxy laminated composite experimentally for validation of optimization results.

Originality of the thesis can be summarized as follows:

1) Comparison studies about the stochastic search algorithms for optimization of laminated composites are very few in literature. Although important individual studies have been made, it is not appear that there is any adequate stochastic optimization algorithm universally accepted by researchers under general load conditions. In this thesis, results of three popular stochastic search optimization algorithms have been compared and investigated. Therefore present study fills a gap in laminated composite design and optimization.

2) In the present thesis, both of multi-objective and single-objective optimization approaches have been considered to verify the optimization studies, mathematically. However, in literature, either single-objective or multi-objective approach have been used for composite design and optimization.

3) This thesis includes implementation of "MATLAB Optimization Toolbox" for the optimization of the two different materials carbon/epoxy and E-glass/epoxy laminated composites. It is shown how the commercial product MATLAB can be adapted to the composite design and optimization problems.

4) Since the optimized carbon/epoxy composites which are obtained in this study are dimensionally stable, they can be used as candidate materials for space applications especially in satellite structures.

CHAPTER 2

COMPOSITE MATERIALS

Definition of composite is flexible and can be defined as a structural material that consists of two or more chemically distinct constituents (*reinforcing phase* and *matrix*) that are bound together at a macroscopic level. The reinforcing phase material may be in the form of fibers, sheets, particles or various other geometries. The matrix phase materials of the composites are generally continuous and can be plastic, metal or ceramic. The main advantage of the fiber-reinforced composite materials over the conventional counterparts such as steel, aluminum, copper, titanium, alloys etc., is the high strength to weight ratio and stiffness to weight ratio (see Table 2.1). The ratio of the material strength to the material density is called as specific strength and specific modulus can also be defined as the material elastic modulus per unit material density. These two parameters have important implications on the wide variety of engineering and aerospace applications of fiber-reinforced composite materials (Kaw, 2006).

Since many fiber-reinforced composite materials have much lower coefficient of thermal expansion (CTE) than metals, laminated composites tend to demonstrate a better dimensional stability over a large temperature range. However, it should be taken into consideration that the differences in thermal expansion between metals and composite materials lead to thermal stresses if they are being joined together. Another significant temperature related property is thermal conductivity. For example, in some applications in electronic packaging technology, fiber-reinforced composites can surpass over metals due to the combination of their high thermal conductivity–weight ratio and low CTE (Mallick, 2007). In addition to the temperature related properties, composites exhibit more superior properties than single phase material. For example, some of carbon reinforced composites are ten times stronger than steel and lighter. However, manufacturing techniques used in composite production increase the cost of composites. Therefore, the main challenge of the composite world is to reduce cost of the laminated materials (Staab, 1999). The most commonly used advanced composites are polymer matrix composites (PMCs) which have a polymer (e.g., epoxy, polyester, Vinyl Ester, urethane) reinforced by fibers (e.g., carbon, graphite, aramids, kevlar).

Table 2.1. Specific modulus and specific strength values of fibers, epoxy matrix composites, and Bulk Metals(Source: Kaw, 2006)

Material Units	Specific gravity	Young's Modulus (GPa)	Ultimate strength (MPa)	Specific Modulus (GPa-m^3/kg)	Specific Strength (MPa-m^3/kg)
Graphite fiber	1.8	230.00	2067	0.1278	1.148
Aramid fiber	1.4	124.00	1379	0.08857	0.9850
Glass fiber	2.5	85.00	1550	0.0340	0.6200
Unidirectional graphite/epoxy	1.6	181.00	1500	0.1131	0.9377
Unidirectional glass/epoxy	1.8	38.60	1062	0.02144	0.5900
Cross-ply graphite/epoxy	1.6	95.98	373.0	0.06000	0.2331
Cross-ply glass/epoxy	1.8	23.58	88.25	0.01310	0.0490
Quasi-isotropic graphite/epoxy	1.6	69.64	276.48	0.04353	0.1728
Quasi-isotropic glass/epoxy	1.8	18.96	73.08	0.01053	0.0406
Steel	7.8	206.84	648.1	0.02652	0.08309
Aluminum	2.6	68.95	275.8	0.02652	0.1061

PMCs are the most common composites because of their superior properties such as low cost, high strength, and easy to manufacture. However, selection of that has some disadvantages as low operating temperatures, high coefficients of thermal and moisture expansion, and low elastic properties in certain directions.

Ordinary metals, such as steel and aluminum alloys, are isotropic, due to exhibiting the same property values for all directions. However, a fiber-reinforced composite is not isotropic materials because of that the properties depend on the direction of measurement.

Laminate which is made by stacking a number of very thin layers of fibers can be defined as assemblages of layers of fiber-reinforced composite materials. In order to control the stacking sequence of various layers in a composite laminate properties

including in-plane stiffness, bending stiffness, strength, and coefficients of thermal expansion, it can be generated.

Since having properties that differ according to the direction of measurement the design of a fiber-reinforced composite structure is much more difficult than traditional metal structure. However, advantage of fiber-reinforced composite materials is that it provides opportunity of tailoring its properties according to the design requirements. The design flexibility provides reinforce a composite structure in the directions of major stresses, increase its stiffness in a preferred direction, and produce dimensionally stable structures. In addition to the directional dependence of properties of fiber-reinforced composite materials, there are some of significant differences between metals and composites. For instance, metallic materials usually show yielding and plastic deformation. All fiber-reinforced composite materials are elastic in their tensile stress–strain characteristics. However, inherent heterogeneity of these materials provides mechanisms for energy absorption on a microscopic scale. A laminate made up of composite materials can show little by little deterioration in properties, depending on

Table 2.2. Thermal properties of the materials
(Source: Mallick, 2007)

Material	Density (g/cm^3)	Coefficient of Thermal Expansion ($10^{-6}/^{o}C$)	Thermal Conductivity ($W/m^{o}K$)	Ratio of Thermal Conductivity to Weight ($10^{-3}m^4/s^3\ ^{o}K$)
Plain carbon steels	7.87	11.7	52	6.6
Copper	8.9	17	388	43.6
Aluminum alloys	2.7	23.5	130-220	48.1-81.5
Ti-6Al-4V titanium alloy	4.43	8.6	6.7	1.51
Invar	8.05	1.6	10	1.24
Kll00 carbon fiber epoxy matrix	1.8	-1.1	300	166.7
Glass-fiber epoxy matrix	2.1	11-20	0.16-0.26	0.08-0.12
SiC particle reinforced aluminum	3	6.2-7.3	170-220	56.7-73.3

the type and magnitude of applied loads, but usually would not fail in a catastrophic manner (Mallick, 2007). Damage development and growth processes show considerably different behaviors in metallic materials and composites. Therefore, when the metallic material is substituted with a fiber-reinforced polymer, the differences in behaviour must be considered during the design steps.

Non-corroding behavior of fiber-reinforced polymer matrix composite materials provides an advantage. Dimensional changes or internal stresses can occur in many fiber-reinforced polymer matrix composite because of the fact that they are capable of absorbing moisture or chemicals from the surrounding environment. In order to avoid such an unwanted problem in an engineering application, the surface of the composite material should be protected from moisture or chemicals by an appropriate paint or coating. Many other environmental factors that may cause degradation in the mechanical properties of fiber-reinforced polymer matrix composites are ultraviolet rays, elevated temperatures and corrosive fluids. When a composite structure subjected to high-temperature, oxidation of the matrix as well as adverse chemical reaction between fibers and the matrix should be taken into account especially in metal matrix composites (Mallick, 2007).

The manufacturing processes such as heat treatment, sheet metal, machining, rapid prototyping, casting, and forging are used in traditional materials and they can not be applied to fiber-reinforced polymer matrix composite. In general, the manufacturing process used for composite materials require considerably less energy and lower pressure or force than the processes used for metals. Two significant processes, parts integration and net-shape, have many advantages of using fiber-reinforced polymer matrix composite. Parts integration process reduces the numbers of parts, manufacturing operations, and assembly operations.

2.1. Classification of Composites

Composites can be classified either by the dispersed phase inclusions (particulate, flake, and fibers) or by the type of matrix (polymer, metal, ceramic, and carbon). Figure 2.1 shows the schematic representation of types of composites based on phase inclusions.

Particulate composite materials consist of embedded particles in matrices such

as alloys and ceramics. Since the dispersed phase inclusions are added randomly, they can be assumed as isotropic. Improved strength, increased operating temperature, and oxidation resistance are some of the advantages of particulate composites. The use of aluminum particles in rubber; silicon carbide particles in aluminum; and gravel, sand, and cement to make concrete are typical examples of them.

Flake composites consist of thin, flat reinforcements of matrices. Glass, mica, aluminum, and silver can be used as typical flake materials in composites. Main advantages of preferring flake composites are high out-of-plane flexural modulus, higher strength, and low cost. However, they have some drawbacks. For example, flakes cannot be oriented easily and only a limited number of materials are available for use.

Fiber composites consist of matrices as the continuous phase, reinforced fibers (short (discontinuous) or long (continuous)) and an interface. Carbon, graphite, aramids, boron, and kevlar can be selected as fibers for composites and they are generally anisotropic. Resins such as epoxy, vinylester, polyester; metals such as aluminum, magnesium or titanium, and ceramics such as calcium–alumina silicate are examples of matrices. Continuous fiber matrix composite materials include unidirectional or woven fiber laminas. Laminas are stacked on top of each other at various angles to form a multidirectional laminate.

The most commercially produced and common advanced composite materials are polymer matrix composites (PMCs) consisting of a polymer reinforced fibers such as carbon, graphite, aramids, boron, and kevlar. They are the most commonly used composites including their low cost, high strength, and simple manufacturing principles. For example, graphite/ epoxy composites are approximately five times stronger than steel on a weight for weight basis and lighter. These properties allows the composite motor to be larger that improves thrust and performance. The main disadvantages of PMCs can be listed as low operating temperatures, high coefficients of thermal and moisture expansion, and low elastic properties in certain directions. Moisture absorbtion or de-absorbtion of polymers may lead to dimensional changes that is important in aerospace applications. Therefore, so as to avoid this drawback, adjustment of these type of environmental parameters using optimization methods is very important task for designers in polymer matrix composite materials (Kaw, 2006).

Metal matrix composites (MMCs), as the name implies, have a metal matrix. Examples of matrices in such composites include aluminum, magnesium, and titanium and in high temperature applications, cobalt and cobalt-nickel alloy. Carbon, alumina

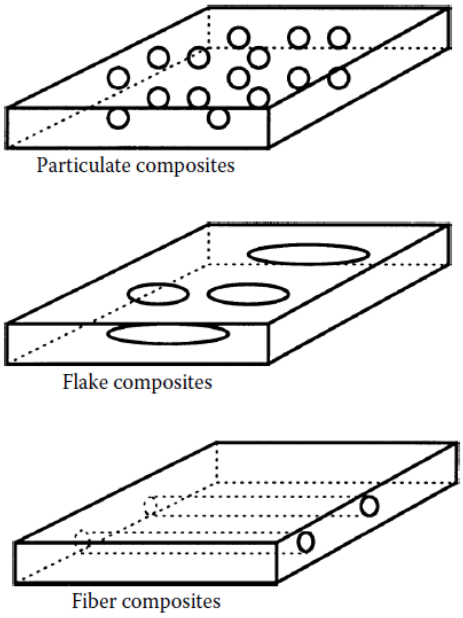

Figure 2.1. Types of composites based on reinforcement shape
(Source: Kaw, 2006).

and silicon carbide are typical fibers used as reinforced materials in MMCs. There are two important purposes to utilize metals as reinforced materials: to increase or decrease their properties to suit the needs of design. For example, the elastic stiffness and strength of metals should be increased, and coefficients of thermal expansion and electrical conductivities of metals can be decreased, by the addition of fibers such as silicon carbide. The main advantages of metal matrix composites can be listed as (i) higher specific strength and modulus by reinforcing low-density metals, such as aluminum beryllium and titanium; (ii) lower coefficients of thermal expansion reinforced by an appropriate fibers (Kaw, 2006). Higher elastic properties; higher service temperature; insensitivity to moisture; higher electric and thermal conductivities; and better wear, fatigue, and flaw resistances are main advantages of MMCs over PMCs. The drawbacks of MMCs over PMCs are higher processing temperatures and higher densities.

Ceramic matrix composites (CMCs) consist of ceramic matrix such as alumina calcium and alumina silicate reinforced by ceramic dispersed phase such as carbon or silicon carbide. Main advantages of CMCs are high strength, hardness, high service temperature limits, chemical inertness, and low density. However, ceramics have low

fracture toughness. Therefore, under tensile or impact loading, ceramic materials fail catastrophically. Reinforcing ceramics with fibers causes gradual failure of the composite and this increases their fracture toughness. Ceramic matrix composites are widely used in high-temperature areas in which metal and polymer matrix composites cannot be used.

Carbon–carbon composites originally have been developed for aerospace applications and consist of carbon fibers in a carbon matrix. These type of composites are utilized in very high-temperature environments of up to 3315°C. Carbon is brittle and flaw sensitive as in ceramic materials. The following advantages can be listed for reinforcement of a carbon matrix : (i) the composite fail gradually (ii) it increase ability to withstand high temperatures, (iii) it provides low creep at high temperatures, (iv) low density, good tensile and compressive strengths, high fatigue resistance, high thermal conductivity, and high coefficient of friction. Disadvantages are high cost, low shear strength, and susceptibility to oxidations at high temperatures (Kaw, 2006).

In this thesis, polymer matrix fiber-reinforced composites (E-glass/epoxy and carbon/epoxy) are considered as design materials.

2.2. Applications

The use of fiber-reinforced composites exists in many engineering fields and are expected to gain increasing applications. If only the major structural applications are selected, following areas can be given as examples: Aircraft, space, automotive components, body armor, sporting goods, boats and marine, infrastructure, water pipes, electronics, bridge, furniture, power industry, oil industry, medical industry, tool handles, ladder rails, oxygen tanks, and power transmission shafts (Mallick, 2007). Since this thesis aims to develop dimensionally stable materials used in space applications, the next section is devoted to this specific application area.

2.2.1. Space Applications

Since fiber-reinforced composites provide weight reduction, it is preferred in space vehicles. The mid-fuselage truss structure, payload bay door, remote manipulator arm, and pressure vessels are various applications in the structure of space shuttles. In

addition to this type of large components, fiber-reinforced polymers are used for many smaller components, such as solar arrays, antennas, and optical platforms. The most important factor in selecting fiber-reinforced polymer matrix composites for these applications is their dimensional stability over a temperature range. Coefficient of thermal expansion (CTE) of a material is very significant parameter to obtain a dimensionally stable structures. Some of carbon fiber-reinforced epoxy composites can be designed to produce a CTE close to zero. Many alloys used in aerospace applications also have a comparable CTE. However, the advantages of carbon fiber-reinforced composites are having a much lower density, higher strength, as well as a higher stiffness–weight ratio. Main reason to utilize carbon fiber-reinforced epoxies in artificial satellites is such a unique combination of mechanical properties and CTE. This type of application can be found in the support structures for mirrors and lenses in the space telescope. It is very significant that the support structures should be designed as dimensionally stable. Because the temperature in space can change between -100°C and 100°C and this type of large changes in the relative positions of mirrors or lenses can lead to some problems in focusing the telescope (Mallick, 2007). Another important space application of fiber-reinforced composites is carbon fiber-reinforced epoxy tubes used in building truss structures for low earth orbit (LEO) satellites and interplanetary satellites. These truss structures support optical benches, solar array panels, antenna reflectors, and other modules.

CHAPTER 3

MECHANICS OF COMPOSITE MATERIALS

The mechanics of materials considers the concepts of stresses, strains, and deformations in structures exposed to mechanical and environmental effects such as temperature, moisture, and radiation. A widely used assumption in the mechanics of traditional materials, such as aluminum, stainless steel, brass, bronze, copper, and lead is that, they are homogeneous and isotropic. Physical properties of a homogeneous material do not depend on the location and properties of an isotropic material are independent of the orientation. For metallic materials unless severely cold-worked the assumption of isotropy is valid since grains in metallic materials are randomly oriented. However, fiber-reinforced composite materials are inhomogeneous and non-isotropic (orthotropic). For this reason, the analysis of mechanics of fiber-reinforced composite materials are much more complicated than that of traditional materials (Mallick, 2007). The mechanical analysis of fiber-reinforced composites are performed in two levels: (i) macromechanical analysis, (ii) micromechanical analysis. These terms can be defined as follows:

Micromechanics: Mechanical analysis of the materials on the level of the individual constituents(the microscopic level). This study is generally performed with the aid of a mathematical model describing the response of each constituent material.

Macromechanics: A study of composite materials behavior wherein the material is presumed homogeneous and the effects of constituent materials are averaged to achieve an apparent response on the macroscopic level.

3.1. Macromechanical Analysis

Classical lamination theory based on classical plate theory is only valid for thin laminates and used to analyze the infinitesimal deformation of laminated structures. In this theory, it is assumed that laminate is thin and wide, perfect bounding exists between laminas, there exist a linear strain distribution through the thickness and all laminas are macroscopically homogeneous and behave in a linearly elastic manner

(Kaw, 2006). Thin laminated composite structure subjected to mechanical in-plane loading (N_x, N_y) considered in this thesis is shown in Figure 3.1. Cartesian coordinate system *x*, *y* and *z* define global coordinates of the layered material. A layer-wise principal material coordinate system is denoted by 1, 2, 3 and fiber direction is oriented at angle θ to the *x* axis. Representation of laminate convention for the *n*-layered structure with total thickness *h* is given in Figure 3.2

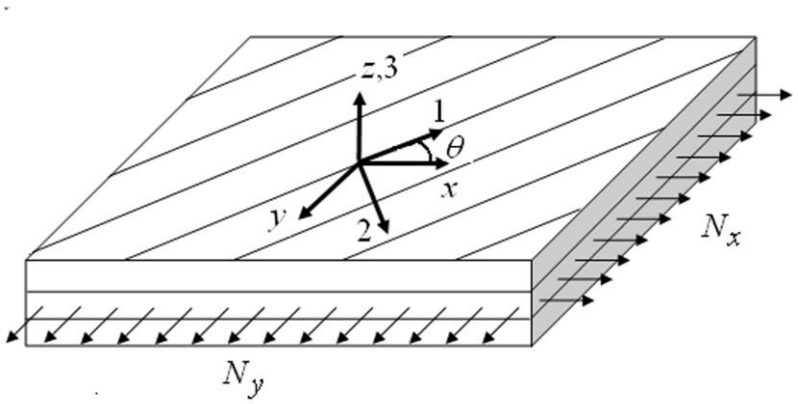

Figure 3.1. A thin fiber-reinforced laminated composite subjected to in plane loading

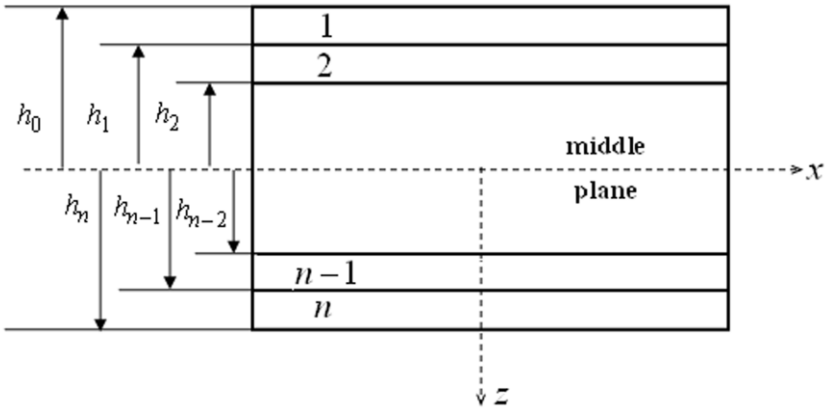

Figure 3.2. Laminate convention.

So as to generalize the total strains including mechanical, thermal and hygral effects following strain expression can be used

$$\begin{bmatrix} \varepsilon_x \\ \varepsilon_y \\ \gamma_{xy} \end{bmatrix} = \begin{bmatrix} \varepsilon_x^M \\ \varepsilon_y^M \\ \gamma_{xy}^M \end{bmatrix} + \begin{bmatrix} \varepsilon_x^T \\ \varepsilon_y^T \\ \gamma_{xy}^T \end{bmatrix} + \begin{bmatrix} \varepsilon_x^H \\ \varepsilon_y^H \\ \gamma_{xy}^H \end{bmatrix} \tag{3.1}$$

where $[\varepsilon]$, $[\varepsilon^M]$, $[\varepsilon^T]$, $[\varepsilon^H]$ are total, mechanical, thermal and hygral strains, respectively.

The stress-strain relation for the *k*-th layer of a composite plate based on the classical lamination theory can be written in the following form

$$\begin{bmatrix} \sigma_x^M \\ \sigma_y^M \\ \sigma_{xy}^M \end{bmatrix}_k = \begin{bmatrix} \overline{Q}_{11} & \overline{Q}_{12} & \overline{Q}_{16} \\ \overline{Q}_{12} & \overline{Q}_{22} & \overline{Q}_{26} \\ \overline{Q}_{16} & \overline{Q}_{26} & \overline{Q}_{66} \end{bmatrix}_k \left(\begin{bmatrix} \varepsilon_x^o \\ \varepsilon_y^o \\ \varepsilon_{xy}^o \end{bmatrix} + z \begin{bmatrix} \kappa_x \\ \kappa_y \\ \kappa_{xy} \end{bmatrix} - \begin{bmatrix} \alpha_x \\ \alpha_y \\ \alpha_{xy} \end{bmatrix}_k \Delta T - \begin{bmatrix} \beta_x \\ \beta_y \\ \beta_{xy} \end{bmatrix}_k \Delta C \right) \tag{3.2}$$

where $[\overline{Q}_{ij}]_k$ are the elements of the transformed reduced stiffness matrix, $[\varepsilon^o]$ is the mid-plane strains $[\kappa]$ is curvatures, $\Delta T, \Delta C$ are temperature and moisture changes, respectively. Here the coefficients of thermal and moisture expansions $[\alpha]_k$, $[\beta]_k$ can be obtained using the following transformation matrix (Kaw, 2006):

$$[T] = \begin{bmatrix} c^2 & s^2 & 2sc \\ s^2 & c^2 & -2sc \\ -sc & sc & c^2 - s^2 \end{bmatrix} \qquad c = Cos\theta, \quad s = Sin\theta \tag{3.3}$$

The elements of transformed reduced stiffness matrix $[\overline{Q}_{ij}]$ appearing in Equation 3.2 can be expressed as in the following form

$$\overline{Q}_{11} = Q_{11}c^4 + Q_{22}s^4 + 2(Q_{12} + 2Q_{66})s^2c^2 \tag{3.4}$$

$$\overline{Q}_{12} = (Q_{11} + Q_{22} - 4Q_{66})s^2c^2 + Q_{12}(c^4 + s^4) \tag{3.5}$$

$$\overline{Q}_{22} = Q_{11}s^4 + Q_{22}c^4 + 2(Q_{12} + 2Q_{66})s^2c^2 \tag{3.6}$$

$$\overline{Q}_{16} = (Q_{11} - Q_{12} - 2Q_{66})sc^3 - (Q_{22} - Q_{12} - 2Q_{66})s^3c \tag{3.7}$$

$$\overline{Q}_{26} = (Q_{11} - Q_{12} - 2Q_{66})cs^3 - (Q_{22} - Q_{12} - 2Q_{66})sc^3 \tag{3.8}$$

$$\overline{Q}_{66} = (Q_{11} + Q_{22} - 2Q_{12} - 2Q_{66})s^2c^2 + Q_{66}(c^4 + s^4) \tag{3.9}$$

where

$$Q_{11} = \frac{E_1}{1 - \nu_{21}\nu_{12}} \tag{3.10}$$

$$Q_{12} = \frac{\nu_{12}E_2}{1 - \nu_{21}\nu_{12}} \tag{3.11}$$

$$Q_{22} = \frac{E_2}{1 - \nu_{21}\nu_{12}} \tag{3.12}$$

$$Q_{66} = G_{12} \tag{3.13}$$

Applied normal force resultants N_x^M, N_y^M and shear force resultant N_{xy}^M (per unit width) on a laminate have the following relations

$$\begin{bmatrix} N_x^M \\ N_y^M \\ N_{xy}^M \end{bmatrix} = \begin{bmatrix} A_{11} & A_{12} & A_{16} \\ A_{12} & A_{22} & A_{26} \\ A_{16} & A_{26} & A_{66} \end{bmatrix} \begin{bmatrix} \varepsilon_x^o \\ \varepsilon_y^o \\ \gamma_{xy}^o \end{bmatrix} + \begin{bmatrix} B_{11} & B_{12} & B_{16} \\ B_{12} & B_{22} & B_{26} \\ B_{16} & B_{26} & B_{66} \end{bmatrix} \begin{bmatrix} \kappa_x \\ \kappa_y \\ \kappa_{xy} \end{bmatrix} - \begin{bmatrix} N_x^T \\ N_y^T \\ N_{xy}^T \end{bmatrix} - \begin{bmatrix} N_x^C \\ N_y^C \\ N_{xy}^C \end{bmatrix} \tag{3.14}$$

The matrices [*A*] and [*B*] appearing in Equation (3.14) can be defined as

$$A_{ij} = \sum_{k=1}^{n} (\overline{Q}_{ij})_k (h_k - h_{k-1}) \tag{3.15}$$

$$B_{ij} = \frac{1}{2} \sum_{k=1}^{n} (\overline{Q}_{ij})_k (h_k^2 - h_{k-1}^2) \tag{3.16}$$

and $[N^T]$, $[N^C]$given in Equation (3.14) are the resultant thermal and hygral forces, respectively:

$$\begin{bmatrix} N_x^T \\ N_y^T \\ N_{xy}^T \end{bmatrix} = \Delta T \sum_{k=1}^{n} \begin{bmatrix} \overline{Q}_{11} & \overline{Q}_{12} & \overline{Q}_{16} \\ \overline{Q}_{12} & \overline{Q}_{22} & \overline{Q}_{26} \\ \overline{Q}_{16} & \overline{Q}_{26} & \overline{Q}_{66} \end{bmatrix}_k \begin{bmatrix} \alpha_x \\ \alpha_y \\ \alpha_{xy} \end{bmatrix}_k (h_k - h_{k-1}) \tag{3.17}$$

$$\begin{bmatrix} N_x^C \\ N_y^C \\ N_{xy}^C \end{bmatrix} = \Delta C \sum_{k=1}^{n} \begin{bmatrix} \overline{Q}_{11} & \overline{Q}_{12} & \overline{Q}_{16} \\ \overline{Q}_{12} & \overline{Q}_{22} & \overline{Q}_{26} \\ \overline{Q}_{16} & \overline{Q}_{26} & \overline{Q}_{66} \end{bmatrix}_k \begin{bmatrix} \beta_x \\ \beta_y \\ \beta_{xy} \end{bmatrix}_k (h_k - h_{k-1}) \tag{3.18}$$

In macromechanical analysis, it is also convenient to introduce the effective elastic properties for symmetric balanced or symmetric cross-ply laminated plates subjected to in-plane loading. The effective thermal and moisture expansion coefficients and elastic moduli are given as follows (Kaw, 2006)

$$\begin{bmatrix} \alpha_x \\ \alpha_y \\ \alpha_{xy} \end{bmatrix} = \begin{bmatrix} \varepsilon_x^0 \\ \varepsilon_y^0 \\ \gamma_{xy}^0 \end{bmatrix}_{\substack{\Delta C=0 \\ \Delta T=1}} = \begin{bmatrix} A_{11}^* & A_{12}^* & A_{16}^* \\ A_{12}^* & A_{22}^* & A_{26}^* \\ A_{16}^* & A_{26}^* & A_{66}^* \end{bmatrix} \begin{bmatrix} N_x^T \\ N_y^T \\ N_{xy}^T \end{bmatrix} \tag{3.19}$$

$$\begin{bmatrix} \beta_x \\ \beta_y \\ \beta_{xy} \end{bmatrix} = \begin{bmatrix} \varepsilon_x^0 \\ \varepsilon_y^0 \\ \gamma_{xy}^0 \end{bmatrix}_{\substack{\Delta C=1 \\ \Delta T=0}} = \begin{bmatrix} A_{11}^* & A_{12}^* & A_{16}^* \\ A_{12}^* & A_{22}^* & A_{26}^* \\ A_{16}^* & A_{26}^* & A_{66}^* \end{bmatrix} \begin{bmatrix} N_x^C \\ N_y^C \\ N_{xy}^C \end{bmatrix} \tag{3.20}$$

$$E_x = \frac{1}{hA_{11}^*},\ E_y = \frac{1}{hA_{22}^*} \tag{3.21}$$

where $[A^*] = [A]^{-1}$.

Now, stresses and strain expressions based on classical lamination theory will be given for local coordinate system (1, 2). The relation between the local and global stresses in an angle lamina can be written as in the following form:

$$\begin{bmatrix} \sigma_1 \\ \sigma_2 \\ \sigma_{12} \end{bmatrix} = [T] \begin{bmatrix} \sigma_x \\ \sigma_y \\ \sigma_{xy} \end{bmatrix} \tag{3.22}$$

Similarly, the local and global strains are also related as follows

$$\begin{bmatrix} \varepsilon_1 \\ \varepsilon_2 \\ \varepsilon_{12} \end{bmatrix} = [R][T][R]^{-1} \begin{bmatrix} \varepsilon_x \\ \varepsilon_y \\ \varepsilon_{xy} \end{bmatrix} \tag{3.23}$$

where $[R] = \begin{bmatrix} 1 & 0 & 0 \\ 0 & 1 & 0 \\ 0 & 0 & 2 \end{bmatrix}$

Both temperature and moisture versus stiffness and strength of polymeric composites is schematically illustrated in Figure 3.3. In this figure, ΔT and ΔC represents the change in temperature and moisture content, respectively (Staab, 1999). It can be observed from the figure, modulus and strength values decrease by exhibiting the similar behavior with the changes of temperature and moisture contents.

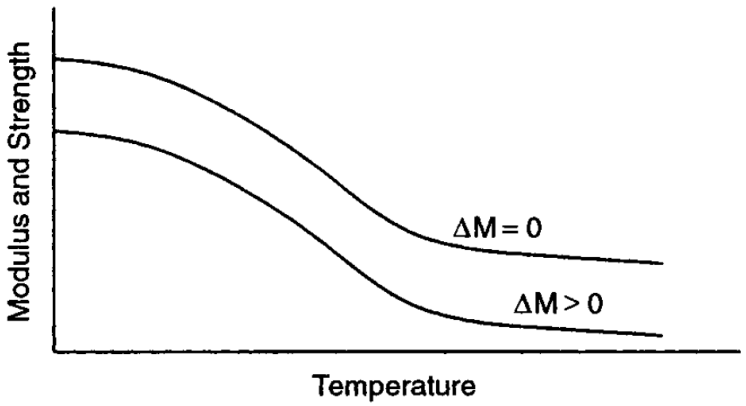

Figure 3.3. Schematic representation of the effects of temperature and moisture on elastic modulus and strength (Source: Staab, 1999).

3.2. Micromechanical Analysis

Simplified micromechanical expressions (Le Rich & Gaudin, 1998) used to predict the stiffness and coefficient of thermal expansion of a lamina using constituent material properties (given in Table 3.1) are as follows

$$E_1 = V_f E_{1f} + (1 - V_f) E_m \tag{3.22}$$

$$E_2 = \frac{E_m}{1 - \sqrt{V_f}\,(1 - E_m / E_{2f})} \tag{3.23}$$

$$G_{12} = \frac{G_m}{1 - \sqrt{V_f}\,(1 - G_m / G_{12f})} \tag{3.24}$$

$$\nu_{12} = V_f \nu_{12f} + (1 - V_f) \nu_m \tag{3.25}$$

$$\alpha_1 = \frac{V_f \alpha_{1f} E_{1f} + (1 - V_f) \alpha_m E_m}{E_1} \tag{3.26}$$

$$\alpha_2 = \alpha_{2f}\sqrt{V_f} + (1-\sqrt{V_f})(1-V_f\nu_m E_{1f}/E_1)\alpha_m \tag{3.27}$$

$$\beta_1 = \frac{(1-V_f)\beta_m E_m}{E_1} \tag{3.28}$$

$$\beta_2 = (1-\sqrt{V_f})\beta_m\left(1+\sqrt{V_f}\,\frac{(1-\sqrt{V_f})E_m}{\sqrt{V_f}E_2+(1-\sqrt{V_f})E_m}\right) \tag{3.29}$$

where indices 1 and 2, *f* and *m* appearing in above equations denote the longitudinal and transverse directions, fiber and matrix properties, respectively. V_f represents the fiber volume fraction of the lamina, *G* is the shear modulus. In these formulations, fibers are assumed to be transversely isotropic.

Table 3.1. Constituent material properties

Fiber Properties	**Matrix Properties**
$E_{1f} = 550.2\,GPa$	$E_{1m} = 4.34\,GPa$
$E_{2f} = 9.52\,GPa$	$E_{2m} = 4.34\,GPa$
$G_{12f} = 6.9\,GPa$	$G_{12m} = 1.59\,GPa$
$\nu_{12f} = 0.2$	$\nu_{12m} = 0.37$
$\alpha_{1f} = -1.35.10^{-6}/^{\circ}C$	$\alpha_{1m} = 43.92.10^{-6}/^{\circ}C$
$\alpha_{2f} = 6.84.10^{-6}/^{\circ}C$	$\alpha_{2m} = 43.92.10^{-6}/^{\circ}C$
$\beta_{1f} =$ ____	$\beta_{1m} = 2000.10^{-6}/\%M$
$\beta_{2f} =$ ____	$\beta_{2m} = 2000.10^{-6}/\%M$

CHAPTER 4

FAILURE CRITERIA IN LAMINATED COMPOSITES

Laminated composite materials are not isotropic. Therefore the conventional failure theories developed for isotropic materials are not applicable to composite. For this reason, many researchers have focused on the subject of failure criteria for fiber-reinforced laminated composite materials over the last four decades. This concept is still today an important research topic for designers. Many different approaches have been proposed that clearly demonstrates failure criteria for fiber-reinforced laminated composites. Even tough it is clear that significant developments have been achieved up to now, there is not any criterion that universally accepted by designers under general loading conditions. Failure criteria of laminated composite materials can be classified as: (i) non-interactive theories (e.g., maximum stress or maximum strain), (ii) interactive theories (e.g., Tsai–Hill, Tsai-Wu or Hoffman) and (iii) partially interactive or failure mode-based theories (e.g., Puck or Hashin-Rotem failure criterion). None of the available failure criteria used in composites is good enough to be used as a sole performance predictor in design. In addition to this, all of the orthotropic failure theories tend to be phenomenological and empirical in nature rather than mechanistic. Failure of a unidirectional laminate begins on the microscopic level. Initial microscopic failures can be classified by local failure modes, such as:

1.Fiber failure

2.Matrix failure

3.Interfacelflaw dominated failures

In this thesis, four of the failure theories (Tsai–Hill, Tsai-Wu Hoffman, Hashin-Rotem) are considered. These theories are briefly explained in the following subsections.

4.1. Tsai-Hill Failure Theory

Tsai-Hill failure theory is firstly derived from the von Mises distortional energy yield criterion for isotropic materials. After some modifications, it is applied to

anisotropic materials like composites. In this theory, it is considered that failure occurs whenever the distortional yield energy equals or exceeds a certain value. The advantage of this theory is that there is interaction between the stress components (σ_1, σ_2, and τ_{12}). Main drawbacks of the criterion are (i) there is no distinction between the tensile and compressive strengths, (ii) it cannot predict different failure modes such as fiber failure, matrix failure, and fiber-matrix interface failure. Tsai-Hill failure criterion for the strengths of the lamina can be represented in the following form. (Mallick, 2007; Kaw, 2004)

$$\frac{\sigma_1^2}{(\sigma_1^F)^2} - \frac{\sigma_1\sigma_2}{(\sigma_1^F)^2} + \frac{\sigma_2^2}{(\sigma_2^F)^2} + \frac{\tau_{12}^2}{(\tau_{12}^F)^2} < 1 \tag{4.1}$$

where

σ_1, σ_2: maximum normal stresses,

τ_{12} : maximum shear stress in the lamina,

σ_1^F: strength in longitudinal direction,

σ_2^F :strength in transverse direction,

τ_{12}^F: shear strength in the 1-2 plane,

4.2. Tsai-Wu Failure Theory

Tsai-Wu failure theory is a a phenomenological failure theory based on total strain energy. According to the theory, failure occurs in the lamina if the following condition is satisfied

$$F_{11}\sigma_1^2 + F_{22}\sigma_2^2 + F_{66}\tau_{12}^2 + F_1\sigma_1 + F_2\sigma_2 + 2F_{12}\sigma_1\sigma_2 < 1 \tag{4.2}$$

where

$$F_{11} = \frac{1}{\sigma_1^T\sigma_1^C}, \quad F_{22} = \frac{1}{\sigma_2^T\sigma_2^C}, \quad F_1 = \frac{1}{\sigma_1^T} - \frac{1}{\sigma_1^C},$$

$$F_2 = \frac{1}{\sigma_2^T} - \frac{1}{\sigma_2^C}, \quad F_{66} = \frac{1}{(\tau_{12}^F)^2}, \quad F_{12} = -\frac{1}{2}\sqrt{F_{11}F_{22}},$$

σ_1^T :tensile strength in longitudinal direction,

σ_1^C : compressive strength in longitudinal direction,

σ_2^T : tensile strength in transverse direction,

σ_2^C compressive strength in transverse direction.

There are two siginifcant advantages of this theory: (i) there is interaction between the stress components and (ii) the theory does distinguish between the tensile and compressive strengths. Main disadvantage of this theory is that in the determination of strength component F_{12} (Daniel & Ishai, 1994).

4.3. Hoffman Failure Theory

The Hoffman failure theory is used a second order polynomial in stress to describe a failure surface in the lamina. Acording to theory, failure is assumed to occur if the following condition is satisfied

$$F_{11}\sigma_1^2 + F_{22}\sigma_2^2 + F_{66}\tau_{12}^2 + F_1\sigma_1 + F_2\sigma_2 + 2F_{12}\sigma_1\sigma_2 < 1 \tag{4.3}$$

where

$$F_{11} = \frac{1}{\sigma_1^T \sigma_1^C}, \quad F_{22} = \frac{1}{\sigma_2^T \sigma_2^C}, \quad F_1 = \frac{1}{\sigma_1^T} - \frac{1}{\sigma_1^C},$$

$$F_2 = \frac{1}{\sigma_2^T} - \frac{1}{\sigma_2^C}, \quad F_{66} = \frac{1}{(\tau_{12}^F)^2}, \quad F_{12} = -\frac{1}{2}(F_{11} + F_{22}).$$

4.4. Hashin-Rotem Failure Theory

Hashin-Rotem failure theory is a partially interactive criteria and includes two failure mechanisms: fiber failure and matrix failure, distinguishing between tension and compression.

$$\sigma_1 = \sigma_1^T$$

(Fiber failure in tension: $(\sigma_1 > 0)$ (4.4)

$$-\sigma_1 = \sigma_1^C \tag{4.5}$$

(Fiber failure in compression: ($\sigma_1 < 0$)

$$\left(\frac{\sigma_2}{\sigma_2^T}\right)^2 + \left(\frac{\tau_{12}}{\tau_{12}^F}\right)^2 = 1 \tag{4.6}$$

(Matrix failure in tension:($\sigma_2 > 0$)

$$\left(\frac{\sigma_2}{\sigma_2^C}\right)^2 + \left(\frac{\tau_{12}}{\tau_{12}^F}\right)^2 = 1 \tag{4.7}$$

(Matrix failure in compression: ($\sigma_2 < 0$)

CHAPTER 5

OPTIMIZATION

Essentially, optimization of a structure can be defined as finding the best design or elite designs by minimizing the specified single or multi-objectives which satisfy all the constraints. Single and multi-objective optimizations are the main approaches used in structural design problems. In single-objective approach, an optimization problem consists of a single-objective function, constraints and bounds. However, the design of some engineering structures generally necessitates the maximization or minimization of often conflicting more than one objectives, simultaneously. In this case, multi-objective formulation is utilized and a set of solutions are obtained with different trade-off which is called as Pareto optimal. Only one solution is to be chosen from the set of solutions for practical engineering usage. There is no such thing as the best solution with respect to all objectives in multi-objective optimization (Pelletier & Vel, 2006)

Composite design problems generally are very complicated and it is impposible to solve by the traditional optimization techniques. In these cases, the use of stochastic optimization methods such as Genetic Algorithms (GA), Generalized Pattern Search Algorithm (GPSA) and Simulated Annealing (SA) are appropriate.

MATLAB Optimization Toolbox is one of the important commercial program toolbox which can be used to solve the design and optimization problems for composites. The toolbox includes a few routines for solving optimization problems using Direct Search (DS), Genetic Algorithm (GA) and Simulated Annealing (SA) methods. All of these methods have been used in the design of composite materials by many researchers. Direct Search functions include two direct search algorithms called the Generalized Pattern Search Algorithm (GPSA) and the Mesh Adaptive Search (MADS) algorithm. The toolbox has optimization solvers *ga, simulannealbnd, patternsearch* for single-objectives and *gamultiobj* for multi-objectives. The multi-objective GA function *gamultiobj* uses a variant of NSGA-II .

5.1. Single-objectiveOptimization

A standard mathematical formulation of the single-objective optimization consists of an objective function, equality and/or inequality constraints and design variables. In our study, the single-objective optimization problem with fiber orientation angles $\theta_1, \theta_2, ..., \theta_n$ is stated as follows

minimize $f(\theta_1, \theta_2, ..., \theta_n)$

such that $g_i(\theta_1, \theta_2, ..., \theta_n) \geq 0 \qquad i = 1, 2, ...r$

$p_j(\theta_1, \theta_2, ..., \theta_n) = 0 \qquad j = 1, 2, ...m$

where f is objective function, $\theta_1, \theta_2, ..., \theta_n$ are the design variables and g, p are the constraints of the problem. In composite design and optimization problems mass, stiffness, displacements, residual stresses, thickness, vibration frequencies, buckling loads and cost are used as objective functions (Gurdal et al., 1999). In this thesis, elastic modulus in *x* direction is considered as objective function of the single-objective optimization problems.

5.2. Multi-objective Optimization

A multi-objective optimization problem can be stated as follows:

minimize $f_1(\theta_1, \theta_2, ..., \theta_n), f_2(\theta_1, \theta_2, ..., \theta_n), ...f_t(\theta_1, \theta_2, ..., \theta_n)$

such that $g_i(\theta_1, \theta_2, ..., \theta_n) \geq 0 \qquad i = 1, 2, ...r$

$p_j(\theta_1, \theta_2, ..., \theta_n) = 0 \qquad j = 1, 2, ...m$

where $f_1, f_2, ...f_t$ represent the objective functions to be minimized simultaneously (Rao, 2009).

The main difficulties in multi-objective optimization problems are to minimize the distance of the generated solutions to the Pareto set and to maximize the diversity of the developed Pareto set. Detail analysis of multi-objective optimization can be found in Deb (2001).

5.3. Stochastic Optimization Algorithms

Stochastic optimization methods are optimization algorithms based on probabilistic elements, either in the objective function with the constraints, or in the algorithm itself or both of them (Spall, 2003). Genetic algorithm, particle swarm optimization, ant colony optimization, simulated annealing, tabu search, harmony search and generalized pattern search algorithm are examples of the stochastic search techniques used in engineering applications. In composite laminate design problems, derivative calculations or their approximations are impossible to obtain or is often costly. Therefore, stochastic search methods have the advantage of requiring no gradient information of the objective functions and the constraints. In this thesis, GA, GPSA and SA have been considered and used without any modification for design of the laminated composites. In the following subsections, steps of the algorithms are briefly overviewed.

5.3.1. Genetic Algorithm

The Genetic Algorithm (GA) is a stochastic optimization and search technique which allows to obtain alternative solutions for some of the complex engineering problems such as increasing composite strength, developing dimensionally stable and light weight structures, etc. GA method utilizes the principles of genetics and natural selection. This method is simple to understand and uses three simple operators: selection, crossover and mutation. Genetic Algorithm always considers a population of solutions instead of a single solution at each iteration. It has some advantages in parallelism and robustness of genetic algorithms. It also improves the chance of finding the global optimum point and helps to avoid local stationary point. However, GA is not guaranteed to find the global optimum solution to a problem. GA has been applied to the design of a variety of composite structures ranging from simple rectangular plates to complex geometries. Genetic algorithms have been widely used in laminate design optimization problems because of the fact that they are suitable for integer programming and able to find global optima (Apalak et al., 2008; Deng et al., 2005; Hufenbach et al., 2001; Park et al., 2008). Details of GA coding in laminated composite design problems are given in literature by many authors (Pelletier & Vel, 2006; Sciuva et al., 2003)

5.3.1.1. Crossover

Crossover is one of the important GA operator that has basic task of creating new children in a reproduction process. This GA step acts combining genetic information taken from a pair of parents. The new generation child should be better than, or at least equivalent, in fitness to its parents. The crossover operator of GA can be utilized first producing a random number to define the crossover point. Then, the gene strings of the related chromosomes are split at the same point in the parents. The left part of parent 1 and the right part of parent 2 are reorganized to create a child. The crossover operator is usually applied with some probability (Spall, 2003).

5.3.1.2. Mutation

Mutation is a genetic operator which is responsible to maintain the genetic diversity from one generation of a population to the next. In mutation operation, the solution can change entirely from the previous solution and so better solution can be obtained. This operation provides a random search capability to GA and it can be useful to find promising areas in the design space. Mutation prevents the algorithm to be trapped in a local minimum. (Gurdal et. al., 1999).

5.3.1.3. Elitist Non-dominated Sorting GA or NSGA-II

The NSGA-II procedure (Deb et al., 2002) is one of the widely used evolutionary multi-objective optimization (EMO) procedures which act to find multiple Pareto-optimal solutions in a multi-objective optimization problem. The procedure has the following three features:

1. It uses an elitist principle,
2. It uses an explicit diversity preserving mechanism, and
3. It emphasizes non-dominated solutions

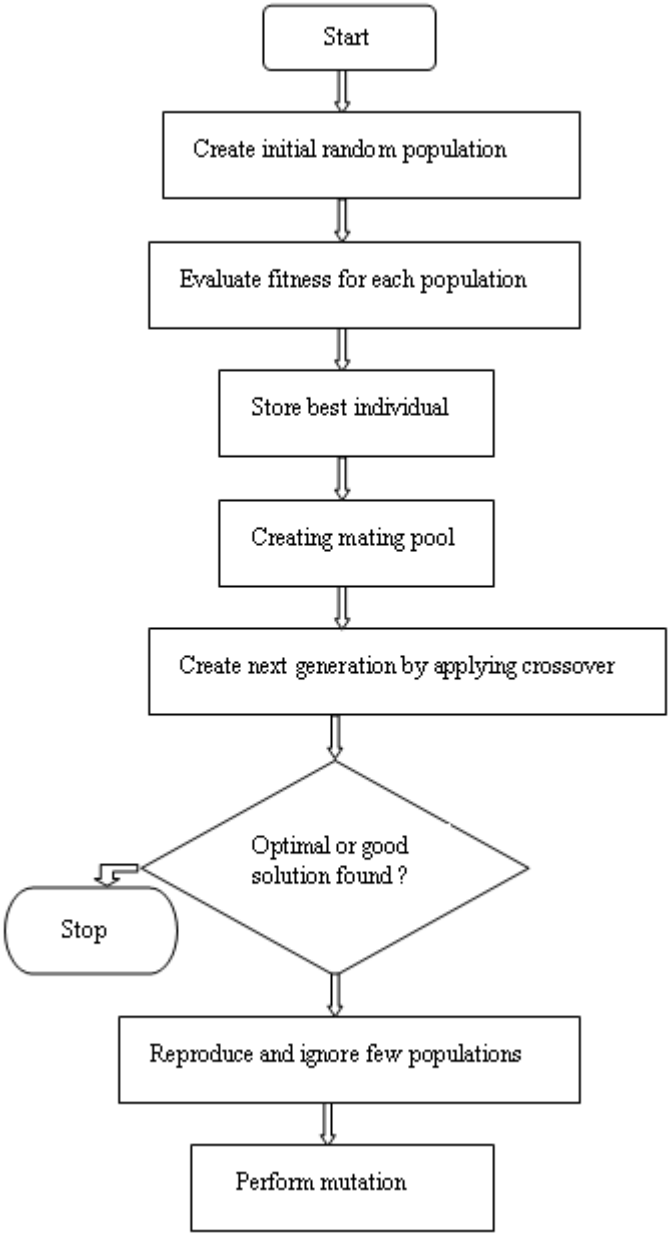

Figure 5.1. Flow chart of Genetic Algorithm
(Source: Sivanandam & Deepa, 2008).

5.3.1.4. Multi-objective Genetic Algorithm in MATLAB

The multi-objective Genetic Algorithm function (*gamultiobj*) utilizes a controlled elitist genetic algorithm. This algorithm is also a variant of Non-Dominated Sorting Genetic Algorithms (NSGA-II). Main difference of controlled elitist GA is that

it favors individuals which increase the diversity of the population even if they have a lower fitness value. An elitist GA always favors individuals with better fitness value. To maintain the diversity of population for convergence to an optimal Pareto front is very significant. This step is achieved by controlling the elite members of the population when the algorithm progresses. The options '*ParetoFraction*' and '*DistanceFcn*' are utilized in order to control the elitism in MATLAB. The first option Pareto fraction limits the number of individuals on the Pareto front. The distance function helps to maintain diversity on a front by favoring individuals that are relatively far away on the front.

5.3.2. Generalized Pattern Search Algorithm (GPSA)

Generalized Pattern Search Algorithm has been defined for derivative-free unconstrained optimization of functions by Torczon (1997) and later extended to take nonlinear constrained optimization problems into account. GPSA is a direct search method which finds a sequence of points that approach the optimal point. Each iteration is divided into two phases: the search phase and the poll phase. In the search phase, the objective function is evaluated at a finite number of points on a mesh. The main task of the search phase is to find a new point that has a lower objective function value than the best current solution which is called the incumbent. In the poll phase, the objective function is evaluated at the neighboring mesh points, so as to see whether a lower objective function value can be obtained (Nicosia, 2008). GPSA has some collection of vectors that form the pattern and has two commonly used positive basis sets; the maximal basis with 2*N* vectors and the minimal basis with *N*+1 vectors.

In order to clarify the algorithm, a laminated composite plate optimization problem including two independent variables θ_1 and θ_2 in the objective function has been considered. In this case, pattern consists of the vectors $v_1=[1 \quad 0]$, $v_2=[0 \quad 1]$ $v_3=[-1 \quad 0], v_4=[0 \quad -1]$ for the positive basis $2N$ or $v_1=[1 \quad 0], v_2=[0 \quad 1]$ $v_3=[-1 \quad -1]$ for the positive basis N+1. The pattern search begins at a provided initial point vector θ_0. In this example problem, $\theta_0=[10 \quad 50]$, the *mesh size* $\Delta^m=5$ and positive basis 2*N* are taken into account. At the first iteration, the following *mesh points* can be calculated as

$[1 \quad 0]\times 5+[10 \quad 50]=[15 \quad 50]$
$[0 \quad 1]\times 5+[10 \quad 50]=[10 \quad 55]$
$[-1 \quad 0]\times 5+[10 \quad 50]=[5 \quad 50]$
$[0 \quad -1]\times 5+[10 \quad 50]=[10 \quad 45]$

and the algorithm computes the objective function at these *mesh points* before polls (Karakaya & Soykasap, 2009; Spall, 2003; Mathworks 2008b). If the algorithm finds an objective function value which is smaller than the value at $\theta_0=[10 \quad 50]$, the poll at corresponding iteration is called as "successful". Supposing the vector [10 55] satisfies the condition, the algorithm sets the next point in the sequence equal to $\theta_1=[10 \quad 55]$. After obtaining a successful poll, the algorithm multiplies the current mesh size by *expansion factor*. For example, if the *expansion factor* is taken as 2, the *mesh size* for the second iteration becomes 5x2=10 and the mesh at the second iteration is to be

$[1 \quad 0]\times 10+[10 \quad 55]=[20 \quad 55]$
$[0 \quad 1]\times 10+[10 \quad 55]=[10 \quad 65]$
$[-1 \quad 0]\times 10+[10 \quad 55]=[0 \quad 55]$
$[0 \quad -1]\times 10+[10 \quad 55]=[10 \quad 45]$

Now, suppose that $\theta_2=[0 \quad 55]$ produce smaller objective function value than the value at $\theta_1=[10 \quad 55]$. This procedure repeats until none of the *mesh points* has a smaller objective function value than the value at last (say *n*) successful poll iteration. This poll is called as "unsuccessful" in the corresponding iteration. In this case, the algorithm does not change the current point at the next iteration as $\theta_{n+1}=\theta_n$

In such a case, the algorithm multiplies the current mesh size by given *contraction factor* and the algorithm then polls with a smaller mesh size. The algorithm stops when any of the stopping criteria conditions satisfied.

5.3.3. Simulated Annealing Algorithm (SA)

Simulated Annealing (SA) is a random-search technique and it is based on the simulation of thermal annealing of heated solids to achieve the minimum function value in a minimization problem (Rao, 2009). It is possible to solve mixed-integer, discrete or continuous optimization problems by using SA. In this algorithm, a new point is randomly generated at each iteration and the algorithm stops when any of the

stopping criteria are satisfied. The distance of the new point from the current point or the extent of the search is based on Boltzmann's probability distribution. The distribution implies the energy of a system in thermal equilibrium at temperature *T*. Boltzmann's probability distribution can be written in the following form (Rao, 2009):

$$P(E) = e^{-E/kT} \tag{5.1}$$

where P(*E*) represents the probability of achieving the energy level *E*, *k* is the Boltzmann's constant and *T* is temperature

Simulated Annealing algorithm has the following steps:

1. Start with an initial vector x_1 and assign a high temperature value to the function

2. Generate a new design point randomly and find the difference between the previous and current function values

3. Specify whether the new point is better than the current point.

4. If the value of a randomly generated number is larger than $e^{-\Delta E/kT}$, accept the point x_{i+1}

5. If the point x_{i+1} is rejected, then the algorithm produces a new design point x_{i+1} randomly. However, it should be noted that the algorithm accepts a worse point based on an acceptance probability (Rao, 2009).

5.4. Matlab Optimization Toolbox

MATLAB Optimization Toolbox includes some routines for solving optimization problems using Direct search (DS), Genetic Algorithm (GA) and Simulated Annealing (SA). All of these methods have been used in design of composite materials by many researchers (Ozgur & Sonmez, 2005; Karakaya & Soykasap, 2009; Pelletier & Vel, 2006). Direct Search functions include two direct search algorithms called the generalized pattern search (GPS) algorithm and the mesh adaptive search (MADS) algorithm. The Toolbox has also some optimization solvers such as *ga*, *gamultiobj*, *simulannealbnd*, *patternsearch* and these solvers can be selected as an optimization algorithm.

5.4.1. Gamultiobj Solver

The *gamultiobj* solver tries to create a set of Pareto optima for a multi-objective minimization. It can be set bounds and linear constraints on variables. To be able to find local Pareto optima, *gamultiobj* solver utilizes the genetic algorithm. It can be specified an initial population, or the solver itself can generate one automatically. The fitness function should return a vector of type double. The population type consists of double, bit string vector, and custom-typed vector. If a custom population type is utilized, the user must write his/her creation, mutation, and crossover functions that accept inputs of that population type. After that, it must be specified the following functions: *Creation function* (CreationFcn), *Mutation function* (MutationFcn), and *Crossover function* (CrossoverFcn). Figure 5.2 represents the parameter selection steps for the multi-objective GA analysis of *gamultiobj* solver user interface. In Table 5.1 Genetic Algorithm parameters for multi-objective approach used in the model problems have been listed.

5.4.2. Ga Solver

GA mode of the toolbox consists of two main part : (i) Problem definition (fitness function, bounds and constraints, number of variables), (ii) Options (Population, Fitness scaling, Selection, Reproduction, Mutation, Crossover, Migration). *Selection* option uses *Tournament* selection function. The aim of using selection function is to determine parents for the next generation based on their scaled values from the objective functions. In order to achive an ideal selection strategy, it should be adjusted its selective pressure and population diversity. *Reproduction* option is related with determination of Genetic Algorithm children creation at each new generation. In the toolbox, *Crossover fraction* is utilized as a sub-option and it specifies the fraction of the next generation that crossover produces. *Crossover fraction* must be a fraction between 0 and 1. *Mutation* option has four different mutation functions such as C*onstraint dependent, Gaussian, Uniform* and *Adaptive feasible*. If there are no constraints or bounds in the specified problem, *Gaussian* sub-option can be selected, otherwise *Adaptive feasible* should be used. In the *Crossover* option, it should be specified the function that performs the crossover in the sub-option *Crossover function*. There exist following six different

crossover functions in the toolbox: *Scattered, Single point, Two point, Intermediate, Heuristic* and *Arithmetic*. Figure 5.3 represents the parameter selection steps for the GA analysis of *ga* solver user interface. In Table 5.2, Genetic Algorithm parameters for single-objective approach used in the model problems have been listed.

5.4.3. Patternsearch Solver

The *Patternsearch* solver interface has two separated parts: problem set up(objective functions, start point, linear inequalities, linear inequalities, lower and upper bounds, nonlinear constraint function and result screen) and options(*Poll, search, mesh, algorithm settings, cache, stopping criteria, plot functions, output function, display to command window, user function evaluation*). *Poll* option consists of the following sub-options: *poll method*, *complete poll* and *polling order*. These sub options are responsible the controlling of the pattern search poll of the mesh points at each iteration. In the *Poll Method*, so as to create the mesh, direct search algorithms (GPSA) or (MADS) algorithms can be specified. There are two patterns for the direct search algorithms: Positive basis 2*N* and the Positive basis *N*+1. *Complete poll* defines whether all the points in the current mesh must be polled at each iteration and it depends on the selection of *on* or *off*. *Polling order* part has three alternatives: *Random*, *success* and *consecutive*. This option specify the types of order. Figure 5.4 represents the parameter selection steps for the GPSA analysis of patternsearch solver user interface. In Table 5.3 generalized pattern search algorithm parameters used in the model problems for single-objective approach have been listed

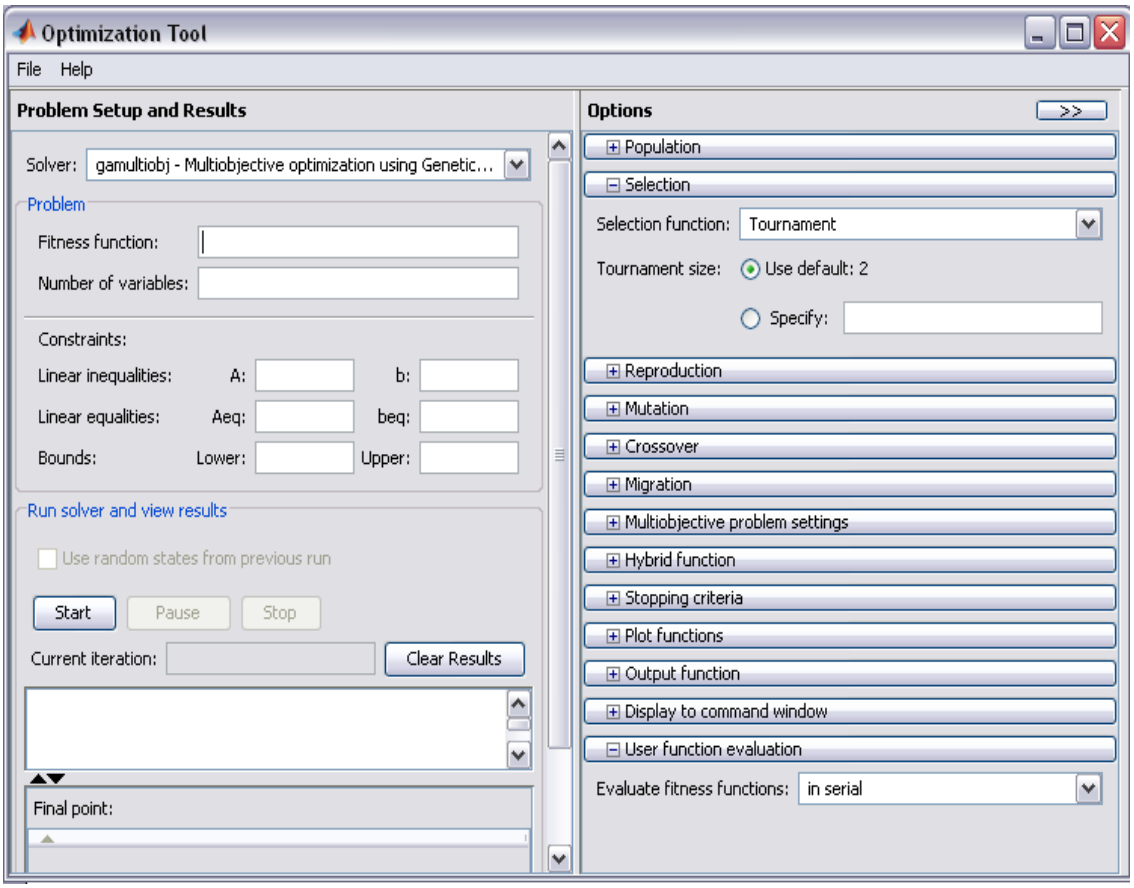

Figure 5.2. Matlab optimization toolbox *gamultiobj* solver user interface.

.

5.4.4. Simulannealbnd Solver

This solver consist of two main parts as in the other MATLAB Optimization Toolbox solvers: (i) Problem set up and results, (ii) Options. In problem set up and results part, *Objective function* represents the fitness of the optimization problem of the user. *Start point* determine the initial point for the Simulated Annealing search. Additionally, lower and upper bounds can be given for the design parameters in the *bounds* sub-options. Options part consists of four sub-options: *annealing parameters*, *acceptance criteria*, *problem type* and *hybrid function*. *Annealing function* define the function that is utilized to generate new points for the next iteration. The *fast annealing* takes random steps with size which is proportional to the temperature whereas *Boltzmann annealing* takes random steps with size proportional to square root of temperature. *Reannealing interval* represent the number of points to accept before re-annealing process. *Temperature*

update function options are:(i) *Exponential temperature update* in this sub-option temperature decreases as 0.95^iteration. (ii) *Logarithmic temperature update* that temperature decreases as 1/log(iteration). (iii) *Linear temperature update* that temperature decreases as 1/iteration. *Initial temperature* represents the temperature at the beginning of the run.. *Data type* sub-option can be set to: *Double* for double-precision numbers. *Hybrid function* determine an alternate solver that runs at specified times

Table 5.1. Genetic Algorithm parameters for multi-objective approach used in the model problems (*gamultiobj* solver)

Population Type	Double vector
Population size	50
Initial range	[-90 -90 ; 90 90]
Selection function	Tournament
Crossover fraction	0.8
Mutation function	Adaptive feasible
Crossover function	Intermediate Ratio=1.0
Migration direction	Both Fraction=0.2, Interval=20
Initial penalty	10
Penalty factor	100
Hybrid Function	None
Stopping criteria	generation=800, Stall generation=800 Function tolerance=10^{-6}

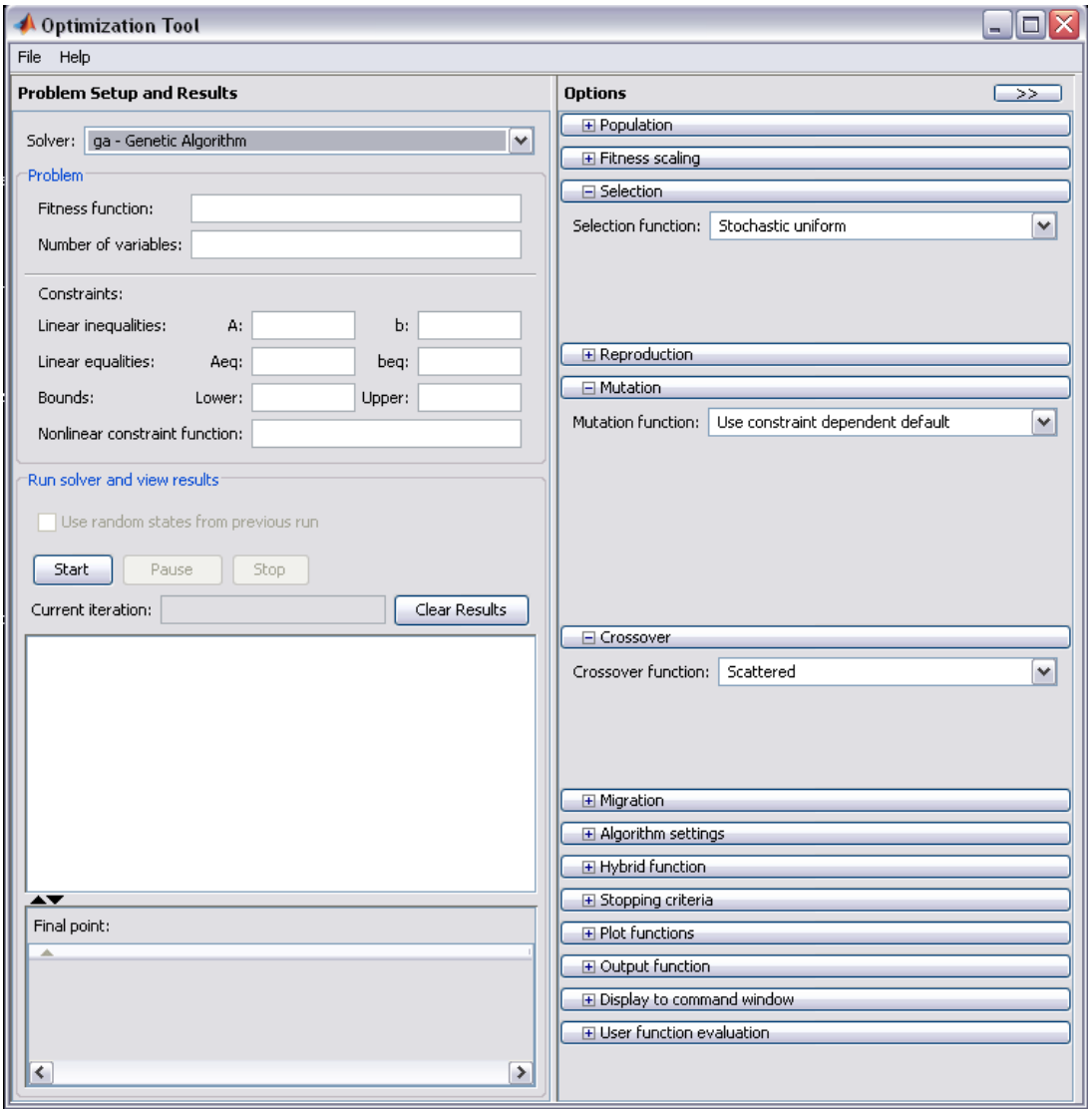

Figure 5.3. Matlab optimization toolbox ga solver user interface.

The selections consist of (i) *fminsearch* that can be used only for unconstrained problems, (ii) *patternsearch* that is used if you specify bounds, (iii) *fminunc* that is utilized only for unconstrained problem, (iv) *fmincon* can be used only for constrained problems. Figure 5.5 represents the parameter selection steps for the SA analysis of simulannealbnd solver user interface. In Table 5.4 Simulated Annealing algorithm parameters used in the model problems for single-objective approach have been listed.

Table 5.2. Genetic Algorithm parameters for single-objective approach used in model problems.

Population Type	Double vector
Population size	20
Creation function	Use constraint dependent
Initial population	[ ]
Initial scores	[ ]
Initial range	[-300;-100]
Scalling function	Top, Quantity=12
Selection function	Tournament Tournament size=7
Elite count	2
Crossover fraction	0.6
Mutation function	Use constraint dependent
Crossover function	Scattered
Migration direction	Both Fraction=0.2, Interval=20
Initial penalty	10
Penalty factor	100
Hybrid Function	None
Stopping criteria	Generation=100, Stall generation=50 Function tolerance=10^-6

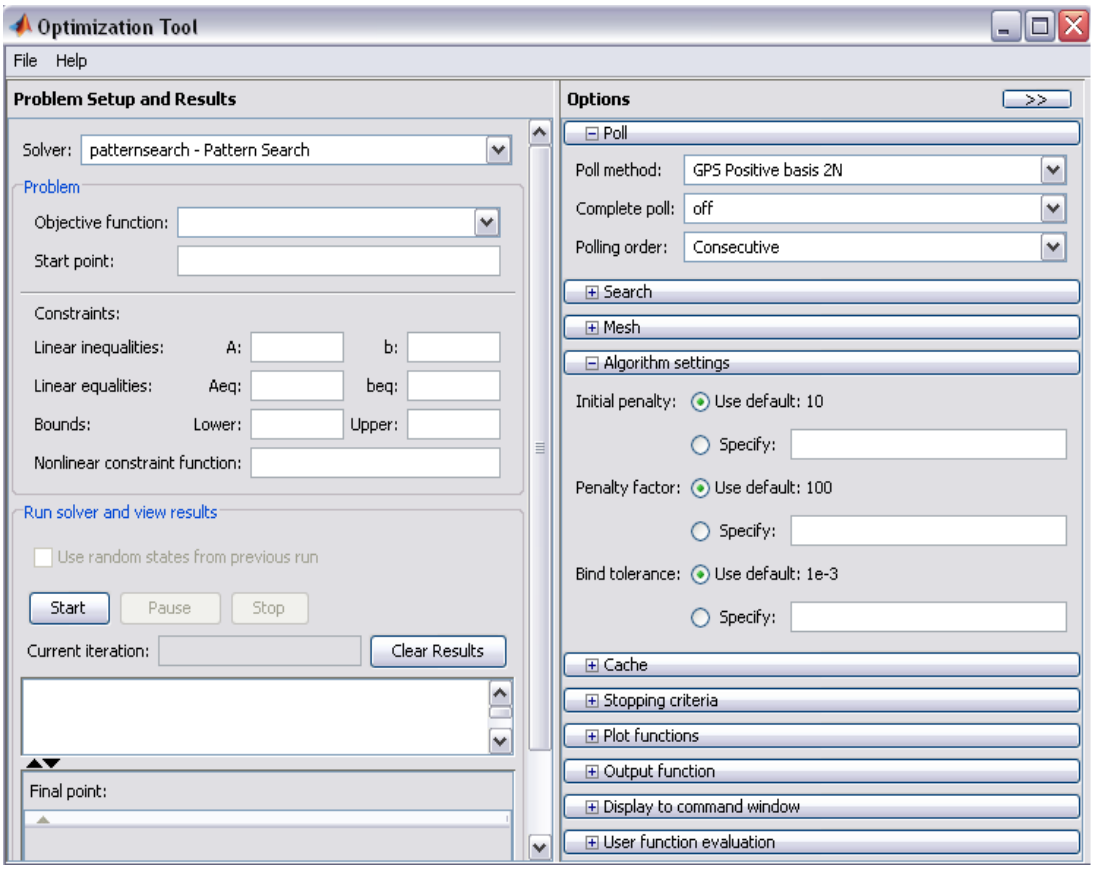

Figure 5.4. Matlab optimization toolbox patternsearch solver user interface.

Table 5.3. GPSA parameters for single-objective approach used in model problems.

Poll Method	GPS Positive basis 2N
Complete poll	off
Polling Order	Consecutive
Complete search	off
Search method	None
Mesh initial size	1.0
Mesh Max size	infinity
Mesh Accelerator	off
Mesh Rotate	on
Mesh Scale	on
Mesh Expansion factor	2.0
Contraction factor	0.5
Initial penalty	1.0
Penalty factor	100
Bind tolerance	10^-3
Stopping criteria	Mesh tolerance=10^-6 Max iterations= 200*numberof variables Max function evaluations=2000*number ofvariables Time limit=infinity X tolerance=10^-6 Function tolerance=10^-6 Nonlinear constraint tolerance=10^-6

.

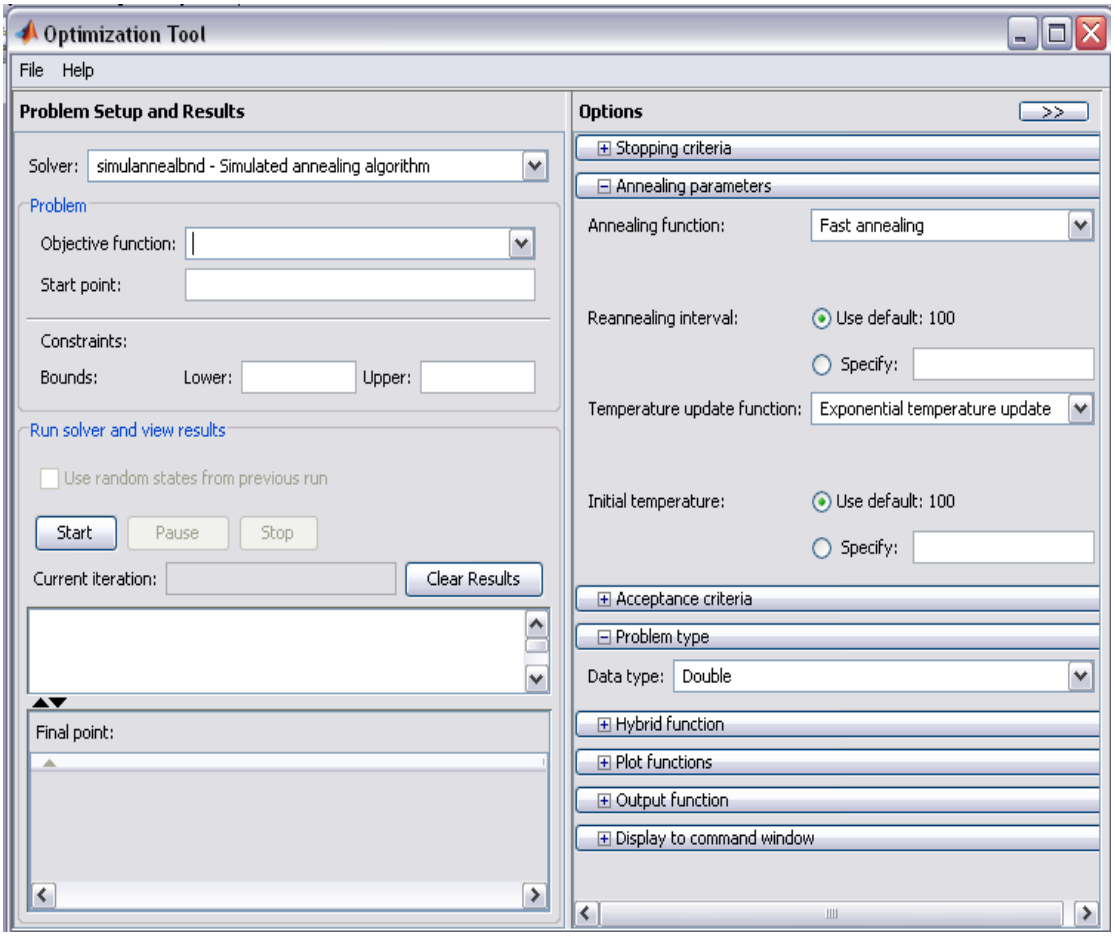

Figure 5.5. Matlab optimization toolbox simulannealbnd solver user interface.

Table 5.4. Simulated Annealing solver parameters for single-objective approach used in the model problems

Annealing function	Fast annealing
Reannealing interval	100
Temperature uptade function	Exponential temperature update
Initial temperature	100
Acceptance probability function	Simulated annealing acceptance
Data type	Double
Stopping criteria	Max iterations= infinity Max function evaluations = 3000*numberof variables Stall iterations = 500*numberofvariables Function tolerance=10^-6

CHAPTER 6

EXPERIMENTAL DETERMINATION OF MATERIAL PROPERTIES

6.1. Background

The oldest and simplest manufacturing method for fiber-reinforced composite structural components is hand layup technique. The main disadvantage of hand layup is that the process is labor-intensive. In recent years, the interests of the automotive industry are much more concentrated on the development of manufacturing methods that can support mass production rates. There are three manufacturing processes for that: compression molding, pultrusion, and filament winding. Even though they have used for many years, analyzing on their basic characteristics and process optimization started in the mid-1970s. Resin transfer molding (RTM) is low pressure closed molding processes that has received important attention in aerospace and automotive industries for its ability to produce very complex shaped composite structures at relatively high production rates. With the introduction of automation techniques into the composite production, fast-curing resins, new fiber forms, high-resolution quality control tools, the manufacturing technology for fiber-reinforced polymer composites has advanced at a remarkably rapid pace (Mallick, 2007). Most widely used manufacturing methods utilized in the fiber-reinforced composite industry are Bag Molding Process, Compression Molding, Pultrusion, Flament Winding, Liquid Composite Molding Processes (1.RTM, 2.SRIM).

6.1.1. Liquid Composite Molding Processes

In Liquid Composite Molding (LCM) processes, involve injecting a a premixed liquid thermoset resin into a dry fiber-packed mold cavity. The main objective of the process is to achieve a full impregnation as the resin fills the space between the fibers. Finally when it cures, it transforms into the matrix. We can describe two LCM

processes, namely Resin Transfer molding (RTM) and Structural Reaction Injection Molding(SRIM). In this study RTM methods are only considered.

6.1.1.1. Resin Transfer Molding (RTM)

RTM is a low pressure, closed molding process, and consist of several layers including two-part mold, strand mat, woven roving, or cloth. In this operation, the mold is closed, and a catalyzed liquid resin is injected into the mold with the aid of a centrally located sprue. The resin should be injected at the lowest point of the mold cavity. The injection pressure is varied from 69 to 690 kPa. When the resins such as epoxy, vinyl ester, methyl methacrylate, polyester or phenolic flows and spreads throughout the mold, they fill the space between the fibers in the dry fiber preform, displace the entrapped air through the air vents in the mold, and coat the fibers. Curing step is relevant to type of the resin catalyst system and it is performed either at room temperature or at an elevated temperature. It is required to trim the outer part to conform to the exact dimensions after the cured part is pulled out of the mold. In this process, it is advantages to use a preform instead of using flat-reinforcing layers, because preform has already the shape of the desired product and this provide good moldability with complicated shapes. Another advantage of using preform is the elimination of the trimming operation, which is often the most labor intensive step in an RTM process.

There are two different version of the RTM process: vacuum assisted RTM (VARTM) and Seemann's Composite Resin Infusion Molding Process (SCRIMP). In contrast to RTM, Vacuum pressure is used in addition to the resin injection system so as to saturate the reinforced fibers into the preform in VARTM. Both VARTM and SCRIMP utilize single-sided, rigid molds. The preform is placed on the hard mold surface and covered with a vacuum bag. Figure 6.1 shows the schematic illustration of VARTM process. In the present thesis, the E-glass/epoxy polymer matrix composites are produced by VARTM method. In Figure 6.2. a VARTM process application prepared in IYTE ME lab is illustrated. Left side is injection (input) part for the epoxy.

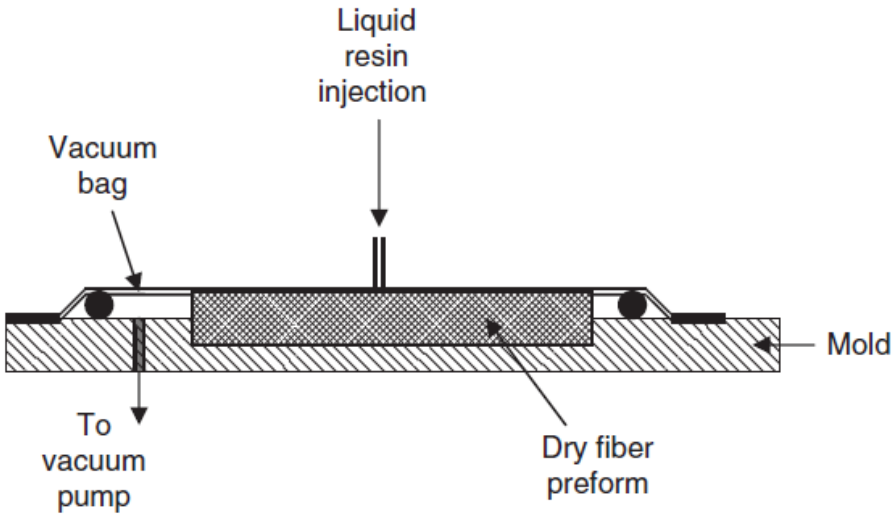

Figure 6.1. Vacuum-assisted resin transfer molding (VARTM) (Source:Mallick, 2007).

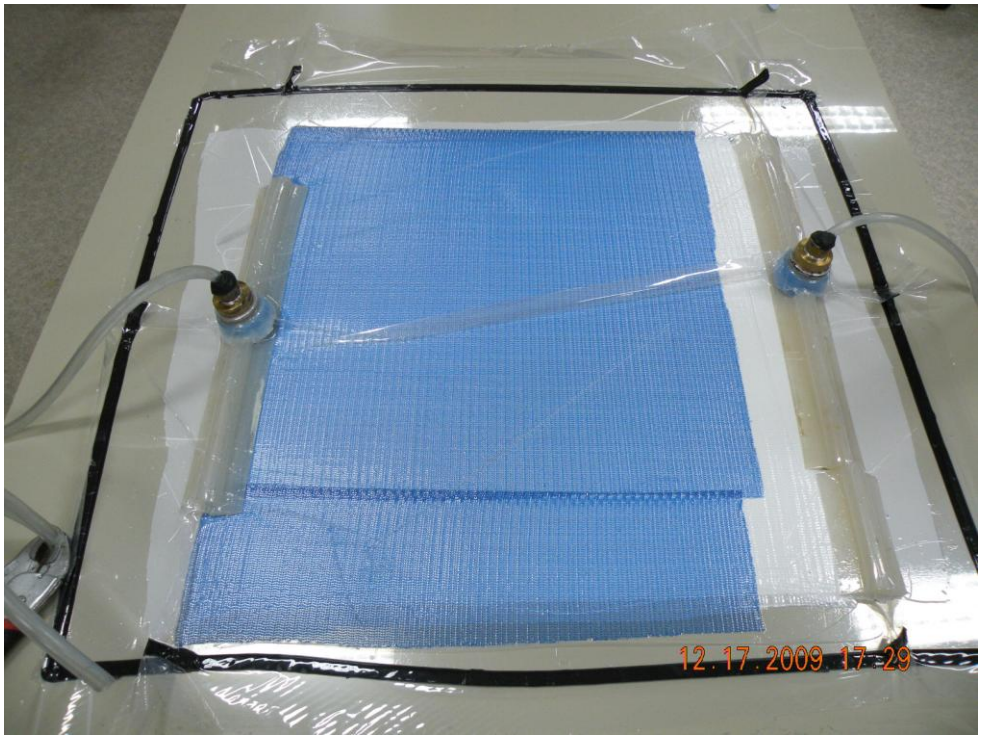

Figure 6.2. VARTM process application prepared in IYTE-ME Lab.

6.2. Determination of Basic Material Properties of the E-Glass/Epoxy

The analysis and design of composite structures require the determination of the basic properties of the lamina for use as an input data. In this part, E-glass/epoxy laminated composite material is characterized in terms of tensile (ASTM D3039-76) and shear (ASTM D7078/D7078M-05) properties (E_1, E_2, ν_{12}, ν_{21}, G_{12}, σ_1^T, σ_2^T) experimentally.

Testing of composite materials has three main objectives

1. determination of basic properties of the unidirectional lamina for use as an input in structural design and analysis
2. verification of analytical predictions of mechanical behavior
3. independent experimental study of material and structural behavior for specific geometries.

Uniaxial tensile tests are conducted on unidirectional laminae to determine the properties longitudinal and transverse Young's moduli E_1, E_2 ; tensile strength in longitudinal and transverse directions σ_1^T, σ_2^T; major Poisson's ratio ν_{12} can be calculated based on the following expressions

$$\sigma_1 = \frac{P}{A},\ E_1 = \frac{\sigma_1}{\varepsilon_1},\ \nu_{12} = -\frac{\varepsilon_2}{\varepsilon_1},\ \sigma_1^T = \frac{P_{ult}}{A} \qquad (6.1a\text{-}d)$$

$$\sigma_2 = \frac{P}{A},\ E_2 = \frac{\sigma_2}{\varepsilon_2},\ \nu_{21} = \nu_{12}\frac{E_2}{E_1},\ \sigma_2^T = \frac{P_{ult}}{A} \qquad (6.2a\text{-}d)$$

Tests are performed using Shimadzu AG1 250 kN (see Figure 6.3) mechanical testing machine and computer for data acquisition. In determination of tensile properties, at least five specimens per test are used. Longitudinal and transverse properties are determined using $[0^\circ]_6$ and $[90^\circ]_6$ unidirectional specimens, respectively. The geometry of the specimens used for longitudinal and transverse properties are given in Figures 6.4 and 6.5. After completing tests, we have obtained stress-strain curves for axial and transverse directions and these curves are given in Figures 6.6 and 6.7, respectively. As seen from these figures the stress-strain behavior is linear and final failure occurs in a catastrophic manner.

Figure 6.3. Shimadzu AG1 250 kN mechanical testing machine.

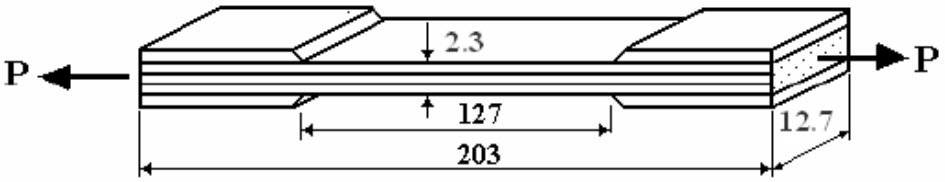

Figure 6.4. Specimen geometry and dimensions for longitudinal properties in tensile test.

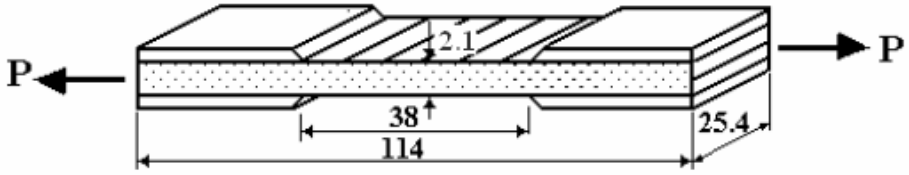

Figure 6.5. Specimen geometry and dimensions for transverse properties in tensile test.

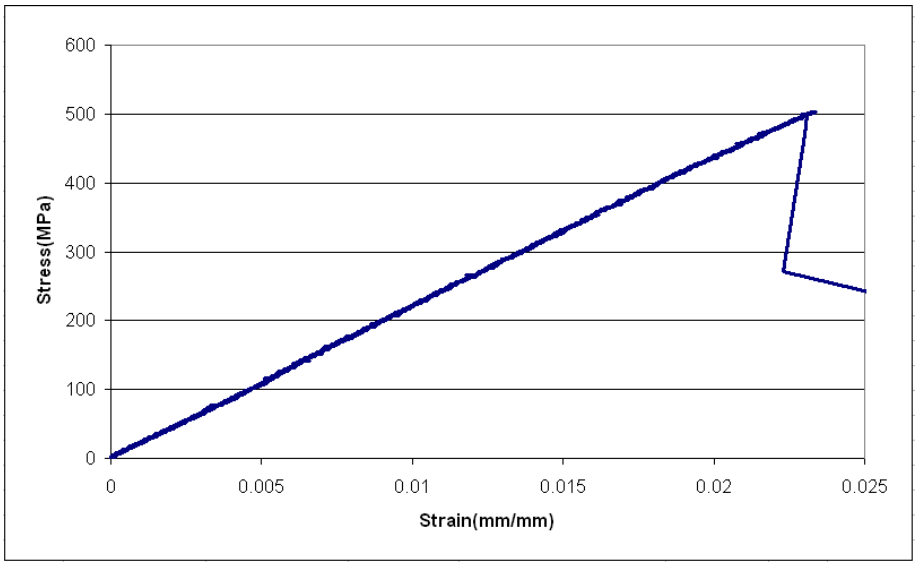

Figure 6.6. Strain-stress curve for E-glass/epoxy unidirectional $[0^\circ]_6$ composite produced by composite lab in IYTE.

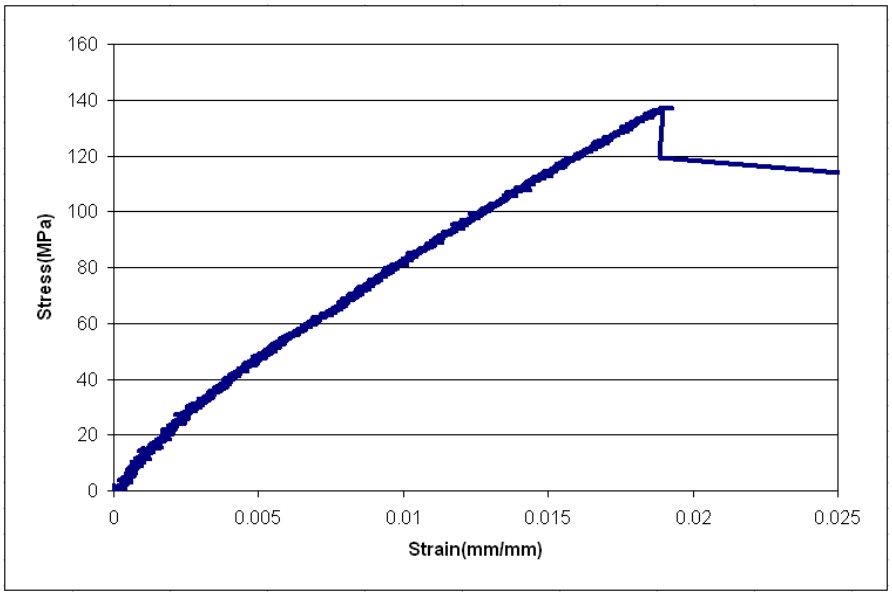

Figure 6.7. Strain-stress curve for E-glass/epoxy unidirectional $[90^\circ]_6$ composite produced by composite lab in IYTE

In order to measure the fiber volume fraction (V_f) of the composite, the burn-out was carried out. Three small rectangular pieces were cut out from the edges and central parts of the polymeric composites. They heated up to 750°C and kept for 1 hour at their temperature using a furnace. Hence, epoxy was burned-out and blow away. The weights

of the sampler before and after born out were measured using a balance. The fiber volume fractions (V_f) of the composites were calculated based on the equation below;

$$V_f = \frac{v_f}{v_f + v_m} \times 100 = \frac{\frac{m_f}{\rho_f}}{\left(\frac{m_f}{\rho_f} + \frac{m_m}{\rho_m}\right)} \times 100 \qquad (6.3)$$

where V_f, v_f, v_m, m_f, m_m, ρ_f, and ρ_m are percentage of fiber volume fraction, volume of fiber, volume of matrix, mass of fiber, mass of matrix, density of fiber, density of matrix of the composites, respectively.

Full characterization of an unidirectional composite requires also the determination of lamina properties under in plane shear loading parallel to the fibers, i.e., shear modulus G_{12}**.** In this thesis, ASTM D 7078/D 7078M-05 Standard test method for shear properties of composite materials by V-notched rail shear method was used for characterization of shear modulus G_{12}. This test method covers the determination of the shear properties of fiber-reinforced composite materials by clamping the ends of a V-notched specimen between two pairs of loading rails (see Figure 6.8). Figures 6.9 and 6.10 also show the spacer blocks and specimen geometry with the dimensions

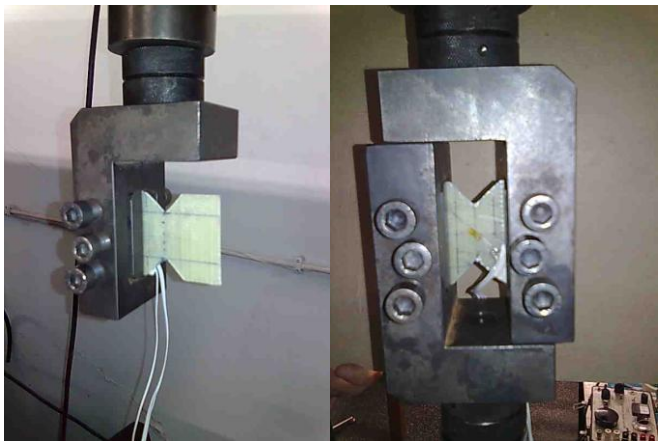

Figure 6.8. Photo of V notched rail shear method specimen and loading fixture located in the Mechanical Engineering Lab of DEU

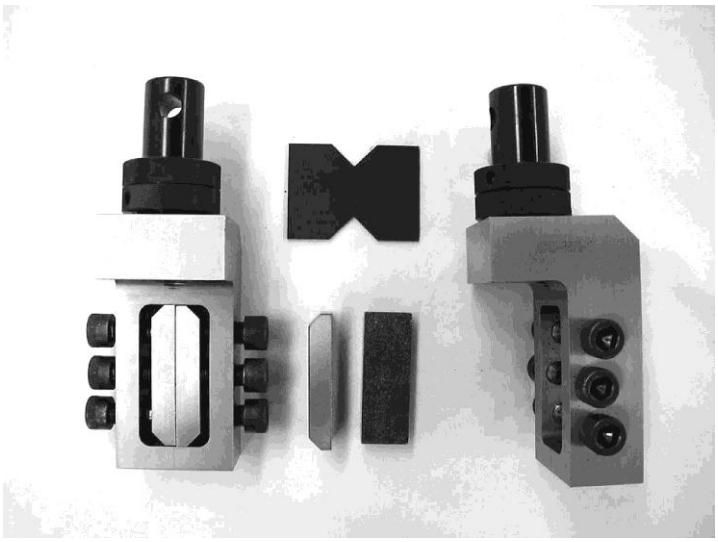

Figure 6.9. Partially assembled fixture with specimen and spacer blocks

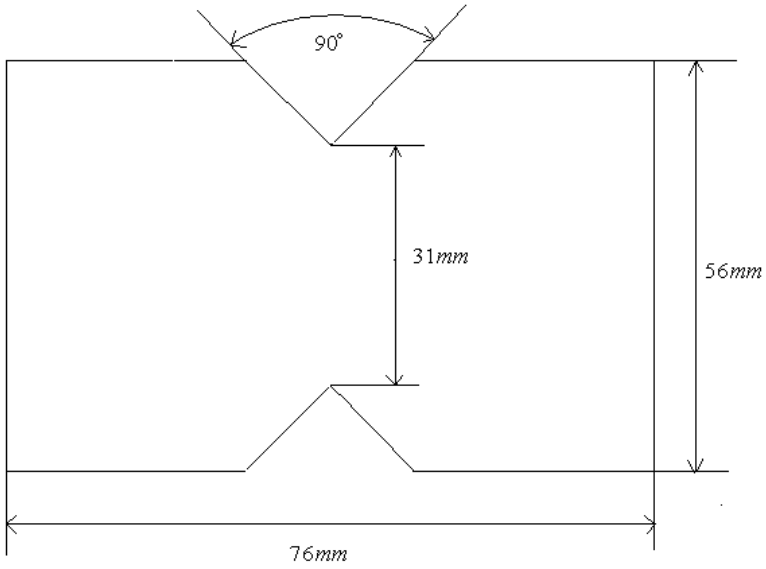

Figure 6.10. V notched rail shear method test specimen dimension and geometry

6.2.1. DMA Q800 Dynamic Mechanical Analyzer

In this thesis, thermal properties of the E-glass/epoxy composites produced in IYTE have been analyzed by using DMA Q800 Dynamic Mechanical Analyzer. Dynamic Mechanical Analysis measures the mechanical properties of materials as a

function of time, temperature and frequency. The Q800 DMA instrument illustrated in Figure 6.11 incorporates unique technology to provide the ultimate in performance, versatility and ease of use. DMA instruments utilize linear drive motor technology (DMT) that provides precise stress control and ultra sensitive optical encoder technology (USOE) so as to measure strain and air bearing. Fundamental imperfection of other rival product is usage of conventional stepper motors, LVDT strain measurement devices, and mechanical springs instead of these (DMT, USOE) technologies. The Q800 DMA instrument can be operated over extremely wide temperature range (-150 to 600°C) and provides multiple modes of deformation such as dual/single cantilever and 3-point bending, tension, compression, and shear. The clamps are individually calibrated for data accuracy and the elegant but simple design facilitates sample mounting.

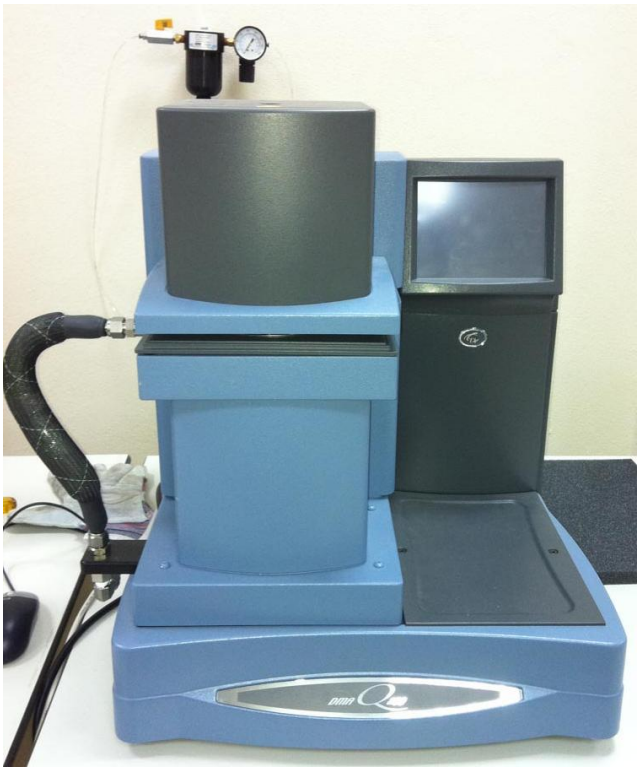

Figure 6.11. DMA Q800 Dynamic Mechanical Analyzer

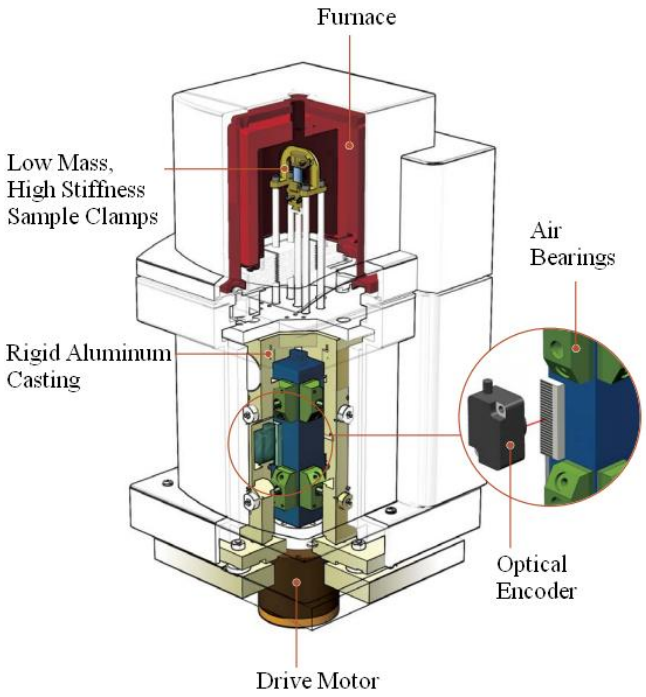

Figure 6.12. Details of DMA Q800 Dynamic Mechanical Analyzer
(Source: http://www.tainstruments.com/)

The main parts of the DMA Q800 instrument are described shortly in the following sections.

6.2.1.1. Drive Motor

DMA Q800 instrument utilizes a non-contact, direct drive motor (see Figure 6.12). The motor provides the oscillatory or static force required. and is constructed of high performance composites that ensure low compliance. Very complicated electronics allow the motor current to be adjusted in small increments. Reproducible forces can be obtained by using the motor and the force can be changed rapidly, enabling a broad spectrum of material properties to be measured.

6.2.1.2. Air Bearing

The force can be transmited by drive motor to an air bearing slide, that is guided by eight porous carbon air bearings. It can be formed a frictionless surface that permits the slide to “float” by two alternatives, pressurized air or nitrogen flows. The slide can

move vertically up to 25 mm. Because of its rectangular shape twisting of the sample can be eliminated. It is possible to characterized films and fibers type weak materials.

6.2.1.3. Optical Encoder

Optical encoder that is used to measure displacement on the DMA Q800 is a type of high-resolution linear. This encoder is based on diffraction patterns of moveable and stationary light through gratings and provide exceptional resolution better than typical LVDT technology. Considerably small amplitudes can be measured accurately. This technology fecilitiates excellent modulus precision and allows the Q800 DMA to characterize a broad range of material.

6.2.1.4. Furnace

The Q800 DMA utilizes a bifilar wound furnace that automatically opens and closes. The furnace design combined with the Gas Cooling Accessory provides for efficient and precise temperature control over the entire temperature range, both in heating, cooling, and isothermal operation. The automatic furnace movement simplifies experimental setup.

6.2.1.5. Low Mass, High Stiffness Sample Clamps

The Q800 features a variety of sample clamps that provide for multiple modes of deformation. The clamps were designed using finite element analysis to provide high stiffness, with low mass, and attach to the drive shaft with a dovetail connection. The clamps are simple to use and adjust, and each is individually calibrated to insure data accuracy. A broad range of samples can be analyzed. The high stiffness minimizes clamp compliance, and the low mass ensures rapid temperature equilibration. The simple, yet elegant designs reduce the time necessary to change clamps and load samples.

6.2.1.6. Rigid Aluminum Casting

The Q800 drive motor, air bearing slide assembly with optical encoder and air bearings are all mounted within a rigid aluminum casting that is temperature controlled. The rigid aluminum housing minimizes system compliance and the temperature-controlled housing ensures precise data.

6.2.1.7. Modes of Deformation

In DMA Q 800 instrument has four different clamp options for various scopes.

1) Dual/Single Cantilever: In this mode, the sample is clamped at both ends and either flexed in the middle (dual cantilever) or at one end (single cantilever). Cantilever bending is a good general-purpose mode for evaluating thermoplastics and highly damped materials (e.g., elastomers). Dual cantilever mode is ideal for studying the cure of supported thermosets.

2) 3-Point Bend: In this mode, the sample is supported at both ends and force is applied in the middle. 3-point bend is considered a "pure" mode of deformation since clamping effects are eliminated. The 50 and 20 mm clamps on the Q800 utilize unique low-friction, roller bearing supports that improve accuracy

3) Compression: In this mode, the sample is placed on a fixed flat surface and an oscillating plate applies force. Compression is suitable for low to moderate modulus materials (e.g., foams and elastomers). This mode can also be used to make measurements of expansion or contraction, and tack testing for adhesives.

4) Tension: In this mode, the sample is placed in tension between a fixed and moveable clamp. In oscillation experiments, the instruments use a variety of methods for applying a static load to prevent buckling and unnecessary creep. The clamps are suitable for both films and fibers. Figure 6.13 shows these clamps bounded to the columns with the samples.

6.3. Measurement of Tg and CTEs for the E-Glass/Epoxy Composite

At temperature below the glass transition temperature (Tg) a composite behaves like a glassy material. At higher temperatures, the composite behaves like a viscoelastic

material. The glass transion is often used to identify the temperature range of the glassy to viscoelastic transition. Tg analysis for the E-glass/epoxy composites produced in IYTE Composite Lab. was performed with a DMA in IYTE Composite Research Lab. The DMA was equipped with the three point bending measuring system with a 20mm bending platform and a 10mm knife edge. The temperature has been changed from 20 ^{o}C to 140 ^{o}C at a heating rate of 4 ^{o}C/min. The sample given in Figure 6.14 was cut to 23 mm length and 3mm in depth, the sample was placed directly on the three point bending platform. After end of the test the graph given in Figure 6.15 as an example have been obtained. Glass transition temperature was determined as the temperature where Tan δ its maximum value It can be seen that, Tg for the composite is obtained as 105 ^{o}C.

The in-plane thermal expansion coefficients (CTEs) of $[0^{\circ}]_6$ and $[90^{\circ}]_6$ E-glass/epoxy was measured as a function of temperature via dynamic mechanical analysis DMA Q800 instrument. It is used in control force mode with a heating rate of 4 ^{o}C/min. A typical sample (see Figure 6.14) dimension is 15 mm × 4 mm × 1.9 mm. The samples are loaded uniaxially with a tensile stress of 0.1 MPa and the change of the sample dimension with increasing temperature is monitored. The CTE have been determined from the slope of the resultant expansion temperature plots. CTEs of the E-glass/epoxy for fiber and transverse to fiber directions are obtained as $\alpha_1 = 10.02.10^{-6}/^{\circ}C$ and $\alpha_2 = 28.41.10^{-6}/^{\circ}C$ based on the formulation given in Equation 6.4. and by determining from the slopes of curves given in Figures 6.16 and 6.17. Experimental determination of the mechanical properties of unidirectional ply under static loading results are also given in Table 6.1.

$$\alpha = \frac{\Delta L}{L \times \Delta T} \tag{6.4}$$

.

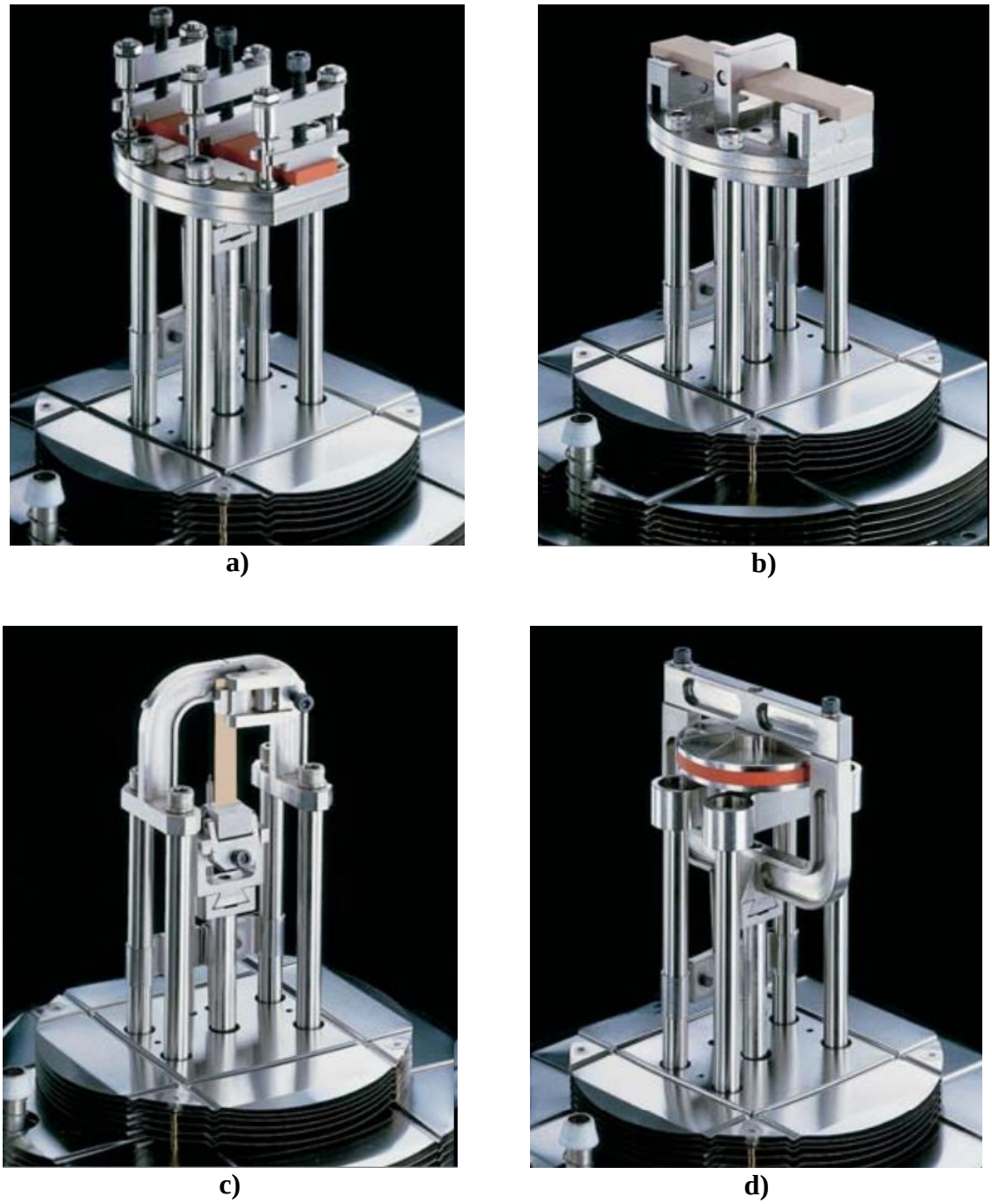

a) **b)**

c) **d)**

Figure 6.13. DMA Q800 clamps a) dual/single cantilever, b) 3-point bend, c) tension, d) compression (Source: http://www.tainstruments.com/)

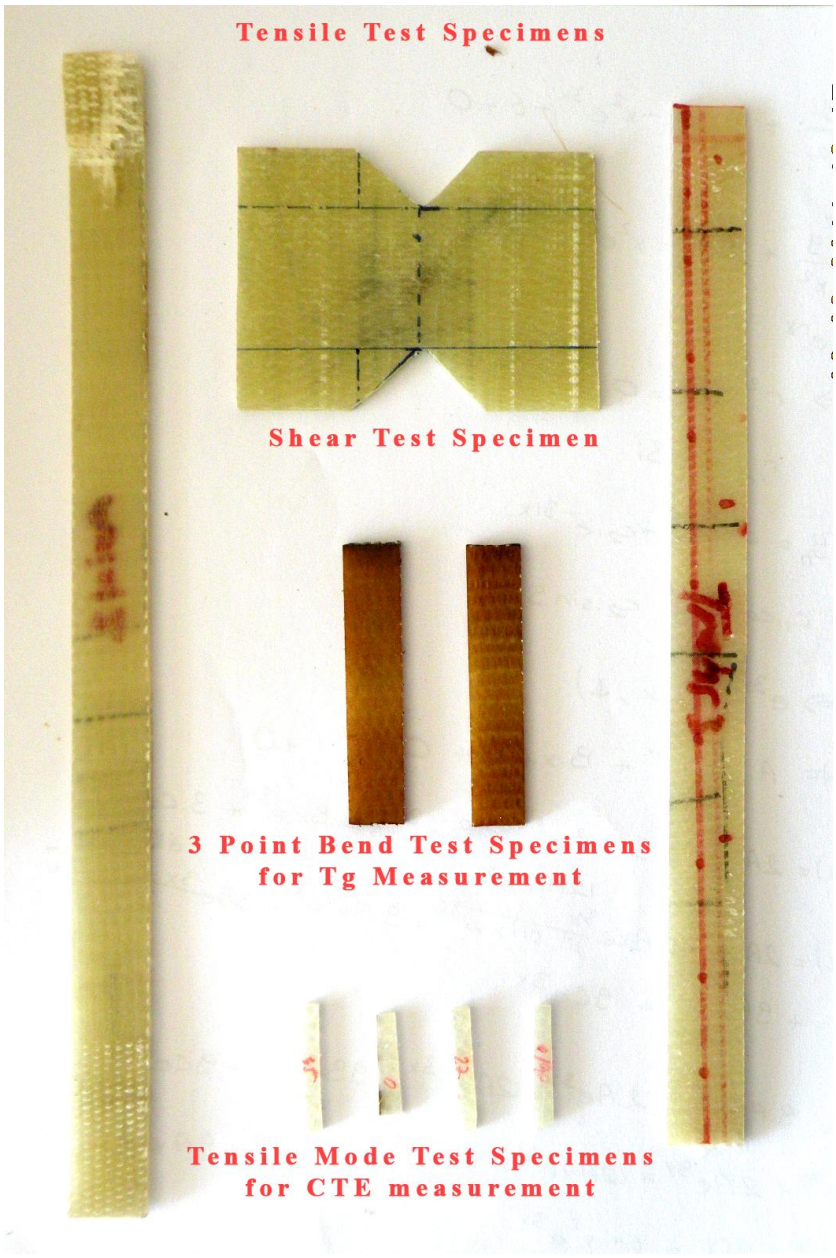

Figure 6.14. E-glass/epoxy specimen geometries used in tensile tests (longitudinal and transverse directions), shear test, 3-point bend test and tensile mode test for CTE calculation

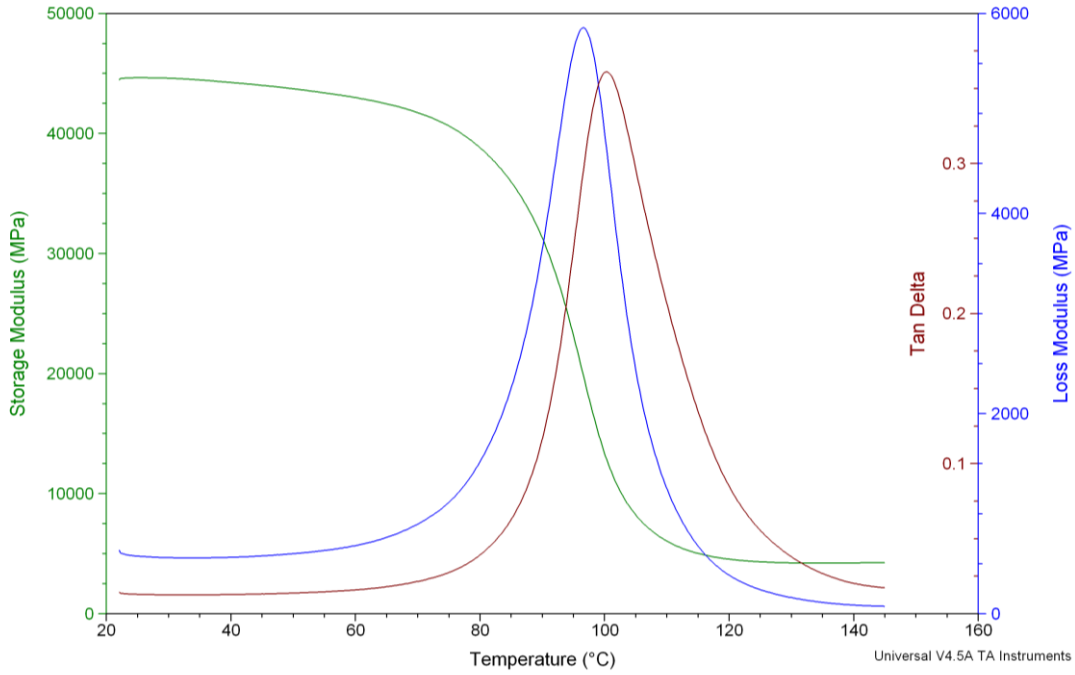

Figure 6.15.Tg analysis result of E-glass Epoxy laminated composite using DMA Q800

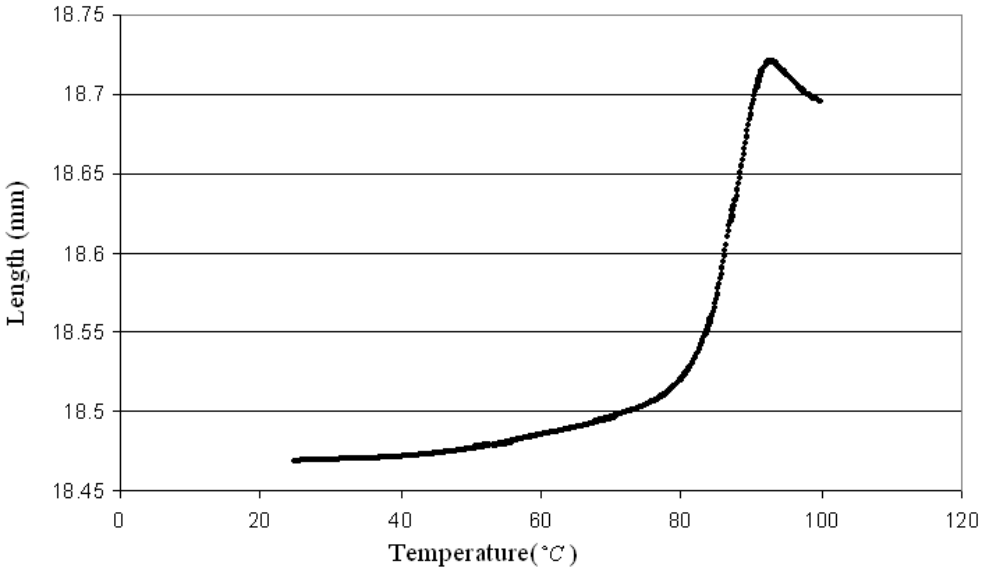

Figure 6.16. Measurement of CTE α_1 of E-glass/epoxy laminated composite using DMA

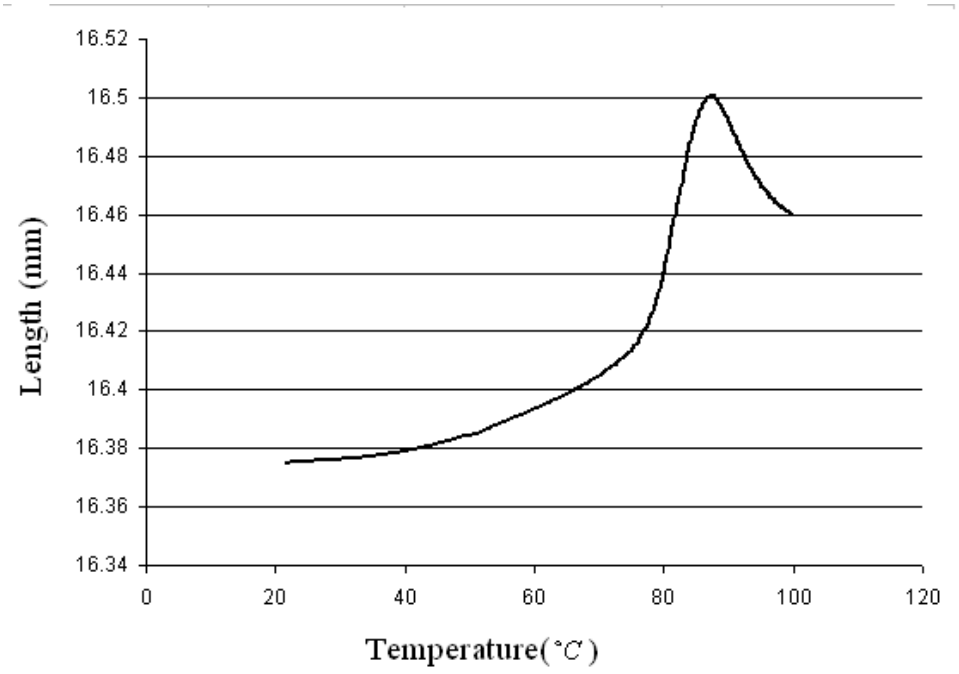

Figure 6.17. Measurement of CTE α_2 of E-glass/epoxy laminated composite using DMA

Table 6.1. Elastic moduli, Poisson's ratio, shear modulus, fiber volume fraction, coefficient of thermal expansions values.

E_1 (GPa)	E_2 (GPa)	ν_{12}	G_{12} (GPa)	V_f	α_1 $(10^{-6}/^{\circ}C)$	α_2 $(10^{-6}/^{\circ}C)$
22.2	11.5	0.33	2	0.41	10.02	28.41

CHAPTER 7

OPTIMIZATION OF DIMENSIONALLY STABLE COMPOSITES

Dimensional stability concept can be defined as a general property of a material, component or structure which enables it to maintain or retain its shape, size or any dimension. From the view point of polymer matrix composites, it can also been defined as the ability of a plastic part to retain the precise shape to which it was molded, cast, or otherwise fabricated (Wolff, 2004). Figure 7.1 presents the definition of dimensionally stable materials in terms of the aerospace range of strains and temperatures.

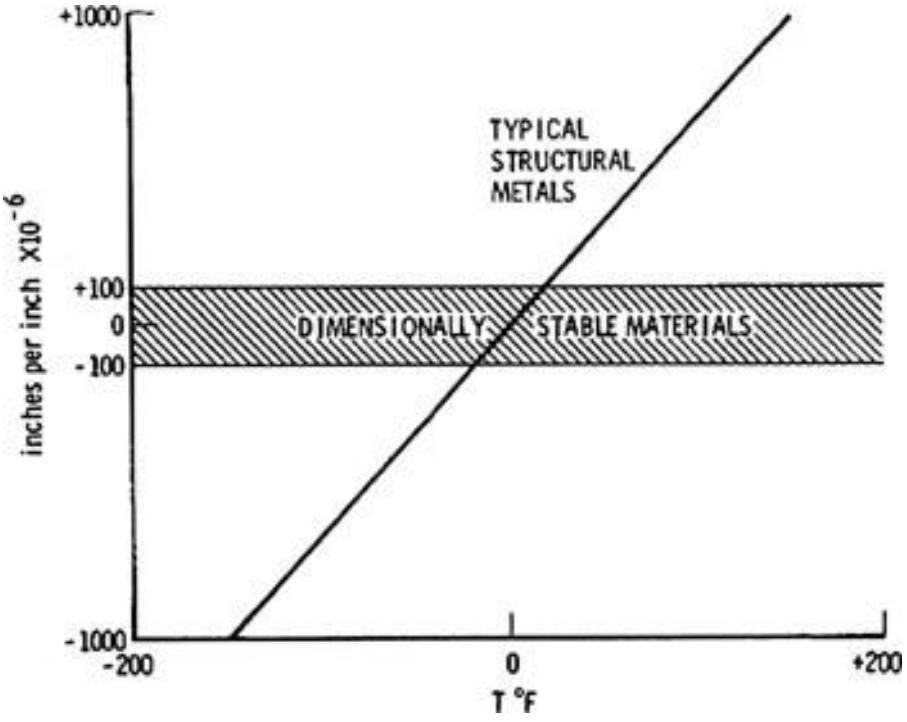

Figure 7.1. Dimensional changes with temperature for dimensionally stable and typical structural materials (Source: Wolff, 2004).

Motivations for dimensionally stable design of a structure or material can be listed as (LeRich & Gaudin, 1998):

1) The designed structure should be light.

2) In order to avoid vibration mode couplings between the launcher and the structure,

the stiffness should be as high as possible.

3) The coefficients of thermal and moisture expansion of the designed structure should be small. Especially in satellite applications these features are very important.

4) Dimensions should be stable through time.

5) Reproducibility of the structure should be taken into consideration. It depends on manufacturing techniques control and on basic materials properties dispersion. Composite sensitivity to ingredients properties dispersions has to be kept as low as possible.

Since carbon fibers have exceptional combinations of strength, stiffness, low density, and low CTE, it is appropriate to consider first when designing stable composites. The linear CTE is one of the most attractive topic in engineering design and analysis. Thermal expansion of polymer or resin matrix composites is very significant parameter in dimensional stability of many lightweight and highly stiff components and structures. The major effect on the linear CTE of a resin matrix composite is the stacking sequences.

In this chapter, stacking sequences optimization problems for symmetric balanced 4 layered $[\theta_1/-\theta_1]_S$; 8 layered $[\pm\theta_1/\pm\theta_2]_S$, $[\theta_1/\theta_2/-\theta_1/-\theta_2]_S$ and $[0/\pm\theta_1/0]_S$; 12 layered $[\pm\theta_1/\pm\theta_2/\pm\theta_3]_S$, $[\theta_1/\theta_2/\theta_3/-\theta_1/-\theta_2/-\theta_3]_S$ and $[\theta_1/-\theta_1/\theta_2/\theta_3/-\theta_2/-\theta_3]_S$; 16 layered $[\pm\theta_1/\pm\theta_2/\pm\theta_3/\pm\theta_4]_S$ E-glass/epoxy and carbon/epoxy laminated composites have been solved by using GA and by drawing the graphical distribution of the objective functions. The objective functions have been obtained using the MATLAB code given in Appendix A. The schematic representation of stacking sequences of the composites are also given in Figures 7.2-7.9. The main problem of the thesis is to design the stacking sequence of the carbon/epoxy and E-glass/epoxy laminated composites having low CTE and high elastic moduli. In order to obtain the composites satisfying these requirements, following optimization problems have been solved and corresponding material parameters have been calculated :

- minimization of α_x only
- minimization of α_y only
- maximization of E_x only
- maximization of E_y only
- Minimizations of α_x and α_y simultaneously

- Maximization of E_x and minimization of α_x simultaneously
- Maximization of E_y and minimization of α_y simultaneously
- Maximizations of E_x and E_y, minimization of α_x simultaneously

After completing optimization process, optimum fiber orientation angles have been obtained. Then failure loads have been calculated with different loading ratios (N_x/N_y=1 to 100 and 1/100 to 1) and thermal changes($\Delta T = -10^\circ C$ to $-110^\circ C$) by using failure criteria Tsai-Hill, Tsai-Wu, Hoffman and Hashin-Rotem for the optimized 8 layered E-glass and carbon/epoxy composites.

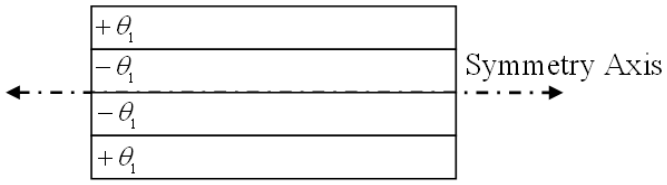

Figure 7.2. Shematic representation of 4 layered symmetric balanced $[\theta_1/-\theta_1]_S$ laminated composites

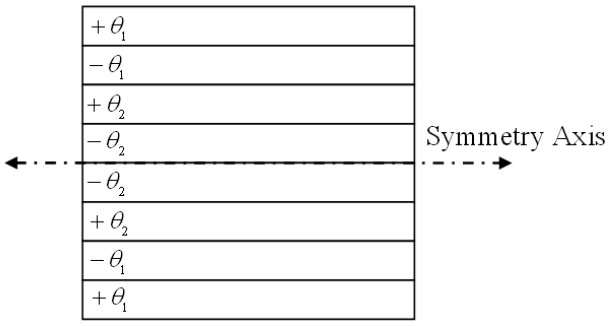

Figure 7.3. Shematic representation of 8 layered symmetric balanced $[\pm\theta_1/\pm\theta_2]_S$ laminated composites

Multi-objective GA and single-objective GA optimization results for $[\theta_1/-\theta_1]_S$ E-glass/epoxy laminated composites are given in Table 7.1. It can be seen from the table, 27.3° and 62.7° are appropriate fiber orientation angles of the composite (model problems 1 and 2) for coefficient of thermal expansion in *x* and *y* directions, respectively. Comparing the results given in Table 7.1 for 27.3° and 62.7° with conventional designs $[\pm 45]_S$ and $[0/90]_S$ (last two lines of the table), it can be seen that

very small CTEs (8.61 instead of 16.83) in *x* and *y* directions have been obtained after optimization. The same results are also observed by drawing variation of CTEs with θ_1 in Figure 7.10.

For model problems 3 and 4, maximum E_x and E_y values as expected are obtained for 0° and 90°, respectively. Variation of Young's Moduli with θ_1 are given in Figure 7.11. As it can be seen from the figure, for 45° and -45°, E_x and E_y have the same value. It can also be observed that maximum E_x and E_y values occur in 0° and 90°, respectively.

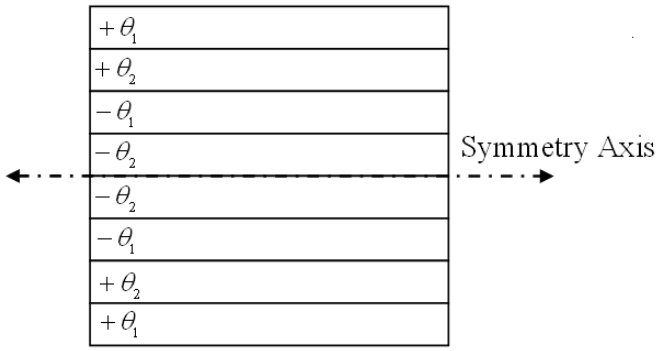

Figure 7.4. Schematic representation of 8 layered symmetric balanced $[\theta_1/\theta_2/-\theta_1/-\theta_2]_S$ laminated composites.

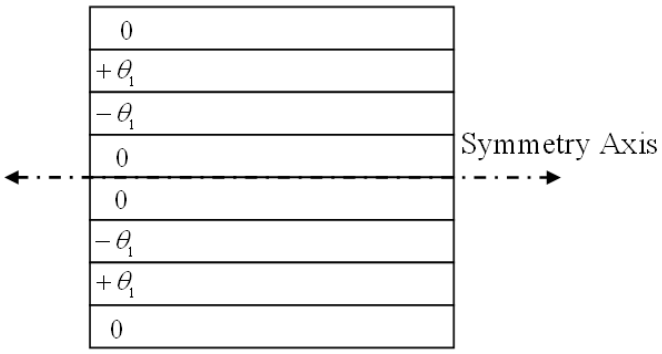

Figure 7.5. Schematic representation of 8 layered symmetric balanced $[0/\pm\theta_1/0]_S$ laminated composites.

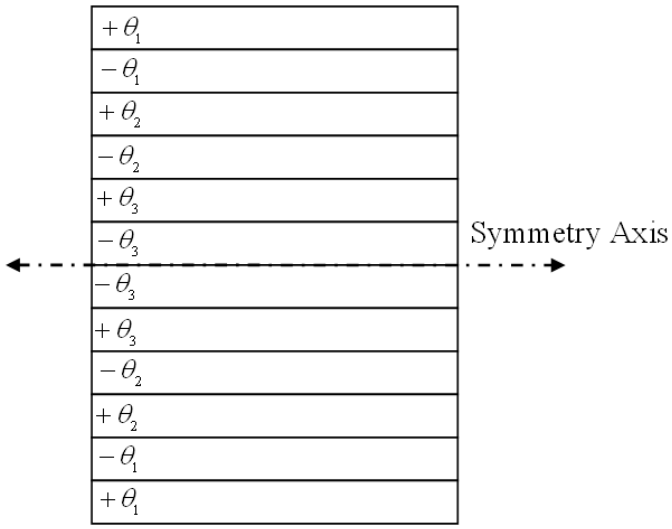

Figure 7.6. Schematic representation of 12 layered symmetric balanced $[\pm\theta_1/\pm\theta_2/\pm\theta_3]_S$ laminated composites.

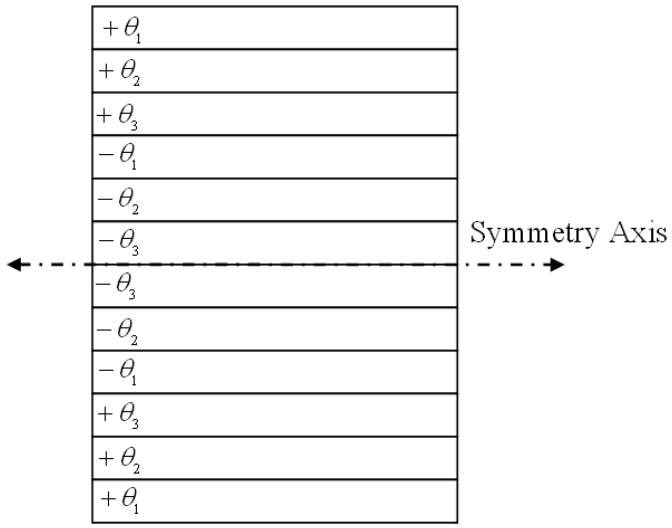

Figure 7.7. Schematic representation of 12 layered symmetric balanced $[\theta_1/\theta_2/\theta_3/-\theta_1/-\theta_2/-\theta_3]_S$ laminated composites

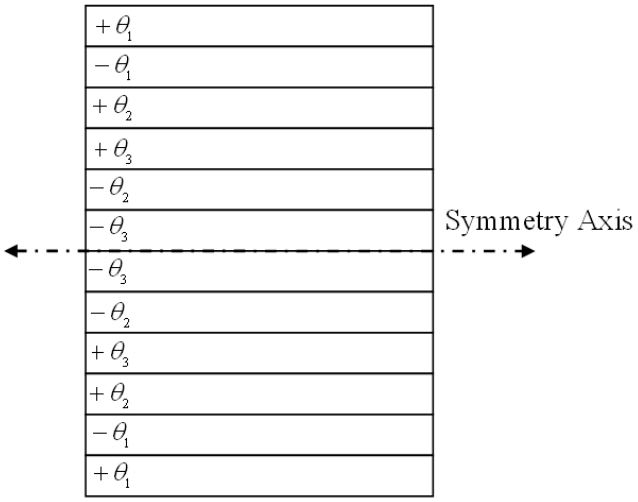

Figure 7.8. Schematic representation of 12 layered symmetric balanced $[\theta_1/-\theta_1/\theta_2/\theta_3/-\theta_2/-\theta_3]_S$ laminated composites

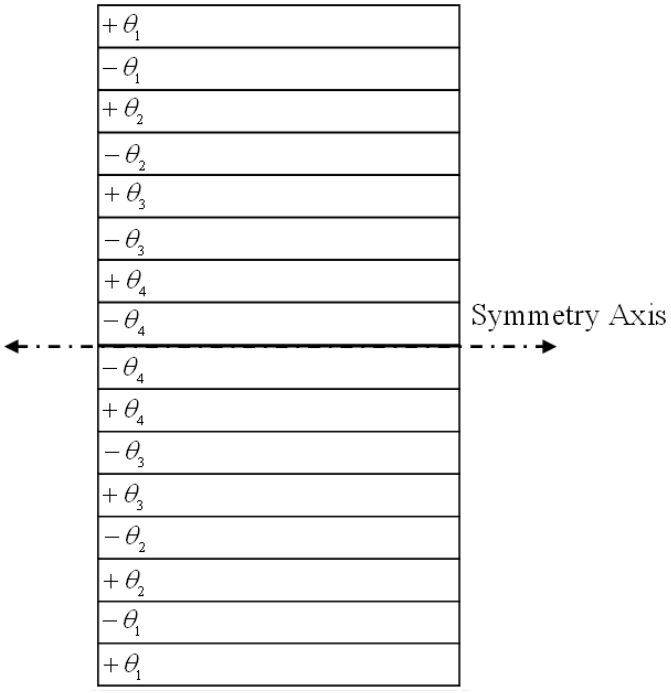

Figure 7.9. Schematic representation of 16 layered symmetric balanced $[\pm\theta_1/\pm\theta_2/\pm\theta_3/\pm\theta_4]_S$ laminated composites

Selected Pareto optimum designs of α_x-α_y, E_x-α_x, E_y-α_y, and E_x-E_y-α_x (model problems 5-8) are listed in Table 7.1. For α_x-α_y multi-objective optimization case, 12 different solutions have been produced. Only one of the solutions of this Pareto set can

be taken into consideration depending on the constraints. For example, if one of your constraint is $E_x > 8.00\ GPa$ then the appropriate designs have the stacking sequences only $[\pm 27.3]_S$, $[\pm 36.8]_S$ and $[\pm 62.7]_S$. Model problem 6 considers maximization of E_x and minimization of α_x simultaneously. As it can be seen from Table 7.1, Pareto set varies between the stacks $[0_4]$ and $[\pm 27.3]_S$. Comparing the set of solutions with conventional designs $[\pm 45]_S$ and $[0/90]_S$, 7 different solutions $[\pm 18.9]_S$, $[\pm 18.4]_S$, $[\pm 17.1]_S$, $[\pm 16.2]_S$, $[\pm 14.4]_S$, $[\pm 6.9]_S$, and $[0_4]$ have been obtained which are better than conventional designs. In model problem 7, multi-objective optimization problem for material parameters E_y-α_y are investigated. After optimization process, 8 different designs $[\pm 70.4]_S$, $[\pm 72.4]_S$, $[\pm 73.0]_S$, $[\pm 74.0]_S$, $[\pm 75.4]_S$, $[\pm 78.4]_S$, $[\pm 80.1]_S$, $[90_4]$ have been produced which is better than conventional designs $[\pm 45]_S$ and $[0/90]_S$.

Table 7.1. Optimizations of 4 layered $[\theta_1/-\theta_1]_S$ E-glass/epoxy laminated composite.

Problem No	Optimization	Stack	E_x (GPa)	E_y (GPa)	α_x ($10^{-6}/^{\circ}C$)	α_y ($10^{-6}/^{\circ}C$)
1	**Min α_x**	$[\pm 27.3]_S$	13.17	8.33	8.61	28.00
2	**Min α_y**	$[\pm 62.7]_S$	8.33	13.17	28.00	8.61
3	**Max E_x**	$[0_4]$	22.20	11.50	10.02	28.41
4	**Max E_y**	$[90_4]$	11.50	22.20	28.41	10.02
5	**Min α_x Min α_y**	$[\pm 27.3]_S$	13.17	8.33	8.61	28.00
		$[\pm 36.8]_S$	8.70	6.84	10.45	24.23
		$[\pm 39.8]_S$	7.74	6.62	12.27	21.84
		$[\pm 42.8]_S$	7.07	6.61	14.71	19.04
		$[\pm 43.7]_S$	6.92	6.66	15.56	18.14
		$[\pm 46.9]_S$	6.62	7.02	18.69	15.04
		$[\pm 48.0]_S$	6.59	7.22	19.83	13.99
		$[\pm 48.4]_S$	6.58	7.30	20.22	13.65
		$[\pm 50.7]_S$	6.64	7.88	22.32	11.89
		$[\pm 51.9]_S$	6.72	8.25	23.25	11.16
		$[\pm 54.6]_S$	7.00	9.25	25.12	9.85
		$[\pm 62.7]_S$	8.33	13.17	28.00	8.61
6	**Max E_x Min α_x**	$[\pm 27.3]_S$	13.17	8.33	8.61	28.00
		$[\pm 24.8]_S$	14.51	8.80	8.67	28.29
		$[\pm 23.0]_S$	15.47	9.13	8.77	28.43
		$[\pm 21.8]_S$	16.10	9.35	8.86	28.49
		$[\pm 21.3]_S$	16.33	9.44	8.89	28.51
		$[\pm 18.9]_S$	17.52	9.85	9.09	28.57
		$[\pm 18.4]_S$	17.72	9.93	9.12	28.57
		$[\pm 17.1]_S$	18.32	10.13	9.23	28.58
		$[\pm 16.2]_S$	18.68	10.27	9.31	28.58
		$[\pm 14.4]_S$	19.40	10.52	9.44	28.56
		$[\pm 6.9]_S$	21.55	11.27	9.88	28.46
		$[0_4]$	22.20	11.50	10.02	28.41

(**cont. on next page**)

Table 7.1. (cont.)

7	**Max E_y Min α_y**	$[90_4]$	11.50	22.20	28.41	10.02
		$[\pm 80.1]_S$	11.03	20.86	28.50	9.74
		$[\pm 78.4]_S$	10.86	20.37	28.52	9.64
		$[\pm 75.4]_S$	10.49	19.35	28.56	9.43
		$[\pm 74.0]_S$	10.30	18.80	28.57	9.32
		$[\pm 73.0]_S$	10.15	18.35	28.58	9.24
		$[\pm 72.4]_S$	10.06	18.10	28.58	9.19
		$[\pm 70.4]_S$	9.73	17.19	28.56	9.03
		$[\pm 69.7]_S$	9.61	16.83	28.54	8.97
		$[\pm 68.3]_S$	9.37	16.12	28.50	8.86
		$[\pm 67.6]_S$	9.24	15.76	28.46	8.81
		$[\pm 65.0]_S$	8.76	14.38	28.27	8.66
		$[\pm 63.5]_S$	8.48	13.60	28.08	8.62
		$[\pm 62.7]_S$	8.33	13.16	27.96	8.61
8	**Max E_x Max E_y Min α_x**	$[0_4]$	22.20	11.50	10.02	28.41
		$[\pm 18.0]_S$	17.94	10.00	9.16	28.58
		$[\pm 20.7]_S$	16.64	9.55	8.94	28.53
		$[\pm 27.3]_S$	13.16	8.33	8.61	27.96
		$[\pm 59.5]_S$	7.75	11.50	27.23	8.75
		$[\pm 62.0]_S$	8.21	12.82	27.84	8.61
		$[\pm 66.7]_S$	9.08	15.30	28.41	8.75
		$[90_4]$	11.50	22.20	28.41	10.02
	Conventional Designs	**$[\pm 45]_S$**	**6.76**	**6.76**	**16.83**	**16.83**
		$[0/90]_S$	**16.95**	**16.95**	**16.83**	**16.83**

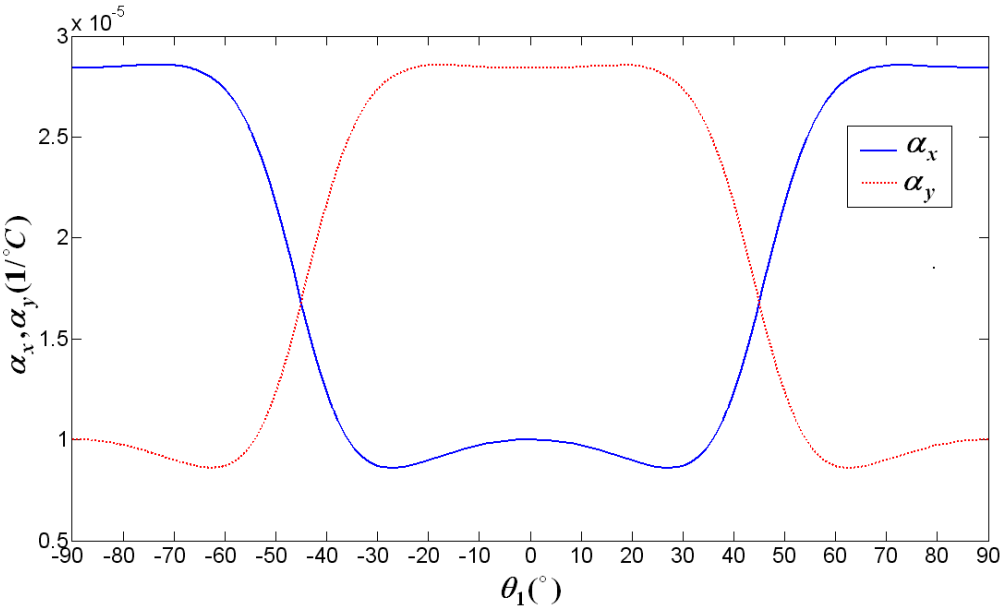

Figure 7.10. Variation of CTEs with θ_1 for 4 layers symmetric balanced $[\theta_1/-\theta_1]_S$ E-glass/epoxy laminated composites.

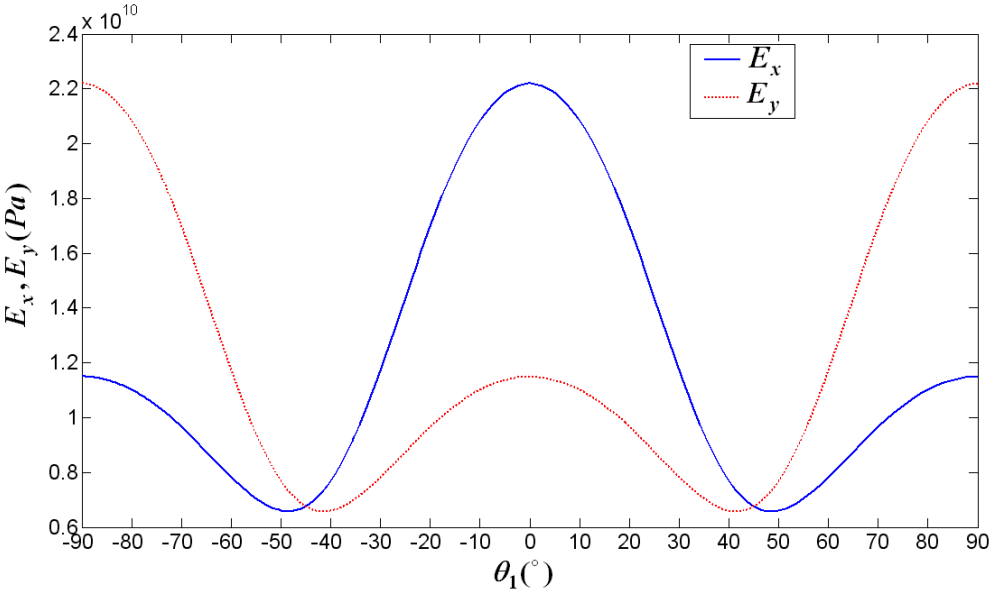

Figure 7.11. Variation of Young's Moduli with θ_1 for 4 layers symmetric balanced $[\theta_1/-\theta_1]_S$ E-glass/epoxy laminated composites.

Table 7.2. gives multi-objective and single-objective GA optimization results for $[\theta_1/-\theta_1]_S$ carbon/epoxy laminated composites. It can be seen from the table, as different from the E-glass/epoxy laminated composites, fiber orientation angles 32°

and 58° minimize the coefficient of thermal expansion in *x* and *y* directions, respectively. However, as in the E-glass/epoxy composite, maximum E_x and E_y values are obtained for 0° and 90°, respectively. Model problem 13 gives the Pareto optimum solutions of the minimizations of α_x and α_y simultaneously. By comparing the set of solutions with the conventional designs given at the end of Table 7.2, it can be concluded that none of the optimum solutions, produced by *MATLAB optimization toolbox*, are better than the results of $[\pm 45]_S$ and $[0/90]_S$. Model problem 14 aims to find the stacking sequences that maximize E_x while minimize α_x. There are 9 candidate designs $[\pm 19.1]_S$, $[\pm 16.8]_S$, $[\pm 15.8]_S$, $[\pm 13.8]_S$, $[\pm 10.0]_S$, $[\pm 9.6]_S$, $[\pm 7.0]_S$, $[\pm 5.9]_S$, and $[0_4]$ in the Pareto set which are better than conventional designs. It should be noted that remaining 4 solutions in the Pareto set of model problem 14 are better from results of $[\pm 45]_S$ and $[0/90]_S$ for only minimization of α_x but not appropriate for maximization of E_x. Model problem 15 devoted to maximization of E_y and minimization of α_y simultaneously. 12 candidate solutions have been obtained by using the solver *gamultiobj* and 7 different designs $[\pm 72.9]_S$, $[\pm 74.6]_S$, $[\pm 75.1]_S$, $[\pm 76.6]_S$, $[\pm 78.4]_S$, $[\pm 81.6]_S$, $[90_4]$ have been found better than the conventional designs. In Figure 7.12, variations of Young's moduli E_x, E_y with θ_1 for 4 layered $[\theta_1/-\theta_1]_S$ carbon/epoxy laminated composites can be seen. Although the distributions of Young's moduli for carbon/epoxy are different from E-glass/epoxy, maximum values of them occur for the same fiber orientation angles (0° and 90°). Figures 7.13-7.14 show variations of coefficients of thermal expansion α_x, α_y and coefficients of moisture expansions β_x, β_y with the fiber orientation angle θ_1 for $[\theta_1/-\theta_1]_S$ carbon/epoxy laminated composites. It should be noted that the behavior of moisture expansion coefficients and thermal expansion coefficients are the same. However, resulting fiber orientation angels automatically minimize the coefficient of moisture expansion (CME) and this gives an important advantage for the materials especially used in satellite structures.

Table 7.2. Optimizations of 4 layered $[\theta_1/-\theta_1]_S$ carbon/epoxy laminated composite.

Problem No	Optimization	Stack	E_x (GPa)	E_y (GPa)	α_x ($10^{-6}/^{\circ}C$)	α_y ($10^{-6}/^{\circ}C$)
9	**Min α_x**	$[\pm 32]_S$	40.78	8.05	-5.24	11.66
10	**Min α_y**	$[\pm 58]_S$	8.05	40.78	11.66	-5.24
11	**Max E_x**	$[0_4]$	277.27	7.05	-1.00	22.42
12	**Max E_y**	$[90_4]$	7.05	277.27	22.42	-1.00
13	**Min α_x Min α_y**	$[\pm 32]_S$	40.78	8.05	-5.24	11.66
		$[\pm 38.8]_S$	21.15	9.75	-4.01	5.38
		$[\pm 41.4]_S$	17.10	10.91	-2.75	2.89
		$[\pm 43.1]_S$	15.10	11.91	-1.65	1.31
		$[\pm 45.2]_S$	13.15	13.48	-0.07	-0.44
		$[\pm 47.8]_S$	11.35	16.10	2.17	-2.28
		$[\pm 49.3]_S$	10.56	18.06	3.54	-3.12
		$[\pm 50.6]_S$	9.98	20.09	4.78	-3.75
		$[\pm 52.6]_S$	9.27	23.95	6.70	-4.48
		$[\pm 58]_S$	8.05	40.78	11.66	-5.24
14	**Max E_x Min α_x**	$[0_4]$	277.3	7.05	-1.00	22.42
		$[\pm 5.9]_S$	268.80	7.05	-1.23	22.17
		$[\pm 7.0]_S$	264.90	7.05	-1.32	22.07
		$[\pm 9.6]_S$	251.70	7.06	-1.60	21.74
		$[\pm 10.0]_S$	249.07	7.06	-1.65	21.68
		$[\pm 13.8]_S$	215.88	7.08	-2.22	20.95
		$[\pm 15.8]_S$	192.46	7.09	-2.58	20.43
		$[\pm 16.8]_S$	179.72	7.11	-2.78	20.14
		$[\pm 19.1]_S$	152.02	7.15	-3.23	19.36
		$[\pm 21.8]_S$	118.50	7.22	-3.81	18.25
		$[\pm 23.1]_S$	104.46	7.27	-4.08	17.63
		$[\pm 25.1]_S$	85.40	7.37	-4.46	16.55
		$[\pm 32]_S$	40.78	8.05	-5.24	11.66

(cont. on next page)

Table 7.2 (cont.)

15	**Max E_y Min α_y**	$[\pm 58]_S$	8.05	40.78	11.66	-5.24
		$[\pm 62.2]_S$	7.56	64.18	14.86	-4.90
		$[\pm 63.2]_S$	7.48	70.86	15.52	-4.77
		$[\pm 67.1]_S$	7.26	106.65	17.73	-4.04
		$[\pm 69.6]_S$	7.18	135.55	18.86	-3.51
		$[\pm 72.9]_S$	7.11	175.75	20.05	-2.85
		$[\pm 74.6]_S$	7.09	197.81	20.54	-2.50
		$[\pm 75.1]_S$	7.08	202.76	20.68	-2.42
		$[\pm 76.6]_S$	7.07	219.56	21.04	-2.16
		$[\pm 78.4]_S$	7.06	236.33	21.41	-1.88
		$[\pm 81.6]_S$	7.06	258.77	21.91	-1.46
		$[90_4]$	7.05	277.3	22.42	-1.00
16	**Max E_x Max E_y Min α_x**	$[0_4]$	277.3	7.05	-1.00	22.42
		$[\pm 15.4]_S$	197.58	7.09	-2.50	20.54
		$[\pm 19.0]_S$	152.52	7.14	-3.22	19.40
		$[\pm 21.4]_S$	122.95	7.21	-3.73	18.43
		$[\pm 23.3]_S$	102.35	7.28	-4.12	17.53
		$[\pm 32]_S$	40.78	8.06	-5.24	11.66
		$[\pm 47.3]_S$	11.66	15.51	1.68	-1.94
		$[\pm 52.6_S$	9.26	24.03	6.76	-4.49
		$[\pm 57.3]_S$	8.17	37.76	11.03	-5.23
		$[\pm 73.5]_S$	7.10	184.46	20.24	-2.72
		$[\pm 77.5]_S$	7.07	228.26	21.23	-2.01
		$[\pm 84.2]_S$	7.05	269.19	22.18	-1.22
		$[\pm 86.4]_S$	7.05	274.38	22.33	-1.08
		$[90_4]$	7.05	277.3	22.42	-1.00
	Conventional Designs	**$[\pm 45]_S$**	**13.31**	**13.31**	**-0.26**	**-0.26**
		$[0/90]_S$	**142.43**	**142.43**	**-0.26**	**-0.26**

Therefore, it is sufficient to minimize the CTE only and not necessary to solve a new optimization problem in order to minimize the CME of the laminated composites (Aydin & Artem 2009).

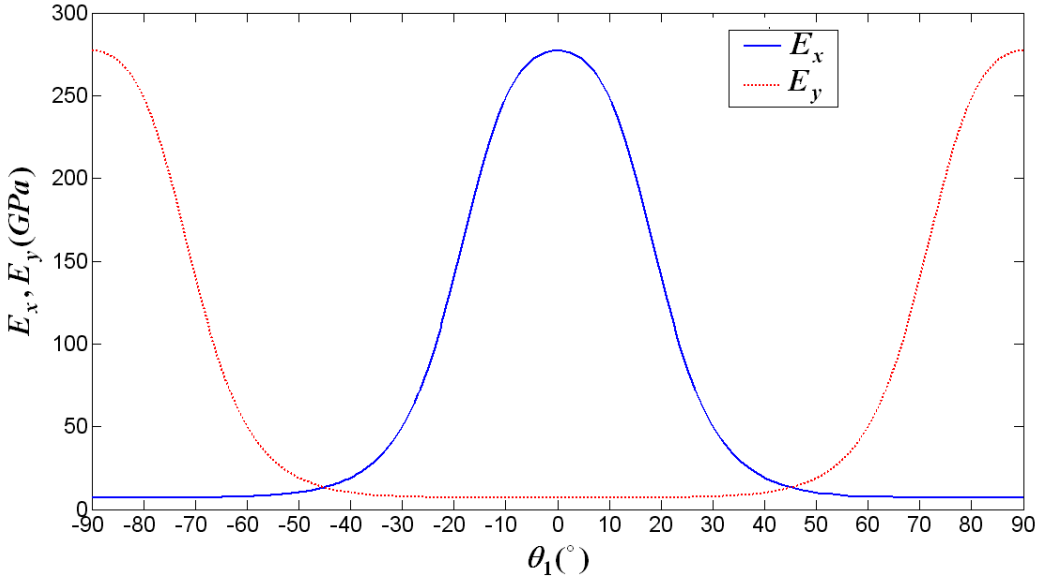

Figure 7.12. Variation of Young's Moduli with θ_1 for 4 layered symmetric balanced $[\theta_1/-\theta_1]_S$ carbon/epoxy laminated composites.

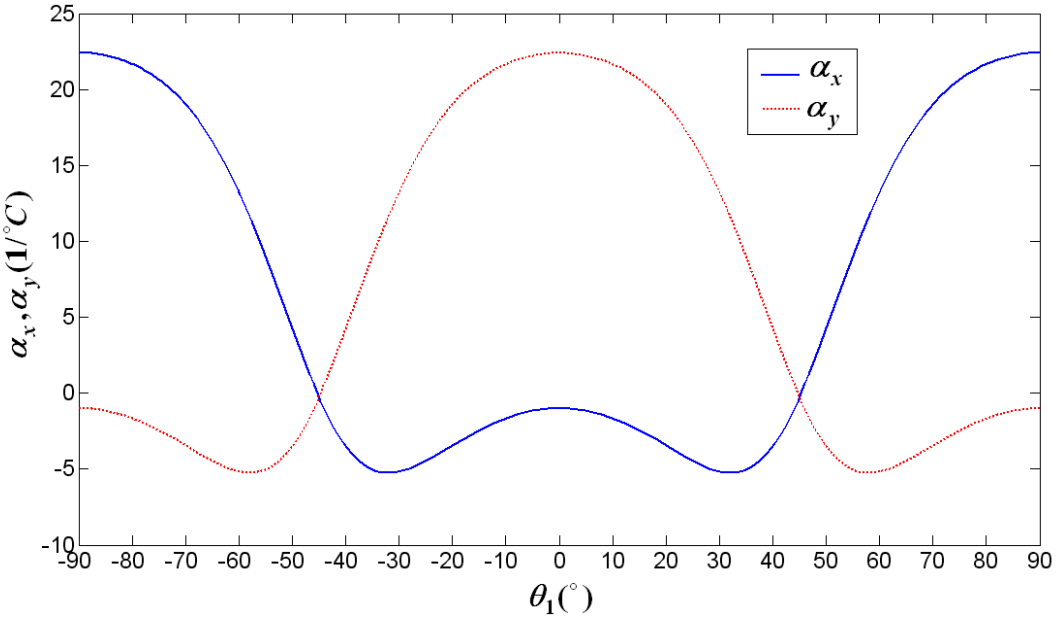

Figure 7.13. Variation of CTEs with θ_1 for 4 layered symmetric balanced $[\theta_1/-\theta_1]_S$ carbon/epoxy laminated composites.

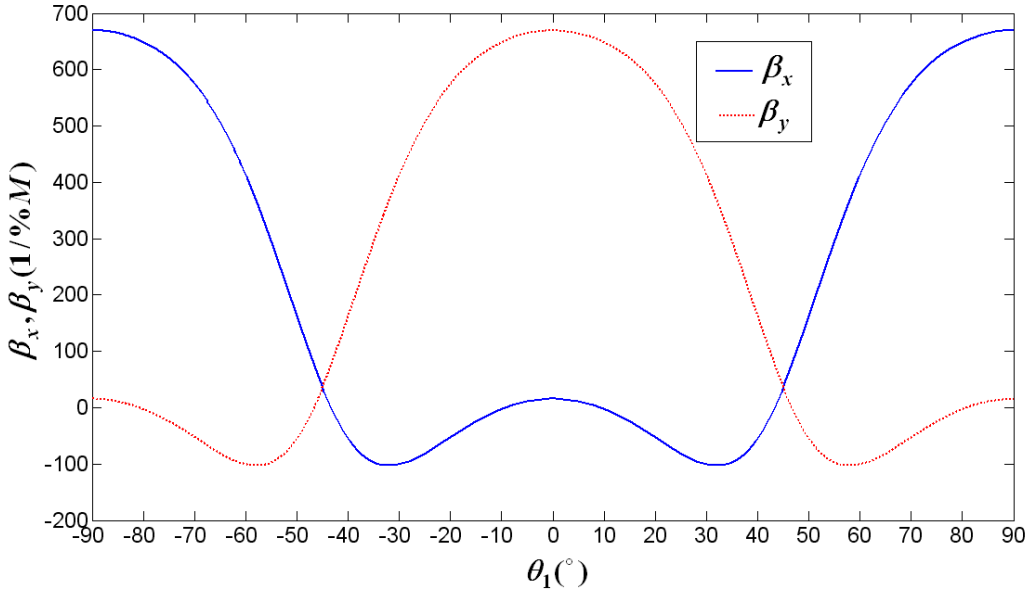

Figure 7.14. Variation of CME with θ_1 for 4 layered symmetric balanced $[\theta_1/-\theta_1]_S$ carbon/epoxy laminated composites.

Multi-objective GA and single-objective GA optimization results for 8 layered $[\pm\theta_1/\pm\theta_2]_S$ E-glass/epoxy laminated composites are given in Table 7.3. As in the optimization for $[\theta_1/-\theta_1]_S$ E-glass/epoxy, It can be seen from the table, 27.3° and 62.7° are appropriate fiber orientation angles of the composite for coefficient of thermal expansion in *x* and *y* directions, respectively. It can be observed that max E_x and E_y values as expected are obtained in 0° and 90°, respectively (see model problems 19 and 20). Selected Pareto optimum designs of α_x-α_y, E_x-α_x, E_y-α_y, and E_x-E_y-α_x are listed in Table 7.3 as model problems 21, 22, 23 and 24, respectively. As it can be seen from results of model problem 22, Pareto set varies between the stacks $[0_8]$ and $[\pm 18.4/\pm 21.7]_S$ Comparing the set of solution with conventional designs, 11 different solutions $[0_8]$, $[\pm 1.4/\pm 8.9]_S$, $[\pm 6.7/\pm 9.0]_S$, $[\pm 9.4/\pm 9.3]_S$, $[\pm 10.0/\pm 15.4]_S$, $[\pm 16.5/\pm 15.4]_S$, $[\pm 14.2/\pm 18.9]_S$, $[\pm 14.5/\pm 20.3]_S$, $[\pm 12.5/\pm 23.2]_S$, $[\pm 15.1/\pm 22.6]_S$, $[\pm 16.1/\pm 22.7]_S$ have been obtained which are better than designs $[\pm 45/\pm 45]_S$ and $[0/90/0/90]_S$. In model problem 23, a multi-objective optimization problem for material parameters E_y-α_y is investigated. After optimization process, 8 different designs $[\pm 71.4/\pm 70.7]_S$, $[\pm 72.4/\pm 71.2]_S$, $[\pm 71.0/\pm 76.9]_S$, $[\pm 78.0/\pm 73.2]_S$, $[\pm 73.1/\pm$

81.0]$_S$, [± 75.4/± 83.4]$_S$, [± 84.5/± 78.0]$_S$, and [± 86.7/± 87.2]$_S$ have been produced better than conventional designs [± 45/± 45]$_S$ and [0/90/0/90]$_S$.

Effect of fiber orientation angle θ_2 on the stiffness characteristics and thermal expansion coefficients for E-glass/epoxy and carbon/epoxy composites can be seen in the Figures 7.15-7.22. Symmetric distributions have been obtained in all cases for both E-glass/epoxy and carbon/epoxy composites. According to variations given in Figure 7.15, E_x values for E-glass/epoxy approximately are in the interval 6-22 GPa. It can be seen from Figures 7.17 and 7.18, for E-glass/epoxy composite, minimum CTE values occur approximately in the θ_1 value intervals $(25^\circ, 35^\circ)$ and $(55^\circ, 65^\circ)$ respectively. Similarly, according to variations for carbon/epoxy composite given in Figures 7.19-7.22, E_x and α_x values approximately are in the intervals (10, 280) GPa and (-5.5, 24)$10^{-6}/^\circ C$. It can be seen from Figures 7.21 and 7.22 for carbon/epoxy composite, minimum CTE values occur approximately in the θ_1 value intervals $(25^\circ, 35^\circ)$ and $(55^\circ, 65^\circ)$, respectively. It should be noted that in order to change the fiber orientation, design types (e.g., $[\theta_1/\theta_2/-\theta_1/-\theta_2]_S$ instead of $[\pm\theta_1/\pm\theta_2]_S$ for 8 layered composites) did not effect the optimum results of single-objective optimizations for α_x or E_x (see model problems 25-28, 41-44 and 49-52 in Tables 7.4, 7.6 and 7.7, respectively). Multi and single-objective GA optimization results for 8 layered symmetric balanced $[0/\pm\theta_1/0]_S$ E-glass/epoxy and carbon/epoxy laminated composites are given in Tables 7.5. and 7.8, respectively.

Table 7.3 Optimizations of 8 layered $[\pm\theta_1/\pm\theta_2]_S$ E-glass/epoxy laminated composite.

Problem No	Optimization	Stack	E_x (GPa)	E_y (GPa)	α_x ($10^{-6}/^{\circ}C$)	α_y ($10^{-6}/^{\circ}C$)
17	**Min α_x**	$[\pm 27.3/\pm 27.3]_S$	13.17	8.33	8.61	28.00
18	**Min α_y**	$[\pm 62.7/\pm 62.7]_S$	8.33	13.17	28.00	8.61
19	**Max E_x**	$[0_8]$	22.20	11.50	10.02	28.41
20	**Max E_y**	$[90_8]$	11.50	22.20	28.41	10.02
21	**Min α_x Min α_y**	$[\pm 62.7/\pm 62.7]_S$	8.33	13.17	28.00	8.61
		$[\pm 56.5/\pm 58.3]_S$	7.41	10.49	26.48	9.08
		$[\pm 53.6/\pm 53.5]_S$	6.87	8.83	24.45	10.29
		$[\pm 47.9/\pm 54.4]_S$	6.82	8.18	22.46	11.79
		$[\pm 55.8/\pm 45.9]_S$	7.00	8.31	22.05	12.13
		$[\pm 56.6/\pm 41.8]_S$	7.41	8.36	20.28	13.63
		$[\pm 42.9/\pm 49.6]_S$	6.85	7.11	18.00	15.69
		$[\pm 27.2/\pm 61.8]_S$	10.86	10.74	16.60	17.07
		$[\pm 20.5/\pm 61.7]_S$	12.48	11.56	15.47	18.27
		$[\pm 55.6/\pm 20.8]_S$	11.86	10.21	14.00	19.96
		$[\pm 31.8/\pm 39.1]_S$	9.40	7.15	10.10	24.79
		$[\pm 23.1/\pm 31.8]_S$	13.18	8.41	8.79	27.66
		$[\pm 27.3/\pm 27.3]_S$	13.17	8.33	8.61	28.00
22	**Max E_x Min α_x**	$[\pm 18.4/\pm 21.7]_S$	16.93	9.66	9.00	28.53
		$[\pm 16.1/\pm 22.7]_S$	17.22	9.77	9.07	28.49
		$[\pm 15.1/\pm 22.6]_S$	17.46	9.86	9.12	28.48
		$[\pm 12.5/\pm 23.2]_S$	17.81	10.00	9.21	28.43
		$[\pm 14.5/\pm 20.3]_S$	18.14	10.08	9.22	28.54
		$[\pm 14.2/\pm 18.9]_S$	18.51	10.21	9.28	28.55
		$[\pm 16.5/\pm 15.4]_S$	18.81	10.30	9.33	28.57
		$[\pm 10.0/\pm 15.4]_S$	19.94	10.71	9.56	28.53
		$[\pm 9.4/\pm 9.3]_S$	21.01	11.08	9.77	28.49
		$[\pm 6.7/\pm 9.0]_S$	21.34	11.20	9.84	28.47
		$[\pm 1.4/\pm 8.9]_S$	21.66	11.31	9.91	28.44
		$[0_8]$	22.20	11.50	10.02	28.41

(cont. on next page)

Table 7.3 (cont.)

23	**Max E_y Min α_y**	$[\pm 62.7/\pm 62.7]_S$	8.33	13.17	28.00	8.61
		$[\pm 65.5/\pm 65.8]_S$	8.89	14.75	28.33	8.69
		$[\pm 69.4/\pm 65.9]_S$	9.26	15.79	28.44	8.83
		$[\pm 70.9/\pm 66.7]_S$	9.46	16.39	28.48	8.92
		$[\pm 67.9/\pm 71.6]_S$	9.63	16.85	28.52	8.99
		$[\pm 71.4/\pm 70.7]_S$	9.84	17.49	28.57	9.08
		$[\pm 72.4/\pm 71.2]_S$	9.96	17.82	28.57	9.14
		$[\pm 71.0/\pm 76.9]_S$	10.28	18.71	28.54	9.32
		$[\pm 78.0/\pm 73.2]_S$	10.51	19.36	28.55	9.45
		$[\pm 73.1/\pm 81.0]_S$	10.66	19.77	28.51	9.53
		$[\pm 75.4/\pm 83.4]_S$	10.91	20.50	28.49	9.67
		$[\pm 84.5/\pm 78.0]_S$	11.09	21.03	28.48	9.78
		$[\pm 86.7/\pm 87.2]_S$	11.45	22.07	28.42	9.99
24	**Max E_x Max E_y Min α_x**	$[0_8]$	22.20	11.50	10.02	28.41
		$[90/0/90/0]_S$	16.95	16.95	16.83	16.83
		$[\pm 64.1/\pm 2.8]_S$	15.35	13.46	14.92	18.93
		$[\pm 56.9/\pm 6.3]_S$	14.57	11.83	13.61	20.57
		$[\pm 27.3/\pm 27.3]_S$	13.17	8.33	8.61	28.00
		$[90/90/90/90]_S$	11.50	22.20	28.41	10.02
		$[\pm 67.2/\pm 85.6]_S$	10.43	18.92	28.34	9.46
		$[\pm 88.8/\pm 58.3]_S$	10.00	16.95	27.54	9.51
		$[\pm 78.2/\pm 63.2]_S$	9.79	17.02	28.20	9.18
	Conventional Designs	**$[\pm 45/\pm 45]_S$**	**6.76**	**6.76**	**16.83**	**16.83**
		$[0/90/0/90]_S$	**16.95**	**16.95**	**16.83**	**16.83**

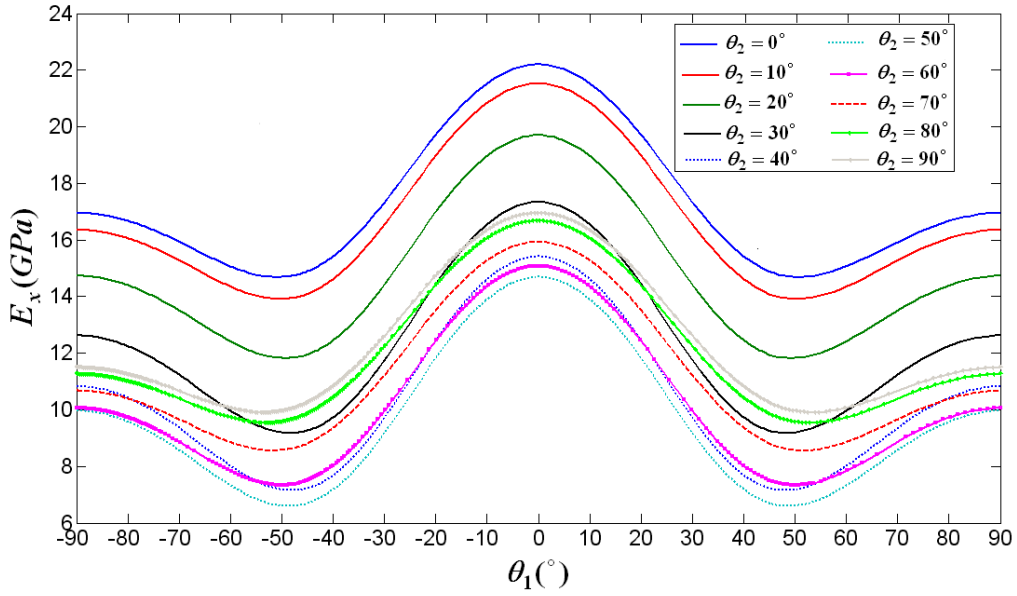

Figure 7.15. Variation of Young's Modulus E_x with θ_1 and θ_2 for 8 layered symmetric balanced $[\pm\theta_1/\pm\theta_2]_S$ E-glass/epoxy laminated composites.

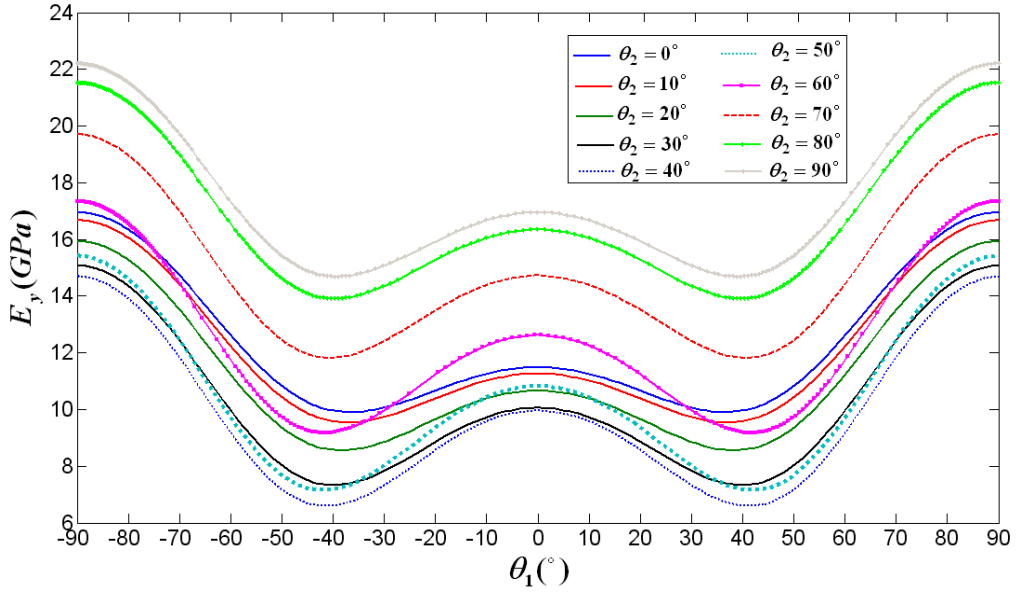

Figure 7.16. Variation of Young's Modulus E_y with θ_1 and θ_2 for 8 layered symmetric balanced $[\pm\theta_1/\pm\theta_2]_S$ E-glass/epoxy laminated composites.

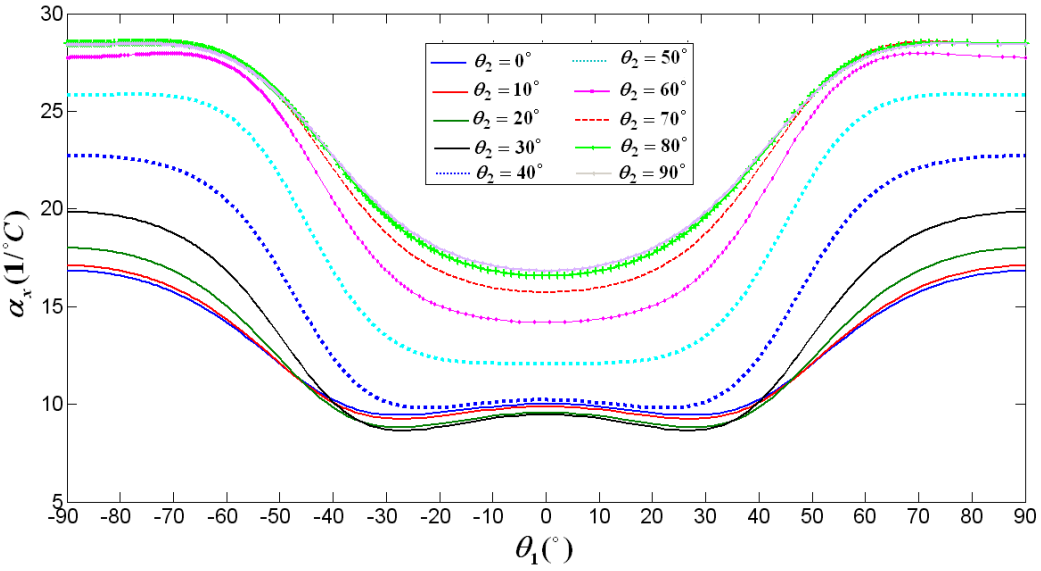

Figure 7.17. Variation of CTE α_x with θ_1 and θ_2 for 8 layered symmetric balanced $[\pm\theta_1/\pm\theta_2]_S$ E-glass/epoxy laminated composites.

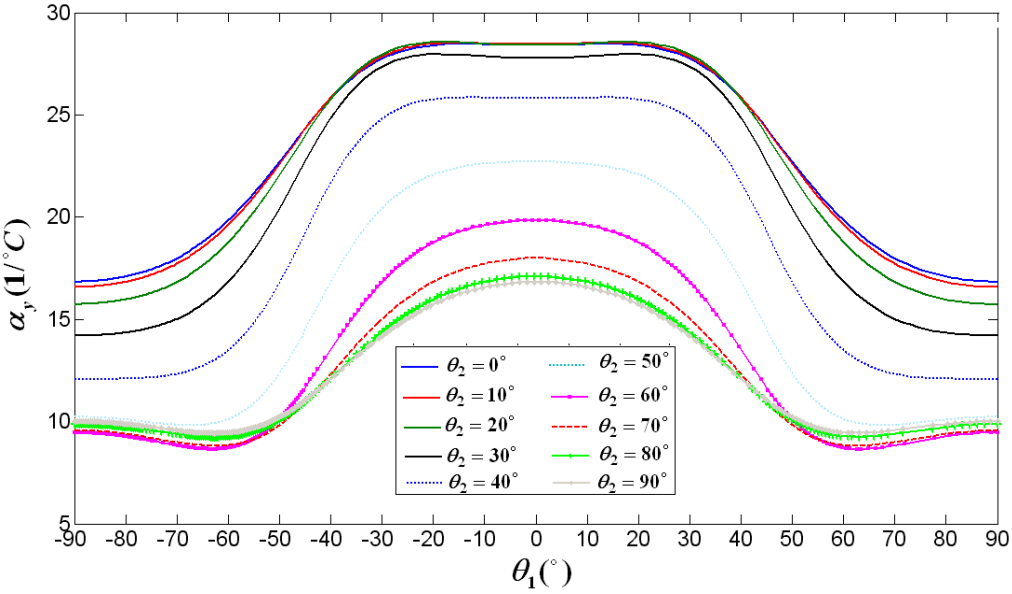

Figure 7.18. Variation of CTE α_y with θ_1 and θ_2 for 8 layered symmetric balanced $[\pm\theta_1/\pm\theta_2]_S$ E-glass/epoxy laminated composites.

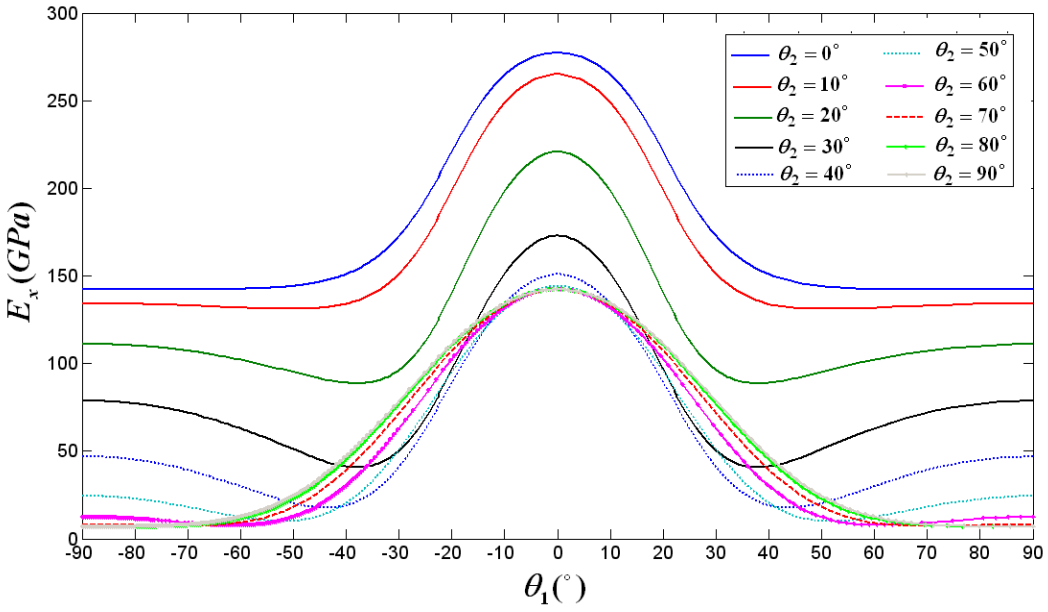

Figure 7.19. Variation of Young's Modulus E_x with θ_1 and θ_2 for 8 layered symmetric balanced $[\pm\theta_1/\pm\theta_2]_S$ carbon/epoxy laminated composites.

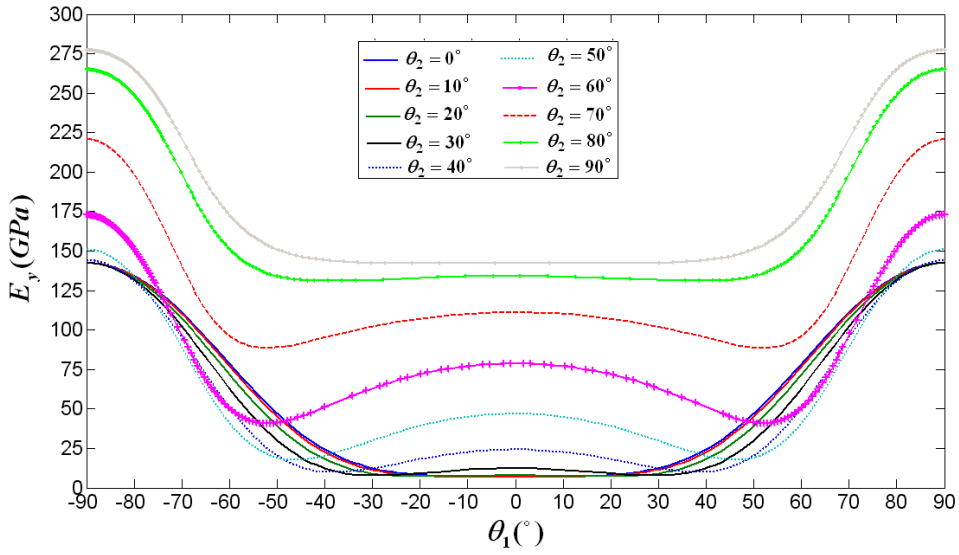

Figure 7.20. Variation of Young's Modulus E_y with θ_1 and θ_2 for 8 layered symmetric balanced $[\pm\theta_1/\pm\theta_2]_S$ carbon/epoxy laminated composites.

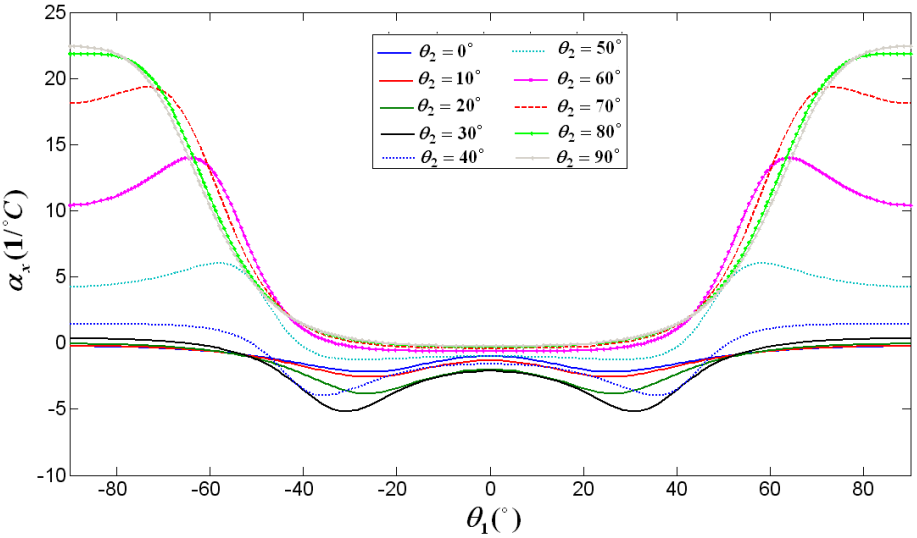

Figure 7.21. Variation of CTE α_x with θ_1 and θ_2 for 8 layered symmetric balanced $[\pm\theta_1/\pm\theta_2]_S$ carbon/epoxy laminated composites.

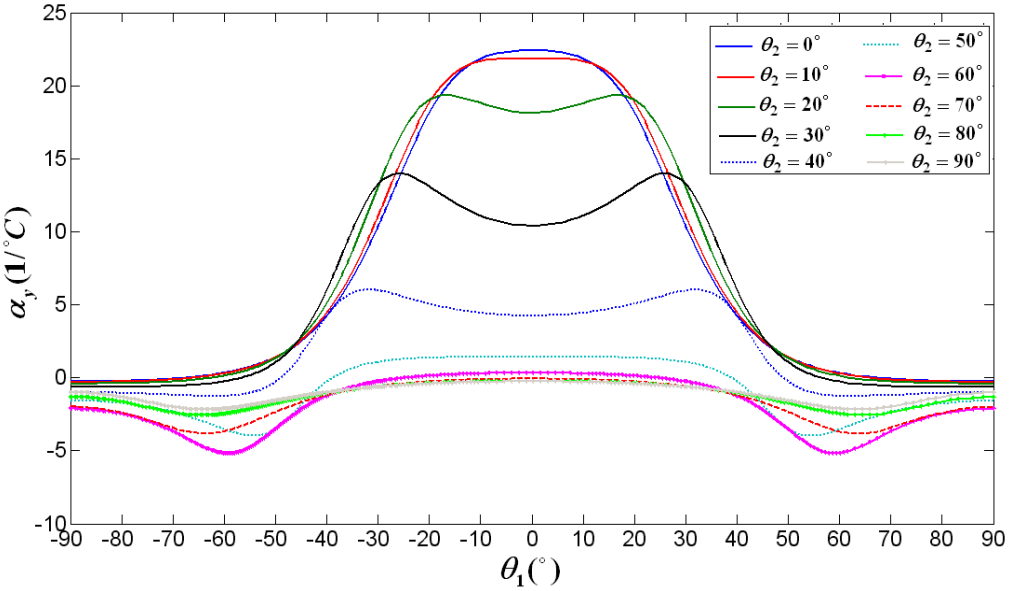

Figure 7.22. Variation of CTE α_y with θ_1 and θ_2 for 8 layered symmetric balanced $[\pm\theta_1/\pm\theta_2]_S$ carbon/epoxy laminated composites.

Table 7.4. Multi-objective GA and single-objective GA optimization results for 8 layered symmetric balanced $[\theta_1/\theta_2/-\theta_1/-\theta_2]_S$ E-glass/epoxy laminated composites.

Problem No	Opt.	Stack	E_x (GPa)	E_y (GPa)	α_x ($10^{-6}/^{\circ}C$)	α_y ($10^{-6}/^{\circ}C$)
25	**Min α_x**	$[27.3/27.3/-27.3/-27.3]_S$	13.17	8.33	8.61	28.00
26	**Min α_y**	$[62.7/62.7/-62.7/-62.7]_S$	8.33	13.17	28.00	8.61
27	**Max E_x**	$[0_8]$	22.20	11.50	10.02	28.41
28	**Max E_y**	$[90_8]$	11.50	22.20	28.41	10.02
29	**Min α_x Min α_y**	$[27.3/27.3/-27.3/-27.3]_S$	13.17	8.33	8.61	28.00
		$[-31.6/33/31.6/33]_S$	10.62	7.45	9.02	26.60
		$[-36.1/35/36.1/35]_S$	9.19	6.98	9.92	25.01
		$[-40.1/35.4/40.1/-35.4]_S$	8.45	6.82	10.82	23.73
		$[-40.2/35.4/40.2/-35.4]_S$	8.44	6.82	11.08	23.37
		$[-41.6/36.3/41.6/36.3]_S$	8.10	6.76	11.78	22.46
		$[-43.6/34.8/43.6/34.8]_S$	8.21	6.93	12.14	22.04
		$[-45.2/35.9/45.2/35.9]_S$	7.90	6.93	13.07	20.90
		$[-45.6/38/45.6/38]_S$	7.05	6.82	13.97	19.86
		$[-47/37.8/47/-37.8]_S$	7.50	6.94	14.54	19.23
		$[-47.1/38.9/47.1/38.9]_S$	7.32	6.89	14.98	18.75
		$[-47.9/39/47.9/39]_S$	7.30	7.00	15.40	18.30
30	**Max E_x Min α_x**	$[0_8]$	22.20	11.50	10.02	28.41
		$[4/13.3/-4/13.3]_S$	20.92	11.06	9.76	28.47
		$[17.7/2.7/-17.7/-2.7]_S$	20.14	10.81	9.63	28.45
		$[13.2/17.1/-13.2/17.1]_S$	19.10	10.41	9.39	28.56
		$[19.6/15.1/-19.6/-15.1]_S$	18.18	10.09	9.22	28.55
		$[15.8/23.7/-15.8/-23.7]_S$	17.02	9.72	9.05	28.45
		$[21.4/23.7/-21.4/-23.7]_S$	15.69	9.22	8.81	28.44
		$[21.4/27.3/-21.4/-27.3]_S$	14.74	8.91	8.75	28.23
		$[24.3/27.1/-24.3/-27.1]_S$	14.02	8.64	8.65	28.16
		$[27.3/\ 27.3/-27.3/-27.3]_S$	13.17	8.33	8.61	28.00

(cont. on next page)

Table 7.4. (cont.)

31	**Max E_y Min α_y**	$[62.7/62.7/-62.7/-62.7]_S$	8.33	13.16	27.96	8.61
		$[65.6/65.8/-65.6/-65.8]_S$	8.89	14.78	28.33	8.70
		$[66.3/70.2/-66.3/-70.2]_S$	9.37	16.10	28.46	8.88
		$[67.8/72.4/-67.8/-72.4]_S$	9.69	17.02	28.52	9.02
		$[69/74.4/-69/-74.4]_S$	9.94	17.74	28.53	9.15
		$[68.4/78.2/-68.4/-78.2]_S$	10.17	18.29	28.47	9.28
		$[70.2/79.8/-70.2/-79.8]_S$	10.40	18.99	28.49	9.40
		$[70.9/83/-70.9/-83]_S$	10.60	19.54	28.47	9.51
		$[73/85.9/-73/-85.9]_S$	10.83	20.21	28.47	9.63
		$[79.4/83.9/-79.4/-83.9]_S$	11.14	21.18	28.48	9.81
		$[90_8]$	11.50	22.20	28.41	10.02
32	**Max E_x Max E_y Min α_x**	$[-84.4/-60.2/84.4/60.2]_S$	9.97	17.14	27.82	9.40
		$[-90/-58.3/90/58.3]_S$	10.00	16.95	27.53	9.51
		$[90_8]$	11.50	22.20	28.41	10.02
		$[\pm 27.3/\pm 27.3]_S$	13.17	8.33	8.61	28.00
		$[1/-66.3/-1/66.3]_S$	15.60	13.97	15.26	18.55
		$[0/90/0/90]_S$	16.95	16.95	16.83	16.83
		$[3/-27.9/-3/27.9]_S$	17.76	10.14	9.42	28.00
		$[-7.6/-1.3/7.6/1.3]_S$	21.79	11.36	9.93	28.44
		$[0_8]$	22.20	11.50	10.02	28.41
	Conventional Designs	**$[\pm 45/\pm 45]_S$**	**6.76**	**6.76**	**16.83**	**16.83**
		$[0/90/0/90]_S$	**16.95**	**16.95**	**16.83**	**16.83**

Table 7.5. Multi-objective GA and single-objective GA optimization results for 8 layered symmetric balanced $[0/\pm\theta_1/0]_S$ E-glass/epoxy laminated composites.

Problem No	Optimization	Stack	E_x (GPa)	E_y (GPa)	α_x ($10^{-6}/^{\circ}C$)	α_y ($10^{-6}/^{\circ}C$)
33	**Min α_x**	$[0/\pm27.3/0]_S$	17.98	10.20	9.43	28.04
34	**Min α_y**	$[0/90/90/0]_S$	16.95	16.95	16.83	16.83
35	**Max E_x**	$[0_8]$	22.20	11.50	10.02	28.41
36	**Max E_y**	$[0/90/90/0]_S$	16.95	16.95	16.83	16.83
37	**Min α_x Min α_y**	$[0/\pm27.3/0]_S$	17.98	10.20	9.43	28.04
		$[0/\pm36.6/0]_S$	15.96	9.90	9.83	26.64
		$[0/\pm48.7/0]_S$	14.71	10.65	11.79	23.15
		$[0/\pm54.3/0]_S$	14.75	11.51	13.01	21.39
		$[0/\pm55.6/0]_S$	14.80	11.75	13.29	21.01
		$[0/\pm60.6/0]_S$	15.12	12.75	14.30	19.70
		$[0/\pm61.8/0]_S$	15.21	13.00	14.52	19.43
		$[0/\pm69.2/0]_S$	15.87	14.57	15.64	18.10
		$[0/90/90/0]_S$	16.95	16.95	16.83	16.83
38	**Max E_x Min α_x**	$[0/\pm27.3/0]_S$	17.98	10.20	9.43	28.04
		$[0/\pm25.7/0]_S$	18.36	10.30	9.44	28.16
		$[0/\pm24/0]_S$	18.77	10.40	9.47	28.26
		$[0/\pm22.8/0]_S$	19.06	10.48	9.49	28.32
		$[0/\pm21.1/0]_S$	19.45	10.60	9.53	28.38
		$[0/\pm20.2/0]_S$	19.66	10.67	9.56	28.40
		$[0/\pm18.4/0]_S$	20.05	10.78	9.62	28.44
		$[0/\pm15.5/0]_S$	20.64	10.97	9.71	28.46
		$[0/\pm13.8/0]_S$	20.95	11.07	9.77	28.46
		$[0/\pm10.4/0]_S$	21.48	11.25	9.87	28.45
		$[0/\pm4.7/0]_S$	22.05	11.45	9.99	28.42

(cont. on next page)

Table 7.5. (cont.)

39	**Max E_y Min α_y**	-	-	-	-	-
		-	-	-	-	-
		-	-	-	-	-
		-	-	-	-	-
		-	-	-	-	-
		-	-	-	-	-
		-	-	-	-	-
		-	-	-	-	-
		-	-	-	-	-
		-	-	-	-	-
		-	-	-	-	-
40	**Max E_x Max E_y Min α_x**	$[0_8]$	22.20	11.50	10.02	28.41
		$[0/\pm11.6/0]_S$	21.30	11.19	9.84	28.46
		$[0/\pm22/0]_S$	19.24	10.54	9.51	28.35
		$[0/\pm27.3/0]_S$	17.98	10.20	9.43	28.04
		$[0/90/90/0]_S$	16.95	16.95	16.83	16.83
		$[0/\pm80.3/0]_S$	16.69	16.39	16.59	17.08
		$[0/\pm73/0]_S$	16.19	15.29	16.05	17.64
		$[0/\pm68.2/0]_S$	15.78	14.36	15.51	18.25
		$[0/\pm60.8/0]_S$	15.13	12.79	14.34	19.65
		$[0/\pm54.2/0]_S$	14.75	11.50	13.00	21.42
	Conventional Designs	**$[\pm 45/\pm 45]_S$**	**6.76**	**6.76**	**16.83**	**16.83**
		$[0/90/0/90]_S$	**16.95**	**16.95**	**16.83**	**16.83**

Table 7.6. Optimizations of $[\pm\theta_1/\pm\theta_2]_S$ 8 layered carbon/epoxy laminated composite.

Problem No	Optimization	Stack	E_x (GPa)	E_y (GPa)	α_x ($10^{-6}/^{\circ}C$)	α_y ($10^{-6}/^{\circ}C$)
41	**Min α_x**	$[\pm 32/\pm 32]_S$	40.78	8.05	-5.24	11.66
42	**Min α_y**	$[\pm 58/\pm 58]_S$	8.05	40.78	11.66	-5.24
43	**Max E_x**	$[0_8]$	277.3	7.05	-1.00	22.42
44	**Max E_y**	$[90_8]$	7.05	277.3	22.42	-1.00
45	**Min α_x Min α_y**	$[\pm 32/\pm 32]_S$	40.78	8.05	-5.24	11.66
		$[\pm 34.5/\pm 36.6]_S$	29.02	8.93	-4.84	8.30
		$[\pm 35.6/\pm 39.0]_S$	25.43	9.76	-4.28	6.43
		$[\pm 36.1/\pm 41.2]_S$	24.08	10.99	-3.58	4.78
		$[\pm 38.4/\pm 42.6]_S$	20.01	11.45	-2.95	3.35
		$[\pm 43.8/\pm 41.3]_S$	16.23	11.96	-1.99	1.77
		$[\pm 41.8/\pm 51.8]_S$	18.42	22.85	0.66	-1.08
		$[\pm 50.2/\pm 46.2]_S$	12.10	17.99	2.27	-2.32
		$[\pm 57.1/\pm 49.6]_S$	11.48	31.79	5.68	-3.70
		$[\pm 58/\pm 58]_S$	8.05	40.78	11.66	-5.24
46	**Max E_x Min α_x**	$[\pm 25.9/\pm 19]_S$	115.9	7.91	-3.66	16.29
		$[\pm 24.6/\pm 18]_S$	127.6	7.75	-3.49	17.05
		$[\pm 20/\pm 18]_S$	152.7	7.18	-3.21	19.28
		$[\pm 14.9/\pm 20.5]_S$	169.4	7.38	-2.89	19.06
		$[\pm 13.8/\pm 18.5]_S$	188.0	7.25	-2.63	19.85
		$[\pm 20.6/\pm 10.2]_S$	194.2	7.77	-2.44	18.50
		$[\pm 4.7/\pm 21.6]_S$	206.9	8.38	-2.16	17.25
		$[\pm 19.5/\pm 2.6]_S$	222.1	7.98	-1.99	18.48
		$[\pm 8.1/\pm 13.7]_S$	239.9	7.16	-1.80	21.17

(cont. on next page)

Table 7.6. (cont.)

47	**Max E_y Min α_y**	$[\pm 88.2/\pm 88.1]_S$	7.05	276.55	22.40	-1.02
		$[\pm 85.5/\pm 72.8]_S$	7.56	231.79	19.80	-1.90
		$[\pm 69.7/\pm 85.8]_S$	8.09	215.44	18.08	-2.08
		$[\pm 67.1/\pm 80.9]_S$	8.40	186.29	16.81	-2.45
		$[\pm 69.6/\pm 74.2]_S$	7.31	164.16	19.16	-2.99
		$[\pm 71.3/\pm 68.6]_S$	7.25	139.57	18.77	-3.41
		$[\pm 67.7/\pm 68.4]_S$	7.23	117.18	18.16	-3.83
		$[\pm 67.1/\pm 63.5]_S$	7.57	90.25	16.24	-4.28
		$[\pm 60.7/\pm 57.8]_S$	8.12	47.89	12.27	-5.05
		$[\pm 58/\pm 58]_S$	8.05	40.63	11.66	-5.24
48	**Max E_x Max E_y Min α_x**	$[\pm 13/\pm 26.5]_S$	149,5	9,1	-2,90	14.63
		$[\pm 1.2/\pm 34.7]_S$	159,5	16,9	-1,90	7.05
		$[\pm 6.5/\pm 31.2]_S$	159,8	13,0	-2,21	9.75
		$[\pm 15.5/\pm 21.2]_S$	161,3	7,4	-3,00	18.77
		$[\pm 11.6/\pm 23.7]_S$	170,2	8,4	-2,69	16.61
		$[\pm 3.9/\pm 29.2]_S$	172,4	11,8	-2,20	11.15
		$[\pm 10.9/\pm 22.1]_S$	181,9	8,0	-2,57	17.64
		$[\pm 5.7/\pm 25.5]_S$	184,1	9,7	-2,31	14.35
		$[\pm 13.7/\pm 18.3]_S$	190,2	7,2	-2,60	19.92
		$[\pm 7.4/\pm 22.7]_S$	193,2	8,5	-2,34	16.73
		$[\pm 1.2/\pm 23.3]_S$	202,6	9,0	-2,15	15.82
		$[\pm 2.5/\pm 20.3]_S$	217,8	8,1	-2,04	17.99
		$[\pm 2.1/\pm 17.4]_S$	234,0	7,6	-1,85	19.61
		$[\pm 0.3/\pm 15.2]_S$	245,9	7,4	-1,67	20.54
	Conventional Designs	**$[\pm 45/\pm 45]_S$**	13.31	13.31	-0.26	-0.26
		$[0/90/0/90]_S$	142.43	142.43	-0.26	-0.26

Table 7.7. Multi-objective GA and single-objective GA optimization results for 8 layered symmetric balanced $[\theta_1/\theta_2/-\theta_1/-\theta_2]_S$ carbon/epoxy laminated composites.

Problem No	Optimization	Stack	E_x (GPa)	E_y (GPa)	α_x ($10^{-6}/^{\circ}C$)	α_y ($10^{-6}/^{\circ}C$)
49	**Min α_x**	$[32/32/-32/-32]_S$	40.78	8.05	-5.24	11.66
50	**Min α_y**	$[58/58/-58/-58]_S$	8.05	40.78	11.66	-5.24
51	**Max E_x**	$[0_8]$	277.3	7.05	-1.00	22.42
52	**Max E_y**	$[90_8]$	7.05	277.3	22.42	-1.00
53	**Min α_x Min α_y**	$[-32/-32/32/32]_S$	40.78	8.05	-5.24	11.63
		$[36.6/35.1/-36.6/-35.1]_S$	27.95	8.92	-4.83	8.12
		$[35.4/40.8/-35.4/-40.8]_S$	25.53	10.90	-3.74	5.22
		$[45.5/17.3/-45.5/-17.3]_S$	104.30	29.88	-1.52	2.52
		$[52.4/46.5/-52.4/-46.5]_S$	12.44	21.51	3.04	-2.73
		$[49.9/53.1/-49.9/-53.1]_S$	10.15	22.77	5.33	3.91
		$[56.2/51.9/-56.2/-51.9]_S$	9.62	29.54	7.42	-4.48
		$[57.7/56.5/-57.7/-56.5]_S$	8.25	37.33	10.81	-5.19
		$[58/58/-58/-58]_S$	8.05	40.78	11.63	-5.24
54	**Max E_x Min α_x**	$[32/-32/-32/32]_S$	40.58	8.05	-5.24	11.66
		$[27.2/-29.6/-27.2/29.6]_S$	60.64	7.75	-4.91	14.17
		$[23.4/-23/-23.4/23]_S$	104.00	7.28	-4.08	17.57
		$[20.7/-22.2/-20.7/22.2]_S$	122.99	7.24	-3.72	18.33
		$[18.7/-20.1/-18.7/20.1]_S$	147.64	7.17	-3.29	19.19
		$[16.5/-20.8/-16.5/20.8]_S$	157.36	7.31	-3.10	19.01
		$[17.8/-15.8/-17.8/15.8]_S$	180.49	7.14	-2.76	20.05
		$[9.8/-21.3/-9.8/21.3]_S$	191.47	7.94	-2.45	18.01
		$[1.9/-13.4/-1.9/13.4]_S$	253.10	7.26	-1.56	21.14
		$[1/-7.3/-1/7.3]_S$	270.99	7.07	-1.17	22.17
		$[0]_8$	277.27	7.05	-1.00	22.42

(cont. on next page)

Table 7.7. (cont.)

55	**Max E_y Min α_y**	$[-58/58/58/-58]_S$	8.05	40.63	11.66	-5.24
		$[-62.1/60.6/62.1/-60.6]_S$	7.69	58.51	14.16	-4.99
		$[-62.9/64.9/62.9/-64.9]_S$	7.51	77.36	15.78	-4.60
		$[-63.4/64.9/63.4/-64.9]_S$	7.46	79.21	16.01	-4.57
		$[-64.3/67.2/64.3/-67.2]_S$	7.46	94.17	16.68	-4.23
		$[-66/70.2/66/70.2]_S$	7.46	119.32	17.58	-3.73
		$[-72.5/67.2/72.5/-67.2]_S$	7.48	140.16	18.09	-3.34
		$[-74.4/67.6/74.4/-67.6]_S$	7.60	153.55	18.12	-3.10
		$[-73.9/71/73.9/71]_S$	7.19	171.34	19.69	-2.90
		$[-76.6/70.7/76.6/70.7]_S$	7.35	185.38	19.50	-2.65
		$[-83.8/80.1/83.8/-80.1]_S$	7.08	259.23	21.85	-1.45
		$[-89.6/82.7/89.6/-82.7]_S$	7.07	271.12	22.17	-1.17
		$[-89.3/85/89.3/-85]_S$	7.06	274.43	22.32	-1.08
56	**Max E_x Max E_y Min α_x**	$[0]_8$	277.27	7.05	-1.00	22.42
		$[4/3.9/-4/-3.9]_S$	273.80	7.05	-1.01	22.31
		$[19/4.1/-19/-4.1]_S$	222.65	7.85	-2.00	18.85
		$[22.5/10.9/-22.5/-10.9]_S$	180.29	8.10	-2.59	17.37
		$[-32/32/32/-32]_S$	40.61	8.06	-5.24	11.66
		$[51/82.6/-51/-82.6]_S$	21.94	142.58	4.81	-1.73
		$[58.2/85/-58.2/-85]_S$	13.73	161.96	9.17	-2.13
		$[60.8/83.9/-60.8/-83.9]_S$	11.64	167.59	11.28	-2.27
		$[79.6/70.9/-79.6/-70.9]_S$	7.52	201.93	19.34	-2.36
		$[86.7/88.8/-86.7/-88.8]_S$	7.06	275.93	22.38	-1.04
		$[86.1/86.2/-86.1/-86.2]_S$	7.05	273.96	22.32	-1.09
	Conventional Designs	**$[\pm 45/\pm 45]_S$**	**13.31**	**13.31**	**-0.26**	**-0.26**
		$[0/90/0/90]_S$	**142.43**	**142.43**	**-0.26**	**-0.26**

Table 7.8. Multi-objective GA and single-objective GA optimization results for 8 layered symmetric balanced $[0/\pm\theta_1/0]_S$ carbon/epoxy laminated composites.

Problem No	Optimization	Stack	E_x (GPa)	E_y (GPa)	α_x ($10^{-6}/^{\circ}C$)	α_y ($10^{-6}/^{\circ}C$)
57	**Min α_x**	$[0/\pm26.3/0]_S$	187.93	10.28	-2.18	13.41
58	**Min α_y**	$[0/90/90/0]_S$	142.43	142.43	-0.26	-0.26
59	**Max E_x**	$[0/0/0/0]_S$	277.27	7.05	-1.00	22.42
60	**Max E_y**	$[0/90/90/0]_S$	142.43	142.43	-0.26	-0.26
61	**Min α_x Min α_y**	$[0/\pm26.3/0]_S$	187.93	10.28	-2.18	13.41
		$[0/\pm29.6/0]_S$	174.38	12.26	-2.13	10.69
		$[0/\pm32.1/0]_S$	166.30	14.28	-2.04	8.82
		$[0/\pm35/0]_S$	159.10	17.29	-1.88	6.85
		$[0/\pm37.5/0]_S$	154.46	20.52	-1.73	5.44
		$[0/\pm40.2/0]_S$	150.75	24.75	-1.56	4.17
		$[0/\pm45.4/0]_S$	146.30	35.23	-1.24	2.41
		$[0/\pm50.4/0]_S$	144.09	48.17	-0.98	1.36
		$[0/90/90/0]_S$	142.43	142.43	-0.26	-0.26
62	**Max E_x Min α_x**	$[0/0/0/0]_S$	277.27	7.05	-1.00	22.42
		$[0/\pm7.1/0]_S$	271.55	7.07	-1.16	22.19
		$[0/\pm10.8/0]_S$	262.75	7.14	-1.36	21.72
		$[0/\pm14.1/0]_S$	250.79	7.31	-1.59	20.92
		$[0/\pm16.2/0]_S$	241.21	7.51	-1.74	20.14
		$[0/\pm18.2/0]_S$	230.81	7.78	-1.88	19.18
		$[0/\pm20.1/0]_S$	220.08	8.14	-2.00	18.06
		$[0/\pm21.7/0]_S$	211.61	8.53	-2.08	16.99
		$[0/\pm23.7/0]_S$	200.98	9.17	-2.15	15.50
		$[0/\pm24.9/0]_S$	194.60	9.63	-2.17	14.55
		$[0/\pm26.3/0]_S$	187.94	10.28	-2.18	13.41

(cont. on next page)

Table 7.8. (cont.)

63	**Max E_y Min α_y**	-	-	-	-	-
		-	-	-	-	-
		-	-	-	-	-
		-	-	-	-	-
		-	-	-	-	-
		-	-	-	-	-
		-	-	-	-	-
		-	-	-	-	-
		-	-	-	-	-
		-	-	-	-	-
		-	-	-	-	-
64	**Max E_x Max E_y Min α_x**	$[0/0/0/0]_S$	277.27	7.05	-1.00	22.42
		$[0/\pm7.1/0]_S$	271.50	7.07	-1.06	22.19
		$[0/\pm12.2/0]_S$	258.20	7.20	-1.46	21.44
		$[0/\pm14.4/0]_S$	249.55	7.33	-1.61	20.82
		$[0/\pm16.3/0]_S$	240.50	7.51	-1.75	20.09
		$[0/\pm18.6/0]_S$	228.27	7.85	-1.91	18.96
		$[0/\pm19.6/0]_S$	223.11	8.03	-1.97	18.38
		$[0/\pm21.4/0]_S$	212.84	8.46	-2.07	17.20
		$[0/\pm22.9/0]_S$	204.76	8.90	-2.13	16.11
		$[0/\pm23.4/0]_S$	202.11	9.07	-2.14	15.73
	Conventional Designs	**$[\pm 45/\pm 45]_S$**	**13.31**	**13.31**	**-0.26**	**-0.26**
		$[0/90/0/90]_S$	**142.43**	**142.43**	**-0.26**	**-0.26**

In Tables 7.9-7.14, multi and single-objective Genetic Algorithm optimization results for 12 layered E-glass/epoxy and carbon/epoxy laminated composites are given. $[\pm\theta_1/\pm\theta_2/\pm\theta_3]_S$, $[\theta_1/\theta_2/\theta_3/-\theta_1/-\theta_2/-\theta_3]_S$, $[\theta_1/-\theta_1/\theta_2/\theta_3/-\theta_2/-\theta_3]_S$ types of orientations have been considered. Outcomes from these cases can be summarized as follows:

1) There is no better solution than conventional designs for multi-objective optimizations of E_y-α_y. Therefore, number of generation and population size should be increased.

2) Consideration of three different fiber orientation angle stack ($[\pm\theta_1/\pm\theta_2/\pm\theta_3]_S$, $[\theta_1/\theta_2/\theta_3/-\theta_1/-\theta_2/-\theta_3]_S$, $[\theta_1/-\theta_1/\theta_2/\theta_3/-\theta_2/-\theta_3]_S$) did not

effect the optimum results of single-objective optimizations for α_x or E_x as in 8 layered cases.

3) From dimensionally stable point of view, the use of $[0/90/0/90/0/90]_S$ instead of $[\pm 45/\pm 45/\pm 45]_S$ are appropriate if you have only conventional angles.

Tables 7.15 and 7.16 show the muti-objective and single-objective Genetic Algorithm optimization results for 16 layered $\left[\pm\theta_1/\pm\theta_2/\pm\theta_3/\pm\theta_4\right]_S$ symmetric balanced E-glass/epoxy and carbon/epoxy laminated composites.

By considering Tables 7.1-7.16, it can be concluded that although the number of independent variables are increased (thickness and weight are increased), no improvement in minimization of α_x and maximization of E_x have been provided. Therefore, investigation of strength of the optimum composites is more important aspect of this study to be able to produce the light-weight composites. For this purpose, having got the optimum ply orientation angles, we can then perform strength analysis using ply failure criteria. In order to evaluate the failure loads of the optimized composites, four different failure criteria Tsai-Hill, Tsai-Wu, Hoffman and Hashin-Rotem are utilized and results have been compared. Loading ratios have been changed from 1 to 100 and 1/100 to 1. In order to see the effect of thermal change to failure loads, the failure loads have been calculated for different ΔT values.

Tables 7.17-7.27 give the results of failure loads in terms of loading ratios, materials, thermal effects, and effects of number of layers for the optimized composite and comparisons. In Table 7.17, tensile failure loads for $\left[\pm 27.3/\pm 27.3\right]_S$ 8 layered E-glass/epoxy composite are listed. It can be seen form the table, for the cases N_x/N_y=1, 1/2, 1/3, 1/5, 1/10 and 1/100, matrix failure (MF) mechanism is effective according to Hashin-Rotem failure criterion. Another observation from the table that, Tsai–Hill failure criterion underestimates the failure loads for all loading ratios. Maximum failure load (N_x=633.748) calculated based on four different failure criteria occurs in the case of N_x/N_y=2 by Hoffman failure criterion. When shear load applied together with biaxial load to the composite, the failure loads have decreased dramatically (e.g., from N_x=463.532 to N_x=152.722 for Tsai-Wu failure criterion).

In Table 7.18, effect of thermal changes to tensile failure loads for $\left[\pm 27.3/\pm 27.3\right]_S$ 8 layered E-glass/epoxy composite is given. It can be seen from the table (i) in all cases matrix failure occurs according to Hashin-Rotem failure criterion, (ii) failure loads decrease with increasing thermal change, (iii) approximately 4 kN/m

decrease have been obtained in failure loads N_x and N_y for thermal change $-110^{\circ}C$.

Table 7.19 gives compression failure loads for $[\pm 27.3/\pm 27.3]_S$ 8 layered E-glass/epoxy composite. It can be observed from the table (i) for the loading ratios N_x/N_y=1, 2, 3, 5, 10 and 100, fiber failure (FF) occurs while matrix failure mechanism is effective for the ratios 1/2, 1/ 3, 1/5, 1/ 10 and 1/100, (ii) Tsai–Hill failure criterion overestimates the failure loads among the others for loading ratios N_x/N_y=1, 2, 3, 5, 10 and 100 but it underestimates the failure loads for the ratios N_x/N_y=1/2, 1/ 3, 1/5, 1/ 10 and 1/100, (iii) Maximum failure load have been calculated by Tsai-Hill criterion (N_x = -539.160) while minimum failure load by using Hoffman theory (Nx = -240.100), (iv) applying shear load, additionally to E-glass/epoxy optimized composite, have decreased the failure loads dramatically (e.g., from N_x=-298.419 kN/m to N_x=-111.625 kN/m for Tsai-Wu failure criterion). By comparing the tensile and compression failure load limits (see Table 7.17 and 7.19) of the E-glass/epoxy composite, it can be concluded that compression limits are smaller than tensile limits according to Tsai-Wu, Hoffman and Hashin-Rotem theories. It should be noted that, since the Tsai–Hill failure criterion does not distinguish between the compressive and tensile strengths, its results for compression and tensile limits are the same.

In Table 7.20, effect of thermal changes to compression failure loads for $[\pm 27.3/\pm 27.3]_S$ 8 layered E-glass/epoxy composite is given. It can be seen form the table that (i) in all cases, fiber failure mechanism is effective based on Hashin-Rotem failure criterion as different from the tensile limit results, (ii) the magnitude of failure loads decreases with increasing thermal change according to Tsai-Wu, Hoffman and Hashin-Rotem criteria. However, an increase is observed in the failure load values calculated by using Tsai-Hill theory, (iii) approximately 5 kN/m decrease has been obtained in failure loads N_x and N_y for thermal change of $-110^{\circ}C$.

In Table 7.21 the stacking sequence $[\pm 72.9/\pm 72.9]_S$ is anti-optimum design for minimization of α_x, and $[0/90/0/90]_S$, $[\pm 45/\pm 45]_S$, $[0/45/0/45]_S$ are conventional designs. Minimum increase occurs in the case of anti-optimum design while maximum increase appears for conventional designs $[0/90/0/90]_S$ and $[\pm 45/\pm 45]_S$ under the thermal change.

In Table 7.22, tensile failure loads for $[\pm 32/\pm 32]_S$ 8 layered carbon/epoxy composite are listed. It can be seen from the table, for all the cases except N_x/N_y=3,

failure occurs in matrix according to Hashin-Rotem failure criterion. Another observation from the table that Tsai–Hill failure criterion underestimates the failure loads among the others for loading ratios N_x/N_y=1, 2, 3, 5, 10 and 100 but it overestimates for the ratios Nx/Ny=1/2, 1/ 3, 1/5, 1/ 10 and 1/100. Maximum failure load (N_x=1349.004 kN/m), calculated from four different failure criteria, occurs in the case of N_x/N_y=3 by Hashin-Rotem failure criterion. The composite have decreased the failure loads moderately (e.g., from N_x=155.204 kN/m to N_x=134.337 kN/m for Tsai-Wu failure criterion) with addition of shear load. In Table 7.23, effect of thermal changes to tensile failure loads for $[\pm 32/\pm 32]_S$ 8 layered carbon/epoxy composite is given. It can be seen form the table that (i) as in the E-glass/epoxy results, in all cases matrix failure occurs according to Hashin-Rotem failure criterion, (ii) failure loads decreases with increasing thermal change, (iii) approximately 30 kN/m decrease, which is 7.5 times bigger than E-glass/epoxy case, has been obtained in failure loads N_x and N_y for thermal change of $-110^{\circ}C$.

Table 7.24 gives compression failure loads for $[\pm 32/\pm 32]_S$ 8 layered E-glass/ epoxy composite. It can be observed from the table that (i) for the loading ratios N_x/N_y= 2, 3 fiber failure occurs however, for the ratios N_x/N_y =1, 5, 10, 100, 1/2, 1/ 3, 1/5, 1/ 10 and 1/100, matrix failure occurs, (ii) for loading ratios N_x/N_y =1, 2, 1/2, 1/3, 1/5, 1/10, 1/100 Tsai-Wu; for N_x/N_y = 3 Tsai-Hill; for N_x/N_y = 5, 10,100 Hashin-Rotem criteria overestimates the failure loads among the others, (iii) maximum magnitude of failure load have been calculated by Tsai-Wu criterion (N_x =-1889.158 kN/m) while minimum failure load have been obtained by using Tsai-Hill (N_y =-99.804 kN/m), (iv) addition of shear load to carbon/epoxy optimized composite have decreased the failure loads moderately (e.g., from N_x =-468.487 kN/m to N_x =-418.018 kN/m for Tsai-Wu failure criterion). By comparing the tensile and compression failure load limits (see Table 7.22 and 7.24) of the E-glass/epoxy composite, it can be concluded that magnitudes of compression limits bigger than tensile limits based on Tsai-Wu, Hoffman and Hashin-Rotem theories.

In Table 7.25, effect of thermal changes to compression failure loads for $[\pm 32/\pm 32]_S$ 8 layered carbon/epoxy composite is given. It can be seen form the table that (i) as different from the E-glass/epoxy results, in all cases matrix failure mechanism is effective based on Hashin-Rotem failure criterion, (ii) the same as E-glass/epoxy results, the magnitude of failure loads decreases with increasing thermal change

according to Tsai-Wu, Hoffman and Hashin-Rotem criteria. However, an increase is observed in the failure load values calculated by using Tsai-Hill theory, (iii) approximately 6 kN/m decrease has been obtained in failure loads N_x and N_y for thermal change of $-110^{\circ}C$.

Effect of stacking sequences with thermal changes to failure loads for different 8 layered carbon/epoxy composite can be seen in Table 7.26. Five distinct stacking sequences; $[\pm 27.3/\pm 27.3]_S$ is optimum, $[90/90/90/90]_S$ is anti-optimum, and $[0/90/0/90]_S$, $[\pm 45/\pm 45]_S$, $[0/45/0/45]_S$ are conventional designs, have been considered. As in E-glass/epoxy, minimum increase occurs in the case of anti-optimum $[90/90/90/90]_S$ while maximum increase appears for conventional designs $[0/90/0/90]_S$ and $[\pm 45/\pm 45]_S$ under the thermal change.

Table 7.27 shows the effect of number of layers to tensile failure loads for optimized E-glass/epoxy and carbon/epoxy laminated composites. Linear increase has been observed in failure loads with linearly increased number of layers in E-glass/epoxy and carbon/epoxy.

Table 7.9. Multi-objective GA, and single-objective GA optimization results for 12 layered symmetric balanced $[\pm\theta_1/\pm\theta_2/\pm\theta_3]_S$ E-glass/epoxy laminated composites.

Problem No	Optimization	Stack	E_x (GPa)	E_y (GPa)	α_x ($10^{-6}/^{\circ}C$)	α_y ($10^{-6}/^{\circ}C$)
65	**Min α_x**	$[\pm 27.3/\pm 27.3/\pm 27.3]_S$	13.17	8.33	8.61	27.96
66	**Min α_y**	$[\pm 62.7/\pm 62.7/\pm 62.7]_S$	8.33	13.17	27.96	8.61
67	**Max E_x**	$[0/0/0/0/0]_S$	22.20	11.50	10.02	28.41
68	**Max E_y**	$[90/90/90/90/90/90]_S$	11.5	22.20	28.41	10.02
69	**Min α_x Min α_y**	$[\pm 27.3/\pm 27.3/\pm 27.3]_S$	13.17	8.33	8.61	27.96
		$[\pm 33.4/\pm 32.7/\pm 32.9]_S$	10.29	7.34	9.15	25.08
		$[\pm 33.3/\pm 35.1/\pm 37.6]_S$	9.31	7.04	9.89	23.48
		$[\pm 39.7/\pm 31.8/\pm 40.7]_S$	8.71	6.99	11.02	18.13
		$[\pm 48/\pm 38.6/\pm 44.3]_S$	7.19	6.90	15.6	18.13
		$[\pm 49.6/\pm 50.9/\pm 45.6]_S$	6.67	7.45	20.43	13.47
		$[\pm 47.4/\pm 51.2/\pm 55.3]_S$	6.83	8.22	22.60	11.68
		$[\pm 54.4/\pm 52.8/\pm 56]_S$	6.99	9.19	24.95	9.96
		$[\pm 56.4/\pm 56.7/\pm 56.5]_S$	7.26	10.08	26.12	9.26
70	**Max E_x Min α_x**	$[0/0/0/0/0]_S$	22.20	11.50	10.02	28.41
		$[\pm 10.1/\pm 6.3/\pm 2.3]_S$	21.54	11.27	9.88	28.45
		$[\pm 16.2/\pm 3.2/\pm 17.8]_S$	19.64	10.62	9.52	28.49
		$[\pm 18.2/\pm 17.4/\pm 12.7]_S$	18.69	10.27	9.31	28.55
		$[\pm 21.2/\pm 19.7/\pm 15.1]_S$	17.57	9.88	9.12	28.53
		$[\pm 25.8/\pm 11.1/\pm 22.9]_S$	16.78	9.67	9.08	28.31
		$[\pm 18.5/\pm 20.3/\pm 23.1]_S$	16.35	9.56	8.96	28.51
		$[\pm 19/\pm 20.5/\pm 26.3]_S$	16.00	9.35	8.89	28.39
		$[\pm 26.2/\pm 19.13/\pm 25.2]_S$	15.18	9.06	8.79	28.30
		$[\pm 25.6/\pm 26.4/\pm 26.2]_S$	13.83	8.56	8.63	28.14

(cont. on next page)

Table 7.9. (cont.)

71	**Max E_y Min α_y**	$[\pm 62.7/\pm 62.7/\pm 62.7]_S$	8.33	13.17	27.96	8.61
		$[\pm 64.6/\pm 64.1/\pm 62.9]_S$	8.55	13.80	28.13	8.63
		$[\pm 65/\pm 65.2/\pm 63.2]_S$	8.67	14.12	28.20	8.65
		$[\pm 64.9/\pm 69.2/\pm 62.7]_S$	8.90	14.72	28.24	8.74
		$[\pm 67.8/\pm 69.9/\pm 65.3]_S$	9.26	15.80	28.43	8.83
		$[\pm 69.5/\pm 69.3/\pm 69.3]_S$	9.56	16.67	28.53	8.95
		$[\pm 67.9/\pm 76.3/\pm 68.7]_S$	9.82	17.35	28.49	9.10
		$[\pm 77.2/\pm 70.2/\pm 69.2]_S$	10.01	17.92	28.52	9.19
		$[\pm 70.6/\pm 73.9/\pm 72.8]_S$	10.06	18.10	28.57	9.20
		$[\pm 83.6/\pm 78.2/\pm 72.5]_S$	10.76	20.07	28.50	9.59
		$[90/90/90/90/90/90]_S$	11.5	22.20	28.41	10.02
72	**Max E_x Max E_y Min α_x**	$[0/0/0/0/0/0]_S$	22.20	11.50	10.02	28.41
		$[\pm 26.3/\pm 1.7/\pm 1]_S$	19.58	10.71	9.64	28.20
		$[\pm 62.7/\pm 62.7/\pm 62.7]_S$	8.33	13.17	27.96	8.61
		$[\pm 69.9/\pm 1.5/\pm 1.6]_S$	18.00	13.69	13.41	21.07
		$[\pm 61.8/\pm 0.9/\pm 1.6]_S$	17.54	12.61	12.56	22.33
		$[\pm 21.3/\pm 15.4/\pm 23.8]_S$	16.84	9.64	9.01	28.46
		$[\pm 25.6/\pm 19.6/\pm 23.2]_S$	15.56	9.18	8.82	28.38
		$[\pm 24.5/\pm 24.9/\pm 27.3]_S$	14.10	8.66	8.65	28.18
		$[\pm 27.3/\pm 27.3/\pm 27.3]_S$	13.17	8.33	8.61	27.96
	Conventional Designs	**$[\pm 45/\pm 45/\pm 45]_S$**	**6.76**	**6.76**	**16.83**	**16.83**
		$[0/90/0/90/0/90]_S$	**16.95**	**16.95**	**16.83**	**16.83**

Table 7.10. Multi-objective GA, and single-objective GA optimization results for 12 layered $[\theta_1/\theta_2/\theta_3/-\theta_1/-\theta_2/-\theta_3]_S$ symmetric balanced E-glass/epoxy laminated composites.

No	Opt.	Stack	E_x (GPa)	E_y (GPa)	α_x ($10^{-6}/^{\circ}C$)	α_y ($10^{-6}/^{\circ}C$)
73	**Min α_x**	$[27.3/27.3/27.3/-27.3/-27.3/-27.3]_S$	13.17	8.33	8.61	27.96
74	**Min α_y**	$[62.7/62.7/62.7/-62.7/-62.7/-62.7]_S$	8.33	13.17	27.96	8.61
75	**Max E_x**	$[0/0/0/0/0/0]_S$	22.20	11.50	10.02	28.41
76	**Max E_y**	$[90/90/90/90/90/90]_S$	11.5	22.20	28.41	10.02
77	**Min α_x Min α_y**	$[51.1/42.8/44.5/-51.1/-42.8/-44.5]_S$	6.88	7.12	17.91	15.78
		$[33.7/34.3/35.3/-33.7/-34.3/-33.7]_S$	9.66	7.13	9.53	25.63
		$[40.7/32.6/31/-40.7/-32.6/-31]_S$	9.75	7.29	9.94	25.09
		$[27.3/27.3/27.3/-27.3/-27.3/-27.3]_S$	13.17	8.33	8.61	24.56
		$[42.7/29.8/33.4/-42.7/-29.8/-33.4]_S$	9.69	7.37	10.31	19.30
		$[48.5/38.7/39.9/-48.5/-38.7/-39.9]_S$	7.47	6.91	14.48	19.15
		$[42.2/41.8/44/-42.2/-41.8/-44]_S$	7.11	6.62	14.61	19.15
		$[34.8/36.8/40.1/-34.8/-36.8/-40.1]_S$	8.62	6.86	10.75	23.81
		$[31.4/33.9/35.5/-31.4/-33.9/-35.5]_S$	10.05	7.27	9.34	26.00
78	**Max E_x Min α_x**	$[27.3/27.3/27.3/-27.3/-27.3/-27.3]_S$	13.17	8.33	8.61	27.96
		$[-26.7/25.8/22.2/26.7/-25.8/-22.2]_S$	14.46	8.80	8.69	28.23
		$[-22.4/25.3/23.3/22.4/-25.3/-23.3]_S$	15.11	9.02	8.74	28.37
		$[-17.6/25.4/25.3/17.6/-25.4/-25.3]_S$	15.55	9.20	8.85	28.32
		$[-19/26.4/16.9/19/-26.4/-16.9]_S$	16.55	9.56	9.00	28.39
		$[-14.5/17.1/21.2/14.5/-17.1/-21.2]_S$	18.05	10.05	9.20	28.54
		$[-19.9/20.7/5.3/19.9/-20.7/-5.3]_S$	18.58	10.27	9.34	28.45
		$[-12.6/3.1/10/12.6/-3.1/-10]_S$	21.00	11.08	9.77	28.48
		$[-12/4.9/5.3/12/-4.9/-5.3]_S$	21.32	11.19	9.84	28.46
		$[-7.4/3.8/5.5/7.4/-3.8/-5.5]_S$	21.75	11.34	9.92	28.44

(cont. on next page)

Table 7.10. (cont.)

79	**Max E_y Min α_y**	$[62.7/-62.7/-62.7/-62.7/62.7/62.7]_S$	8.33	13.17	27.96	8.61
		$[63.4/-66/-63/-63.4/66/63]_S$	8.61	13.94	28.15	8.65
		$[64.2/-69.4/-62.7/-64.2/69.4/62.7]_S$	8.87	14.64	28.22	8.73
		$[70.4/-67.1/-64.8/-70.4/67.1/64.8]_S$	9.22	15.68	28.41	8.83
		$[71.5/-68.7/-65.5/-71.5/68.7/65.5]_S$	9.43	16.25	28.46	8.91
		$[76.1/-74.5/-66.1/-76.1/74.5/66.1]_S$	10.03	17.92	28.47	9.21
		$[80.9/-73.4/-64.6/-80.9/73.4/64.6]_S$	10.11	18.05	28.37	9.28
		$[80.1/-75.9/-64.8/-80.1/75.9/64.8]_S$	10.21	18.34	28.37	9.34
		$[76.8/-79.7/-67.5/-76.8/79.7/67.5]_S$	10.36	18.85	28.46	9.39
		$[78.2/-84.4/-68.2/-78.2/84.4/68.2]_S$	10.59	19.48	28.43	9.52
		$[83.9/-87/-69.3/-83.9/87/69.3]_S$	10.85	20.23	28.41	9.66
80	**Max E_x Max E_y Min α_x**	$[-13/22.5/23.7/13/-22.5/-23.7]_S$	16.98	9.71	9.06	28.42
		$[-11.9/22.4/23.5/11.9/-22.4/-23.5]_S$	17.16	9.78	9.10	28.41
		$[-10.1/19.8/23.3/10.1/-19.8/-23.3]_S$	17.81	10.00	9.21	28.44
		$[-7.6/19.7/23/7.6/-19.7/-23]_S$	18.10	10.11	9.27	28.42
		$[-5.9/15.8/22/5.9/-15.8/-22]_S$	18.94	10.40	9.41	28.45
		$[-5/10.1/19.9/5/-10.1/5]_S$	19.97	10.75	9.60	28.45
		$[-2.9/9.1/19.7/2.9/-9.1/-19.7]_S$	20.17	10.82	9.64	28.44
		$[-1.2/11.5/14.9/1.2/-11.5/-14.9]_S$	20.63	10.96	9.70	28.48
		$[-0.4/13.4/0/0.4/-13.4/0]_S$	21.42	11.23	9.86	28.44
		$[-0.9/10.1/5.6/0.9/-10.1/-5.6]_S$	21.60	11.29	9.89	28.45
		$[0/0/0/0/0/0]_S$	22.20	11.50	10.02	28.41
	Conventional Designs	**$[\pm 45/\pm 45/\pm 45]_S$**	**6.76**	**6.76**	**16.83**	**16.83**
		$[0/90/0/90/0/90]_S$	**16.95**	**16.95**	**16.83**	**16.83**

Table 7.11. Multi-objective GA and single-objective GA optimization results for 12 layered $[\theta_1/-\theta_1/\theta_2/\theta_3/-\theta_2/-\theta_3]_S$ symmetric balanced E-glass/epoxy laminated composites.

No	Opt.	Stack	E_x (GPa)	E_y (GPa)	α_x ($10^{-6}/^{\circ}C$)	α_y ($10^{-6}/^{\circ}C$)
81	**Min α_x**	$[27.3/-27.3/27.3/27.3/-27.3/-27.3]_S$	13.17	8.33	8.61	27.96
82	**Min α_y**	$[-62.7/62.7/62.7/62.7/-62.7/-62.7]_S$	8.33	13.17	27.96	8.61
83	**Max E_x**	$[0/0/0/0/0/0]_S$	22.20	11.50	10.02	28.41
84	**Max E_y**	$[90/90/90/90/90/90]_S$	11.50	22.20	28.41	10.02
85	**Min α_x Min α_y**	$[27.3/-27.3/27.3/27.3/-27.3/-27.3]_S$	13.17	8.33	8.61	27.96
		$[-20.9/20.9/40.4/-35.9/-40.4/35.9]_S$	11.14	8.01	9.93	25.36
		$[-27.5/27.5/37.6/-42.8/-37.6/42.8]_S$	9.53	7.40	10.72	23.98
		$[0.4/-0.4/48.8/-36/-48.8/36]_S$	12.95	9.56	11.43	23.45
		$[-34.3/34.5/45.4/-48.6/-45.4/48.6]_S$	7.68	7.20	14.96	18.78
		$[-20.4/20.4/57.3/-49.9/-57.3/49.9]_S$	10.30	9.84	15.86	17.84
		$[12.7/-12.7/60.8/-53.6/-60.8/53.6]_S$	11.69	11.44	16.43	17.24
		$[-29.2/29.2/48.9/-61.1/-48.9/61.1]_S$	9.10	9.46	17.77	15.91
		$[-51.4/51.4/51.6/-41.5/-51.6/41.5]_S$	6.94	7.63	19.76	14.06
		$[-41.2/41.2/61.5/-53.8/-61.5/53.8]_S$	7.68	9.37	22.31	11.99
		$[-54.2/54.2/54.6/-51.8/-54.6/51.8]_S$	6.89	8.85	24.41	10.33
		$[-62.7/62.7/62.7/62.7/-62.7/-62.7]_S$	8.33	13.17	27.96	8.61
86	**Max E_x Min α_x**	$[7.5/-7.5/2.1/-7.4/-2.1/7.4]_S$	21.68	11.32	9.91	28.45
		$[8/-8/1.3/-14.4/-1.3/14.4]_S$	21.00	11.08	9.78	28.47
		$[13.4/-13.4/3.1/-19.9/-3.1/19.9]_S$	19.70	10.65	9.54	28.47
		$[9.6/-9.6/12.1/-21.2/-12.1/21.2]_S$	19.25	10.49	9.45	28.48
		$[17.2/-17.2/20.5/-10.4/-20.5/10.4]_S$	18.62	10.26	9.32	28.51
		$[17.2/-17.2/20.1/-12.6/-20.1/12.6]_S$	18.44	10.19	9.28	28.54
		$[15.6/-15.6/14.3/-22.5/-14.3/22.5]_S$	18.08	10.07	9.22	28.51
		$[16.4/-16.4/22.3/-17/-22.3/17]_S$	17.62	9.90	9.13	28.53
		$[17/-17/23.3/-26.1/-23.3/26.1]_S$	15.87	9.31	8.89	28.35
		$[26.5/-26.5/23.8/-27.3/-23.8/27.3]_S$	13.94	8.61	8.65	28.14

(cont. on next page)

Table 7.11. (cont.)

87	**Max E_y Min α_y**	$[-62.7/62.7/-62.7/-62.7/62.7/62.7]_S$	8.33	13.17	27.96	8.61
		$[-65.4/65.4/-63.5/-63.5/63.5/63.5]_S$	8.60	13.94	28.16	8.64
		$[-64.1/64.1/-64.8/-66/64.8/66]_S$	8.76	14.39	28.26	8.67
		$[-67.5/67.5/-63.5/-67/63.5/67]_S$	8.96	14.94	28.32	8.73
		$[-67.8/67.8/-65.7/-66.5/65.7/66.5]_S$	9.08	15.29	28.40	8.76
		$[-71/71/-64.2/-68.8/64.2/68.8]_S$	9.33	15.96	28.41	8.88
		$[-69.7/69.7/-68.6/-67.1/68.6/67.1]_S$	9.40	16.21	28.49	8.88
		$[-70/70/-67.8/-68.7/67.8/68.7]_S$	9.46	16.40	28.51	8.91
		$[-74.3/74.3/-67.7/-67.7/67.7/67.7]_S$	9.65	16.88	28.50	9.01
		$[-74.2/74.2/-69.1/-71.4/69.1/71.4]_S$	9.92	17.69	28.55	9.13
		$[-77.6/77.6/-70.2/-69.8/70.2/69.8]_S$	10.06	18.06	28.52	9.21
88	**Max E_x Max E_y Min α_x**	$[0.4/-0.4/-0.5/-11.7/0.5/11.7]_S$	21.60	11.29	9.90	28.44
		$[2.6/-2.6/-6.3/-23.2/6.3/23.2]_S$	19.85	10.75	9.62	28.34
		$[2.5/-2.5/-6.2/-26.1/6.2/26.1]_S$	19.41	10.64	9.60	28.23
		$[9/-9/-17.2/-23.8/17.2/23.8]_S$	18.23	10.16	9.29	28.42
		$[9.6/-9.6/-22.4/-20.2/22.4/20.2]_S$	17.94	10.05	9.22	28.45
		$[0.6/-0.6/-2.6/-63.7/2.6/63.7]_S$	17.62	12.86	12.78	21.99
		$[0.5/-0.5/-9/-55.6/9/55.6]_S$	16.91	11.64	11.77	23.51
		$[9.8/-9.8/-25.5/-27.6/25.5/27.6]_S$	16.18	9.51	9.07	28.12
		$[18.4/-18.4/-25.7/-23.8/25.7/23.8]_S$	15.63	9.22	8.84	28.36
		$[19.3/-19.3/-26.2/-27.6/26.2/27.6]_S$	14.74	8.92	8.77	28.19
		$[25.4/-25.4/-22.6/-27.4/22.6/27.4]_S$	14.34	8.75	8.69	28.21
	Conventional Designs	**$[\pm 45/\pm 45/\pm 45]_S$**	**6.76**	**6.76**	**16.83**	**16.83**
		$[0/90/0/90/0/90]_S$	**16.95**	**16.95**	**16.83**	**16.83**

Table 7.12. Multi-objective GA and single-objective GA optimization results for 12 layered symmetric balanced $[\pm\theta_1/\pm\theta_2/\pm\theta_3]_S$ carbon/epoxy laminated composites.

No	Opt.	Stack	E_x (GPa)	E_y (GPa)	α_x ($10^{-6}/^{\circ}C$)	α_y ($10^{-6}/^{\circ}C$)
89	**Min α_x**	$[\pm32/\pm32/\pm32]_S$	40.78	8.05	-5.24	11.66
90	**Min α_y**	$[\pm58/\pm58/\pm58]_S$	8.05	40.78	11.66	-5.24
91	**Max E_x**	$[0/0/0/0/0/0]_S$	277.27	7.05	-1.00	22.42
92	**Max E_y**	$[90/90/90/90/90/90]_S$	7.05	277.27	22.42	-1.00
93	**Min α_x Min α_y**	$[\pm32/\pm32/\pm32]_S$	40.78	8.05	-5.24	11.66
		$[\pm32/\pm34.5/\pm33.9]_S$	35.62	8.46	-5.10	10.18
		$[\pm31.5/\pm36/\pm34.8]_S$	34.62	8.95	-4.84	9.20
		$[\pm32/\pm36.1/\pm35.8]_S$	32.82	9.06	-4.79	8.76
		$[\pm31.9/\pm37.8/\pm35.8]_S$	32.36	9.59	-4.52	7.91
		$[\pm31.3/\pm39.4/\pm35.9]_S$	33.53	10.51	-4.13	6.95
		$[\pm31.7/\pm40.5/\pm34.2]_S$	35.10	10.96	-3.96	6.67
		$[\pm31.6/\pm41.8/\pm37.7]_S$	32.13	12.23	-3.46	5.12
		$[\pm31.8/\pm43.4/\pm37.6]_S$	32.70	13.43	-3.10	4.34
		$[\pm31.6/\pm46.9/\pm36.5]_S$	37.89	17.37	-2.34	2.94
		$[\pm30.2/\pm52.3/\pm39.2]_S$	44.82	27.50	-1.29	1.10
		$[\pm28.8/\pm54.4/\pm39.8]_S$	50.68	33.17	-1.03	0.73
94	**Max E_x Min α_x**	$[\pm32/\pm32/\pm32]_S$	40.78	8.05	-5.24	11.66
		$[\pm30.5/\pm27.9/\pm26.6]_S$	61.71	7.86	-4.83	13.99
		$[\pm25.9/\pm24.8/\pm26.5]_S$	79.95	7.44	-4.56	16.09
		$[\pm22.4/\pm25.8/\pm26.6]_S$	88.16	7.59	-4.32	16.11
		$[\pm21.5/\pm21.9/\pm23.5]_S$	113.56	7.28	-3.89	17.90
		$[\pm23.3/\pm20.7/\pm17.1]_S$	137.05	7.46	-3.40	18.07
		$[\pm20.4/\pm14.8/\pm20.2]_S$	159.65	7.36	-3.05	18.92
		$[\pm22.5/\pm8.5/\pm20.1]_S$	174.12	8.06	-2.69	17.38
		$[\pm14.7/\pm11.5/\pm20.3]_S$	194.87	7.45	-2.48	19.40
		$[\pm17.6/\pm8.4/\pm15.4]_S$	211.96	7.34	-2.24	20.05
		$[\pm6.4/\pm10.2/\pm17.5]_S$	233.26	7.39	-1.89	20.31
		$[\pm2.5/\pm5.8/\pm14.2]_S$	256.43	7.24	-1.49	21.25

(cont. on next page)

Table 7.12. (cont.)

95	**Max E_y Min α_y**	$[\pm 83.6/\pm 88.3/\pm 80.3]_S$	7.09	266.05	21.98	-1.29
		$[\pm 72.8/\pm 81.9/\pm 79.3]_S$	7.32	229.64	20.47	-1.96
		$[\pm 81.6/\pm 77.5/\pm 68.3]_S$	7.84	206.55	18.54	-2.24
		$[\pm 71.1/\pm 74/\pm 79.1]_S$	7.34	197.34	19.76	-2.46
		$[\pm 73.5/\pm 77/\pm 64]_S$	8.39	162.38	16.36	-2.80
		$[\pm 71.5/\pm 71/\pm 68.4]_S$	7.24	144.28	18.90	-3.34
		$[\pm 66.6/\pm 75.2/\pm 63.9]_S$	8.27	127.88	15.81	-3.36
		$[\pm 69.8/\pm 70.1/\pm 66.8]_S$	7.31	127.63	18.25	-3.61
		$[\pm 64.8/\pm 68.5/\pm 64.5]_S$	7.52	96.20	16.61	-4.16
		$[\pm 60.4/\pm 60/\pm 63]_S$	7.83	57.86	13.78	-4.94
		$[\pm 58.5/\pm 58.7/\pm 59.3]_S$	7.94	44.58	12.32	-5.21
96	**Max E_x Max E_y Min α_x**	$[\pm 86.7/\pm 83.8/\pm 84.4]_S$	7.06	271.03	22.22	-1.17
		$[\pm 75.3/\pm 80.9/\pm 80]_S$	7.15	237.83	21.14	-1.84
		$[\pm 66.3/\pm 83/\pm 84]_S$	8.58	219.01	17.02	-1.97
		$[\pm 59.3/\pm 82.2/\pm 83.9]_S$	11.48	196.87	11.94	-1.96
		$[\pm 52.6/\pm 82.8/\pm 81.2]_S$	16.62	182.33	7.54	-1.73
		$[\pm 44.3/\pm 81.9/\pm 83]_S$	27.51	179.34	3.90	-1.31
		$[\pm 31.7/\pm 75.8/\pm 83.9]_S$	51.39	170.13	1.40	-0.90
		$[\pm 11.9/\pm 8.7/\pm 56.1]_S$	170.96	46.62	-0.97	1.68
	Conventional Designs	**$[\pm 45/\pm 45/\pm 45]_S$**	**13.31**	**13.31**	**-0.26**	**-0.26**
		$[0/90/0/90/0/90]_S$	**142.43**	**142.43**	**-0.26**	**-0.26**

Table 7.13. Multi-objective GA and single-objective GA optimization results for 12 layered $[\theta_1/\theta_2/\theta_3/-\theta_1/-\theta_2/-\theta_3]_S$ symmetric balanced carbon/epoxy laminated composites

No	Opt.	Stack	E_x (GPa)	E_y (GPa)	α_x ($10^{-6}/^{\circ}C$)	α_y ($10^{-6}/^{\circ}C$)
97	**Min α_x**	$[32/32/32/-32/-32/-32]_S$	40.78	8.05	-5.24	11.66
98	**Min α_y**	$[58/58/58/-58/-58/-58]_S$	8.05	40.78	11.66	-5.24
99	**Max E_x**	$[0/0/0/0/0/0]_S$	277.27	7.05	-1.00	22.42
100	**Max E_y**	$[90/90/90/90/90/90]_S$	7.05	277.27	22.42	-1.00
101	**Min α_x Min α_y**	$[30.7/30.8/-30.2/-30.7-30.8/30.2]_S$	47.49	7.86	-5.19	12.81
		$[29.9/34.1/-29.7/-29.9/-34.1/29.7]_S$	46.42	8.44	-4.92	11.51
		$[29.8/34.9/-30.1/-29.8/-34.9/30.1]_S$	45.44	8.68	-4.83	10.97
		$[30.1/37.9/-30.1/-30.1/-37.9/30.1]_S$	44.88	10.01	-4.29	8.86
		$[29.1/38.8/-29.5/-29.1/-38.8/29.5]_S$	49.12	10.84	-3.96	8.23
		$[29.9/39.8/-29.7/-29.9/-39.8/29.7]_S$	47.40	11.38	-3.81	7.51
		$[29/42.1/-29.8/-29/-42.1/29.8]_S$	51.70	13.59	-3.23	5.97
		$[24.2/42.1/-27.4/-24.2/-42.1/27.4]_S$	72.91	15.47	-2.77	5.87
		$[21.4/43.4/-26.6/-21.4/-43.4/26.6]_S$	86.67	18.10	-2.36	5.05
		$[15.8/43.7/-24.5/-15.8/-43.7/24.5]_S$	112.69	20.62	-1.99	4.73
102	**Max E_x Min α_x**	$[0/0/0/0/0/0]_S$	277.27	7.05	-1.00	
		$[6.8/0.8/-0.2/-6.8/-0.8/0.2]_S$	273.81	7.07	-1.10	22.27
		$[4.2/3.0/-13.5/-4.2/-3.0/13.5]_S$	259.67	7.22	-1.42	21.41
		$[3.0/15.1/-20.4/-3.0/-15.1/20.4]_S$	211.70	7.81	-2.17	18.74
		$[16.8/19/-7.1/-16.8/-19/7.1]_S$	204.23	7.55	2.32	19.30
		$[22.8/10.6/-17.7/-22.8/-10.6/17.7]_S$	176.39	7.85	2.69	17.94
		$[18.2/17/-18.8/-18.2/-17/18.8]_S$	165.28	7.14	-3.01	19.69
		$[24.7/20/-17.9/-24.7/-20/17.9]_S$	131.90	7.60	-3.46	17.57
		$[26.6/20.5/-20.2/-26.6/-20.5/20.2]_S$	115.08	7.77	-3.71	16.64
		$[23.9/24.6/-23.2/-23.9/-24.6/23.2]_S$	96.67	7.33	-4.22	17.16
		$[27.5/23.1/-31.2/-27.5/-23.1/31.2]_S$	73.01	8.46	-4.34	13.39
		$[27.2/28/-29.5/-27.2/-28/29.5]_S$	61.45	7.68	-4.92	14.38

(cont. on next page)

Table 7.13. (cont.)

103	**Max E_y Min α_y**	$[57.9/-57.9/-57.9/-57.9/57.9/57.9]_S$	8.07	40.36	11.58	-5.24
		$[60.9/-61.4/-62.2/-60.9/61.4/62.2]_S$	7.65	59.39	14.32	-4.99
		$[61.3/-63.4/-60.7/-61.3/63.4/60.7]_S$	7.72	61.88	14.33	-4.89
		$[63.1/-64.2/-62.7/-63.1/64.2/62.7]_S$	7.50	72.36	15.53	-4.72
		$[64.4/-64.3/-62.4/-64.4/64.3/62.4]_S$	7.51	75.47	15.68	-4.64
		$[66.1/-65.5/-59.6/-66.1/65.5/59.6]_S$	8.16	79.73	14.35	-4.29
		$[66.5/-66.6/-62.2/-66.5/66.6/62.2]_S$	7.67	89.04	15.94	-4.27
		$[66.6/-72.7/-60.4/-66.6/72.7/66.6/]_S$	8.84	110.15	14.13	-3.52
		$[74.8/-70.4/-62.6/-74.8/70.4/62.6]_S$	8.47	137.49	15.63	-3.16
		$[74.6/-74.7/-62.8/-74.6/74.7/62.8]_S$	8.63	154.70	15.68	-2.86
		$[80.8/-75.1/-62.5/-80.8/75.1/62.5]_S$	9.28	176.84	14.85	-2.45
104	**Max E_x Max E_y Min α_x**	$[32/32/32/-32/-32/-32]_S$	40.78	8.05	-5.24	11.66
		$[0/0/0/0/0/0]_S$	277.27	7.05	-1.00	22.42
		$[-56.3/-52.5/2.8/56.3/52.5/2.8]_S$	98.12	71.79	-0.54	0.09
		$[-54.3/-18.5/5.4/54.3/18.5/-5.4]_S$	159.67	42.37	-1.06	1.88
		$[-50/-36.9/24.8/50/36.9/-24.8]_S$	60.70	26.72	-1.62	1.93
		$[-24.9/-28.4/30.4/24.9/28.4/-30.4]_S$	65.79	8.03	-4.66	13.87
		$[-43/-33.8/20.3/43/33.8/-20.3]_S$	72.31	18.40	-2.40	4.47
		$[-40.9/-40.6/25.7/40.9/40.6/-25.7]_S$	47.17	16.31	-2.68	4.12
		$[-3.5/-5.1/7.7/3.5/5.1/-7.7]_S$	269.60	7.06	-1.21	22.16
		$[-36.2/-12.3/10.6/36.2/12.3/-10.6]_S$	167.37	14.77	-1.99	8.48
		$[-3.5/-21.5/11.8/3.5/21.5/-11.8]_S$	218.20	7.99	-2.05	18.38
		$[-12.9/-15.9/2.1/12.9/15.9/-2.1]_S$	236.22	7.34	-1.85	20.53
		$[-10.5/-20.7/11.8/10.5/20.7/-11.8]_S$	206.85	7.61	-2.27	19.17
		$[-35.1/-23.8/24.9/35.1/23.8/-24.9]_S$	76.43	10.11	-3.77	10.79
		$[-55.8/-49.2/3/55.8/49.2/-3]_S$	99.36	64.31	-0.65	0.28
	Conventional Designs	**$[\pm 45/\pm 45/\pm 45]_S$**	**13.31**	**13.31**	**-0.26**	**-0.26**
		$[0/90/0/90/0/90]_S$	**142.43**	**142.43**	**-0.26**	**-0.26**

Table 7.14. Multi-objective GA and single-objective GA optimization results for 12 layered $[\theta_1/-\theta_1/\theta_2/\theta_3/-\theta_2/-\theta_3]_S$ symmetric balanced carbon/epoxy laminated composites

No	Opt.	Stack	E_x (GPa)	E_y (GPa)	α_x ($10^{-6}/^{\circ}C$)	α_y ($10^{-6}/^{\circ}C$)
105	**Min α_x**	$[-32/32/-32/-32/32/32]_S$	40.78	8.05	-5.24	11.66
106	**Min α_y**	$[58/-58/-58/-58/58/58]_S$	8.05	40.78	11.66	-5.24
107	**Max E_x**	$[0/0/0/0/0/0]_S$	277.27	7.05	-1.00	22.42
108	**Max E_y**	$[90/90/90/90/90/90]_S$	7.05	277.27	22.42	-1.00
109	**Min α_x Min α_y**	$[32/-32/-32/-32/32/32]_S$	40.78	8.05	-5.24	11.66
		$[32.2/-32.2/33.8/-34.1/-33.8/34.1]_S$	35.76	8.38	-5.14	10.35
		$[32.2/-32.2/36.3/-34.7/-36.3/34.7]_S$	33.28	8.91	-4.87	9.06
		$[32.2/-32.2/34/-38.3/-34/38.3]_S$	33.72	9.60	-4.52	8.10
		$[32.2/-32.2/35.4/-39.2/-35.4/39.2]_S$	32.14	10.09	-4.29	7.23
		$[32.2/-32.2/33.2/-40.4/-33.2/40.4]_S$	35.61	10.85	-4.01	6.86
		$[32.2/-32.2/34.6/-41.9/-34.6/41.9]_S$	34.35	11.85	-3.64	5.74
		$[32.2/-32.2/35.4/-43.9/-35.4/43.9]_S$	34.84	13.61	-3.11	4.48
		$[32.4/-32.4/44.7/-45.1/-44.7/45.1]_S$	29.76	18.05	-1.86	1.84
		$[32.4/-32.4/48.4/-46.7/-48.4/46.7]_S$	31.33	23.65	-1.07	0.69
		$[32.3/-32.3/53.8/-42.4/-53.8/42.4]_S$	37.86	29.78	-0.83	0.39
		$[32.4/-32.4/55.6/-48.8/-55.6/48.8]_S$	36.19	38.97	-0.09	-0.42
110	**Max E_x Min α_x**	$[32/-32/32/32/-32/-32]_S$	40.78	8.05	-5.24	11.66
		$[29.7/-29.7/26.4/27.8/-26.4/-27.8]_S$	63.71	7.74	-4.83	14.40
		$[28.8/-28.8/26/24.5/-26/-24.5]_S$	75.59	7.71	-4.55	15.18
		$[26/-26/25.1/19.5/-25.1/-19.5]_S$	103.10	-7.77	-3.94	16.23
		$[23.3/-23.3/24.6/15.8/-24.6/-15.8]_S$	128.51	7.88	-3.44	16.75
		$[21.4/-21.4/17.1/20.1/-17.1/-20.1]_S$	146.45	7.29	-3.29	18.82
		$[10.8/-10.8/18.3/17.4/-18.3/-17.4]_S$	194.49	7.34	-2.51	19.71
		$[15.6/-15.6/12/10.9/-12/-10.9]_S$	224.37	7.14	-2.07	20.90
		$[7/-7/4.2/6.4/-4.2/-6.4]_S$	268.69	7.06	-1.23	22.15
		$[0.4/-0.4/0.3/0/-0.3/0]_S$	277.25	7.05	-1.00	22.42

(cont. on next page)

Table 7.14. (cont.)

111	**Max E_y Min α_y**	$[-79.3/79.3/-79.4/-80.3/79.4/80.3]_S$	7.06	246.48	21.62	-1.70
		$[-77.8/77.8/-76.4/-79.2/76.4/79.2]_S$	7.09	230.93	21.22	-1.97
		$[-72.4/72.4/-77.7/-79.5/77.7/79.5]_S$	7.27	217.14	20.38	-2.17
		$[-70.5/70.5/-75.4/-73.3/75.4/73.3]_S$	7.23	178.57	19.71	-2.78
		$[-69/69/-76.7/-69.7/76.7/69.7]_S$	7.51	162.87	18.56	-2.96
		$[-68.1/68.1/-70.9/-68.6/70.9/68.6]_S$	7.26	130.89	18.50	-3.57
		$[-65.1/65.1/-68.8/62.8/68.8/-62.8]_S$	7.73	93.91	15.97	-4.14
		$[-62.1/62.1/-64/-66.8/64/66.8]_S$	7.68	81.73	15.56	-4.42
		$[-64.3/64.3/-62.4/-64.7/62.4/64.7]_S$	7.51	76.36	15.71	-4.62
		$[-61.4/61.4/-62.4/-64.5/62.4/64.5]_S$	7.66	68.74	14.93	-4.74
		$[-58/58/-58/-58/58/58]_S$	8.05	40.78	11.66	-5.24
112	**Max E_x Max E_y Min α_x**	$[0/0/0/0/0/0]_S$	277.27	7.05	-1.00	22.42
		$[-16.2/16.2/4/14/-4/-14]_S$	230.08	7.35	-1.95	20.38
		$[-26/26/-2.4/-59.8/2.4/59.8]_S$	144.56	54.57	-0.89	1.05
		$[-16.6/16.6/30.7/26.1/-30.7/-26.1]_S$	102.78	9.50	-3.48	12.71
		$[-78.1/78.1/18/-74.2/-18/74.2]_S$	79.58	163.65	0.45	-0.64
		$[-32/32/32/32/-32/-32]_S$	40.78	8.05	-5.24	11.66
		$[-83.6/83.6/-41.1/-84.4/41.1/84.4]_S$	33.23	182.65	3.01	-1.16
		$[-83.6/83.6/-82/-50/82/50]_S$	19.62	182.93	6.14	-1.57
		$[-84.6/84.6/-83/-60/83/60]_S$	11.16	201.17	12.40	-1.93
		$[-84.5/84.5/-84.4/-69.5/84.4/69.5]_S$	7.91	233.49	18.87	-1.82
		$[-84.8/84.8/-84.9/-84.9/84.9/84.9]_S$	7.05	271.15	22.23	-1.17
	Conventional Designs	**$[\pm 45/\pm 45/\pm 45]_S$**	**13.31**	**13.31**	**-0.26**	**-0.26**
		$[0/90/0/90/0/90]_S$	**142.43**	**142.43**	**-0.26**	**-0.26**

Table 7.15. Multi-objective GA and single-objective GA optimization results for 16 layered $[\pm\theta_1/\pm\theta_2/\pm\theta_3/\pm\theta_4]_S$ symmetric balanced E-glass/epoxy laminated composites.

No	Opt.	Stack	E_x (GPa)	E_y (GPa)	α_x ($10^{-6}/^{\circ}C$)	α_y ($10^{-6}/^{\circ}C$)
113	**Min α_x**	$[\pm 27.3/\pm 27.3/\pm 27.3/\pm 27.3]_S$	13.17	8.33	8.61	27.96
114	**Min α_y**	[±62.7/±62.7/±62.7/±62.7]	8.33	13.17	27.96	8.61
115	**Max E_x**	$[0/0/0/0/0/0/0/0]_S$	22.20	11.50	10.02	28.41
116	**Max E_y**	$[90/90/90/90/90/90/90/90]_S$	11.5	22.20	28.41	10.02
117	**Min α_x Min α_y**	$[\pm 27.3/\pm 27.3/\pm 27.3/\pm 27.3]_S$	13.17	8.33	8.61	27.96
		$[\pm 32.8/\pm 44.4/\pm 27.7/\pm 41.4]_S$	9.39	7.41	11.05	23.53
		$[\pm 31.5/\pm 44/\pm 27.4/\pm 40.1]_S$	9.68	7.47	10.69	24.05
		$[\pm 31.9/\pm 43.5/\pm 27.6/\pm 38.4]_S$	9.74	7.44	10.43	24.40
		$[\pm 29/\pm 38.1/\pm 27.3/\pm 32.2]_S$	11.10	7.71	9.15	26.52
		$[\pm 28.6/\pm 43.5/\pm 27.3/\pm 36]_S$	10.42	7.67	10.01	25.10
		$[\pm 29.4/\pm 37.1/\pm 27.4/\pm 32.1]_S$	11.14	7.70	9.07	26.65
		$[\pm 29/\pm 43.1/\pm 27.4/\pm 33.2]_S$	10.66	7.71	9.77	25.50
		$[\pm 32.4/\pm 28.6/\pm 27.4/\pm 34.8]_S$	11.43	7.77	8.90	26.98
		$[\pm 31.9/\pm 43.8/\pm 27.6/\pm 41.1]_S$	9.55	7.44	10.83	23.84
		$[\pm 30.5/\pm 31.2/\pm 27.4/\pm 32.5]_S$	11.58	7.79	8.79	27.20
		$[\pm 28.1/\pm 42.8/\pm 27.2/\pm 33.1]_S$	10.83	7.77	9.69	25.65
118	**Max E_x Min α_x**	$[0/0/0/0/0/0/0/0]_S$	22.20	11.50	10.02	28.41
		$[\pm 16.4/\pm 1.7/\pm 1/\pm 3.7]_S$	21.28	11.19	9.84	28.43
		$[\pm 1.5/\pm 21.6/\pm 0.7/\pm 0.9]_S$	20.79	11.05	9.78	28.37
		$[\pm 7/\pm 18/\pm 4.3/\pm 11.4]_S$	20.50	10.92	9.68	28.47
		$[\pm 17.6/\pm 13.6/\pm 4/\pm 13.6]_S$	19.91	10.71	9.56	28.51
		$[\pm 15.4/\pm 13.7/\pm 13.8/\pm 20.9]_S$	18.74	10.30	9.33	28.54
		$[\pm 15/\pm 19.4/\pm 16.8/\pm 15.4]_S$	18.49	10.20	9.27	28.56
		$[\pm 24.7/\pm 20/\pm 20.4/\pm 22]_S$	16.09	9.36	8.87	28.46
		$[\pm 21.5/\pm 22/\pm 23.5/\pm 23.7]_S$	15.63	9.20	8.80	28.44
		$[\pm 27.5/\pm 26.8/\pm 27.3/\pm 25.6]_S$	13.44	8.43	8.62	28.03

(cont. on next page)

Table 7.15. (cont.)

119	**Max E_y Min α_y**	$[\pm 62.7/\pm 62.7/\pm 62.7/\pm 62.7]_S$	8.33	13.17	27.96	8.61
		$[\pm 65.3/\pm 71.7/\pm 61.3/\pm 75.5]_S$	9.44	16.13	28.25	8.99
		$[\pm 67.6/\pm 69.4/\pm 61.3/\pm 69.8]_S$	9.18	15.47	28.31	8.84
		$[\pm 66/\pm 75.9/\pm 61.3/\pm 77.5]_S$	9.73	16.87	28.23	9.14
		$[\pm 66.4/\pm 78.9/\pm 61.3/\pm 82.5]_S$	10.01	17.57	28.18	9.29
		$[\pm 65.4/\pm 72.6/\pm 61.3/\pm 76.1]_S$	9.51	16.31	28.24	9.03
		$[\pm 64.1/\pm 69.8/\pm 61.3/\pm 68.8]_S$	8.99	14.94	28.22	8.79
		$[\pm 60.7/\pm 67.2/\pm 61.4/\pm 68.7]_S$	8.72	14.16	28.06	8.74
		$[\pm 68/\pm 79.8/\pm 61.3/\pm 84.5]_S$	10.13	17.94	28.19	9.35
		$[\pm 61.4/\pm 71.4/\pm 61.3/\pm 74.7]_S$	9.25	15.51	28.10	8.96
		$[\pm 66.4/\pm 70.1/\pm 61.3/\pm 75.1]_S$	9.40	16.03	28.27	8.96
120	**Max E_x Max E_y Min α_x**	$[0/0/0/0/0/0/0/0]_S$	22.20	11.50	10.02	28.41
		$[\pm 9.5/\pm 2.6/\pm 14.8/\pm 15.9]_S$	20.32	10.85	9.64	28.49
		$[\pm 2.6/\pm 72.7/\pm 0.1/\pm 2.5]_S$	19.15	13.41	12.62	22.43
		$[\pm 22.9/\pm 8.7/\pm 16.8/\pm 27.1]_S$	17.22	9.83	9.16	28.31
		$[0/0/90/90/90/90/0/0]_S$	16.95	16.95	16.83	16.83
		$[\pm 14.7/\pm 30.4/\pm 16/\pm 26.9]_S$	15.89	9.41	9.04	28.07
		$[\pm 13.6/\pm 89.9/\pm 60.5/0/0]_S$	15.57	14.61	15.93	17.78
		$[\pm 25.7/\pm 26.2/\pm 23.9/\pm 25.3]_S$	14.26	8.72	8.66	28.23
		$[\pm 80.7/\pm 89.8/\pm 72.2/0/0]_S$	13.77	18.41	21.31	13.28
		$[\pm 55.4/\pm 89.9/\pm 89.8/0/0]_S$	13.47	16.96	20.47	13.78
		$[\pm 27.3/\pm 27.3/\pm 27.3/\pm 27.3]_S$	13.17	8.33	8.61	27.96
	Conventional Designs	**$[\pm 45/\pm 45/\pm 45/\pm 45]_S$**	**6.76**	**6.76**	**16.83**	**16.83**
		$[0/90/0/90/0/90/0/90]_S$	**16.95**	**16.95**	**16.83**	**16.83**

Table 7.16. Multi-objective GA and single-objective GA optimization results for 16 layered $[\pm\theta_1/\pm\theta_2/\pm\theta_3/\pm\theta_4]_S$ symmetric balanced carbon/epoxy laminated composites.

No	Opt.	Stack	E_x (GPa)	E_y (GPa)	α_x ($10^{-6}/^{\circ}C$)	α_y ($10^{-6}/^{\circ}C$)
121	**Min α_x**	$[\pm32/\pm32/\pm32/\pm32]_S$	40.78	8.05	-5.24	11.66
122	**Min α_y**	$[\pm58/\pm58/\pm58/\pm58]_S$	8.05	40.78	11.66	-5.24
123	**Max E_x**	$[0/0/0/0/0/0/0/0]_S$	277.27	7.05	-1.00	22.42
124	**Max E_y**	$[90/90/90/90/90/90/90/90]_S$	7.05	277.27	22.42	-1.00
125	**Min α_x Min α_y**	$[\pm32/\pm32/\pm32/\pm32]_S$	40.78	8.05	-5.24	11.66
		$[\pm34.3/\pm34.2/\pm34.6/\pm34.3]_S$	32.08	8.48	-5.11	9.59
		$[\pm35.6/\pm36/\pm40.2/\pm36]_S$	26.56	9.78	-4.32	6.64
		$[\pm37.1/\pm37.2/\pm42.3/\pm41.6]_S$	22.12	11.28	-3.29	4.08
		$[\pm51.1/\pm55.9/\pm38.7/\pm56.5]_S$	20.43	38.90	2.06	-1.88
		$[\pm47.6/\pm54.4/\pm49.4/\pm54.2]_S$	11.43	25.11	4.62	-3.47
		$[\pm51.5/\pm52.4/\pm49.8/\pm56.1]_S$	10.29	25.87	5.90	-4.03
		$[\pm54/\pm51.1/\pm51.9/\pm56.7]_S$	9.83	27.92	6.84	-4.33
		$[\pm54.7/\pm55.3/\pm54.1/\pm51.3]_S$	9.31	28.00	7.55	-4.61
		$[\pm55.3/\pm56.9/\pm54.8/\pm56.2]_S$	8.54	32.87	9.62	-5.07
		$[\pm56.9/\pm57/\pm57/\pm56.9]_S$	8.23	36.58	10.76	-5.21
		$[\pm58/\pm58/\pm58/\pm58]_S$	8.05	40.78	11.66	-5.24
126	**Max E_x Min α_x**	$[0/0/0/0/0/0/0/0]_S$	277.27	7.05	-1.00	22.42
		$[\pm32/\pm32/\pm32/\pm32]_S$	40.78	8.05	-5.24	11.66
		$[\pm22.2/\pm19.9/\pm20.1/\pm12.6]_S$	156.77	7.56	-3.05	18.28
		$[\pm25/\pm25/\pm26/\pm25]_S$	83.98	7.39	-4.48	16.43
		$[\pm19/\pm18.8/\pm25.1/\pm22.6]_S$	125.79	7.57	-3.57	17.48
		$[\pm4.4/\pm12.3/\pm23.6/\pm11.6]_S$	215.26	8.12	-2.08	18.02
		$[\pm4.5/\pm1.2/\pm0.4/\pm15.1]_S$	262.15	7.28	-1.37	21.26
		$[\pm18.9/\pm16.2/\pm24.1/\pm18.7]_S$	148.25	7.52	-3.20	18.19
		$[\pm8.2/\pm14.7/\pm4.7/\pm7.4]_S$	253.09	7.20	-1.56	21.32
		$[\pm15.6/\pm15.5/\pm17.5/\pm14.6]_S$	192.46	7.12	-2.58	20.33

(cont. on next page)

Table 7.16. (cont.)

127	**Max E_y Min α_y**	[±60.1/±78.4/±71.9/±36.3] s	32.63	136.42	2.61	-1.34
		[±57.9/±58.8/±60.6/±55.9] s	8.36	43.58	11.37	-5.02
		[±60.7/±77.7/±72.1/±46.8] s	18.62	125.83	5.71	-2.04
		[±60.4/±70/±69.3/±54.3] s	11.04	92.52	10.22	-3.30
		[±59.3/±73.3/±70.8/±55.4] s	11.53	104.82	10.04	-3.04
		[±60.6/±78.8/±72.4/±24.2] s	52.99	150.12	1.16	-0.91
		[±57/±57.1/±57.1/±56.4] s	8.25	36.43	10.70	-5.20
		[±60/±78.2/±72.1/±44] s	21.95	128.08	4.58	-1.82
		[±59.4/±75.5/±70.3/±53.7] s	12.74	109.55	8.97	-2.79
		[±60.4/±78.3/±72.3/±32.9] s	38.13	141.25	2.06	-1.18
		[±61.3/±78.2/±72.4/±15.4] s	65.97	155.90	0.73	-0.76
128	**Max E_x Max E_y Min α_x**	[±32/±32/±32/±32] s	40.78	8.05	-5.24	11.66
		[0/0/0/0/0/0/0/0] s	277.27	7.05	-1.00	22.42
		[±0.3/±8.6/±7.4/±16.8] s	249.75	7.35	-1.61	20.78
		[±6.2/±18.7/±21.6/±1.7] s	215.49	8.10	-2.08	18.06
		[±12.2/±42.3/±31.5/±51.6] s	87.05	33.60	-1.36	1.74
		[±29.8/±31.1/±30.4/±42] s	48.42	11.98	-3.63	7.02
		[±21.3/±30.8/±33.4/±41.2] s	63.89	13.86	-3.10	6.48
		[±6/±53.9/±23.6/±42.7] s	113.68	39.97	-1.17	1.58
		[±5.1/±45.3/±62.3/±35.9] s	95.35	57.72	-0.74	0.42
		[±35.7/±43.6/±39/±45.9] s	23.14	14.32	-2.23	2.29
		[±8.5/±61.8/±62.7/±65.6] s	71.45	121.53	0.32	-0.65
	Conventional Designs	**[± 45/± 45/± 45/± 45]$_S$**	**13.31**	**13.31**	**-0.26**	**-0.26**
		[0/90/0/90/0/90/0/90]$_S$	**142.43**	**142.43**	**-0.26**	**-0.26**

Table 7.17. Tensile failure loads for $[\pm 27.3/\pm 27.3]_S$ 8 layered E-glass/epoxy laminated composite.

Loading Cases	**TENSILE LIMITS (kN/m)**			
	Tsai-Hill	**Tsai-Wu**	**Hoffman**	**Hashin-Rotem**
Nx/Ny=1	Nx=301.325 Ny=301.325	Nx=463.532 Ny=463.532	Nx=470.342 Ny=470.342	Nx(FF)=563.036 Ny(FF)=563.036 Nx(MF)=309.582 Ny(MF)=309.582
Nx/Ny=2	Nx=488.894 Ny=244.447	Nx=627.422 Ny=313.711	Nx=633.748 Ny=316.874	Nx(FF)= 569.352 Ny(FF)=284.676 Nx(MF)= 664.698 Ny(MF)=332.349
Nx/Ny=3	Nx=537.6 Ny=179.200	Nx=611.769 Ny=203.923	Nx=615.195 Ny=205.065	Nx(FF)= 571.488 Ny(FF)=190.496 Nx(MF)= 1197.08 Ny(MF)=399.028
Nx/Ny=5	Nx=539.16 Ny=107.832	Nx=574.47 Ny=114.894	Nx=575.805 Ny=115.161	Nx(FF)= 573.21 Ny(FF)=114.642 Nx(MF)= 1170.71 Ny(MF)=234.142
Nx/Ny=10	Nx=516.32 Ny=51.632	Nx=538.810 Ny=53.881	Nx=539.010 Ny=53.901	Nx(FF)=574.510 Ny(FF)=57.451 Nx(MF)=1132.400 Ny(MF)=113.240
Nx/Ny=100	Nx=483.900 Ny=4.839	Nx=504.700 Ny=5.047	Nx=504.200 Ny=5.042	Nx(FF)=575.700 Ny(FF)=5.757 Nx(MF)=969.000 Ny(MF)=9.690
Nx/Ny=1/2	Nx=148.028 Ny=296.056	Nx=197.795 Ny=395.590	Nx=199.194 Ny=398.388	Nx(FF)= 550.814 Ny(FF)=1101.628 Nx(MF)= 144.595 Ny(MF)=289.190
Nx/Ny=1/3	Nx=96.1313 Ny=288.394	Nx=116.895 Ny=350.684	Nx=117.372 Ny=352.117	Nx(FF)= 539.112 Ny(FF)=1617.336 Nx(MF)= 93.949 Ny(MF)=281.847
Nx/Ny=1/5	Nx=56.147 Ny=280.734	Nx=63.045 Ny=315.226	Nx=63.182 Ny=315.912	Nx(FF)= 517.139 Ny(FF)=2585.695 Nx(MF)=55.178 Ny(MF)=275.891
Nx/Ny=1/10	Nx=27.432 Ny=274.322	Nx=29.044 Ny=290.444	Nx=29.075 Ny=290.750	Nx(FF)=469.318 Ny(FF)=4693.176 Nx(MF)=27.140 Ny(MF)=271.404
Nx/Ny=1/100	Nx=2.682 Ny=268.192	Nx=2.699 Ny=269.893	Nx=2.670 Ny=269.960	Nx(FF)=176.136 Ny(FF)=17613.637 Nx(MF)=2.674 Ny(MF)=267.366
Nx=Ny=Nxy	Nx=175.442 Ny=175.442	Nx=152.722 Ny=152.722	Nx=152.486 Ny=152.486	Nx(FF)= 237.515 Ny(FF)=237.515 Nx(MF)= 573.651 Ny(MF)=573.651

Table 7.18. Effect of thermal changes to tensile failure loads for $[\pm 27.3/\pm 27.3]_S$ 8 layered E-glass/epoxy laminated composite.

Loading Cases	**TENSILE LIMITS (kN/m)**			
	Tsai-Hill	**Tsai-Wu**	**Hoffman**	**Hashin-Rotem**
Nx/Ny=1 $\Delta T = 0^{\circ}C$	Nx=300.890 Ny=300.890	Nx=463.194 Ny=463.194	Nx=470.003 Ny=470.003	Nx(FF)=563.649 Ny(FF)=563.649 Nx(MF)=309.582 Ny(MF)= 309.582
Nx/Ny=1 $\Delta T = -10^{\circ}C$	Nx=300.890 Ny=300.890	Nx=463.194 Ny=463.194	Nx=470.003 Ny=470.003	Nx(FF)=563.649 Ny(FF)=563.649 Nx(MF)=308.921 Ny(MF)=308.921
Nx/Ny=1 $\Delta T = -20^{\circ}C$	Nx=300.451 Ny=300.451	Nx=462.849 Ny=462.849	Nx=469.657 Ny=469.657	Nx(FF)=564.263 Ny(FF)=564.263 Nx(MF)=308.258 Ny(MF)=308.258
Nx/Ny=1 $\Delta T = -30^{\circ}C$	Nx=300.009 Ny=300.009	Nx=462.499 Ny=462.499	Nx=468.305 Ny=469.305	Nx(FF)=564.877 Ny(FF)=564.877 Nx(MF)=307.592 Ny(MF)=307.592
Nx/Ny=1 $\Delta T = -50^{\circ}C$	Nx=299.114 Ny=299.114	Nx=461.779 Ny=461.779	Nx=468.582 Ny=468.582	Nx(FF)=566.105 Ny(FF)=566.105 Nx(MF)=306.255 Ny(MF)=306.255
Nx/Ny=1 $\Delta T = -70^{\circ}C$	Nx=298.205 Ny=298.205	Nx=461.035 Ny=461.035	Nx=467.835 Ny=467.835	Nx(FF)=567.332 Ny(FF)=567.332 Nx(MF)=304.909 Ny(MF)=304.909
Nx/Ny=1 $\Delta T = -90^{\circ}C$	Nx=297.281 Ny=297.281	Nx=460.266 Ny=460.266	Nx=467.062 Ny=467.062	Nx(FF)=568.560 Ny(FF)=568.560 Nx(MF)=303.554 Ny(MF)=303.554
Nx/Ny=1 $\Delta T = -110^{\circ}C$	Nx=296.342 Ny=296.342	Nx=459.472 Ny=459.472	Nx=466.263 Ny=466.263	Nx(FF)=569.788 Ny(FF)=569.788 Nx(MF)=302.191 Ny(MF)=302.191

Table 7.19. Compression failure loads for $[\pm 27.3/\pm 27.3]_S$ 8 layered E-glass/epoxy laminated composite.

Loading Cases	**COMPRESSION LIMITS (kN/m)**			
	Tsai-Hill	**Tsai-Wu**	**Hoffman**	**Hashin-Rotem**
Nx/Ny=1	Nx=-301.325 Ny=-301.325	Nx=-298.419 Ny=-298.419	Nx=-301.325 Ny=-301.325	Nx(FF)=-254.274 Ny(FF)=-254.274 Nx(MF)=-309.582 Ny(MF)=-309.582
Nx/Ny=2	Nx=-488.894 Ny=-244.447	Nx=-304.306 Ny=-152.153	Nx=-305.786 Ny=-152.893	Nx(FF)= -257.126 Ny(FF)=-128.563 Nx(MF)= -664.698 Ny(MF)= -332.349
Nx/Ny=3	Nx=-537.6 Ny=-179.200	Nx=-286.272 Ny=-95.424	Nx=-287.019 Ny=-95.673	Nx(FF)= -258.093 Ny(FF)=-86.031 Nx(MF)= -1197.08 Ny(MF)=-399.028
Nx/Ny=5	Nx=-539.16 Ny=-107.832	Nx=-267.93 Ny=-53.586	Nx=-268.22 Ny=-53.644	Nx(FF)= 258.87 Ny(FF)=51.774 Nx(MF)= -1251.49 Ny(MF)=-250.298
Nx/Ny=10	Nx=-516.320 Ny=-51.632	Nx=-253.340 Ny=-25.334	Nx=-253.380 Ny=-25.338	Nx(FF)=-259.460 Ny(FF)=-25.946 Nx(MF)=-1134.460 Ny(MF)=-113.446
Nx/Ny=100	Nx=-483.900 Ny=-4.839	Nx=-240.300 Ny=-2.403	Nx=-240.100 Ny=-2.401	Nx(FF)=-260.000 Ny(FF)=-2.600 Nx(MF)=-982.600 Ny(MF)=-9.826
Nx/Ny=1/2	Nx=-148.028 Ny=-296.056	Nx=-190.404 Ny=-380.808	Nx=-191.700 Ny=-383.400	Nx(FF)=- 248.755 Ny(FF)=-497.510 Nx(MF)= -200.103 Ny(MF)=-400.205
Nx/Ny=1/3	Nx=-96.1313 Ny=-288.394	Nx=-128.973 Ny=-386.919	Nx=-129.555 Ny=-388.664	Nx(FF)= -243.47 Ny(FF)=-730.410 Nx(MF)= -128.607 Ny(MF)=-385.822
Nx/Ny=1/5	Nx=-56.1468 Ny=-280.734	Nx=-76.5364 Ny=-382.682	Nx=-76.7386 Ny=-383.693	Nx(FF)= -233.547 Ny(FF)=-1167.733 Nx(MF)= -74.848 Ny(MF)=-374.240
Nx/Ny=1/10	Nx=-27.432 Ny=-274.322	Nx=-37.528 Ny=-375.275	Nx=-37.579 Ny=-375.786	Nx(FF)=-211.950 Ny(FF)=-2119.499 Nx(MF)=-36.559 Ny(MF)=-365.594
Nx/Ny=1/100	Nx=-2.682 Ny=-268.192	Nx=-3.663 Ny=-366.343	Nx=-3.665 Ny=-366.467	Nx(FF)=-79.545 Ny(FF)=-7954.546 Nx(MF)=-3.579 Ny(MF)=-357.883
Nx=Ny=Nxy	Nx=-229.707 Ny=-229.707	Nx=-111.625 Ny=-111.625	Nx=-111.740 Ny=-111.740	Nx(FF)= -107.265 Ny(FF)=-107.265 Nx(MF)= -623.179 Ny(MF)=-623.179

Table 7.20. Effect of thermal changes to compression failure loads for 8 layered $[\pm 27.3/\pm 27.3]_S$ E-glass/epoxy laminated composite.

Loading Cases	**COMPRESSION LIMITS (kN/m)**			
	Tsai-Hill	**Tsai-Wu**	**Hoffman**	**Hashin-Rotem**
Nx/Ny=1 $\Delta T = 0^{\circ}C$	Nx=-301.325 Ny=-301.325	Nx=-298.419 Ny=-298.419	Nx=-301.325 Ny=-301.325	Nx(FF)=-254.274 Ny(FF)= -254.274 Nx(MF)=-309.582 Ny(MF)= -309.582
Nx/Ny=1 $\Delta T = -10^{\circ}C$	Nx=-301.757 Ny=-301.757	Nx=-298.020 Ny=-298.020	Nx=-300.822 Ny=-300.822	Nx(FF)= -253.660 Ny(FF)=-253.660 Nx(MF)= 440.001 Ny(MF)=-440.001
Nx/Ny=1 $\Delta T = -20^{\circ}C$	Nx=-302.184 Ny=-302.184	Nx=-297.616 Ny=-297.616	Nx=-300.412 Ny=-300.412	Nx(FF)= -253.046 Ny(FF)=-253.046 Nx(MF)=- 440.563 Ny(MF)=-440.563
Nx/Ny=1 $\Delta T = -30^{\circ}C$	Nx=-302.609 Ny=-302.609	Nx=-297.205 Ny=-297.205	Nx=-299.995 Ny=-299.995	Nx(FF)= -252.433 Ny(FF)=-252.433 Nx(MF)=- 441.122 Ny(MF)=-441.122
Nx/Ny=1 $\Delta T = -50^{\circ}C$	Nx=-303.446 Ny=-303.446	Nx=-296.366 Ny=-296.366	Nx=-299.142 Ny=-299.142	Nx(FF)= -251.205 Ny(FF)=-251.205 Nx(MF)= -442.231 Ny(MF)=-442.231
Nx/Ny=1 $\Delta T = -70^{\circ}C$	Nx=-304.270 Ny=-304.270	Nx=-295.502 Ny=-295.502	Nx=-298.265 Ny=-298.265	Nx(FF)= -249.977 Ny(FF)=-249.977 Nx(MF)= -443.327 Ny(MF)=-443.327
Nx/Ny=1 $\Delta T = -90^{\circ}C$	Nx=-305.079 Ny=-305.079	Nx=-294.613 Ny=-294.613	Nx=-297.362 Ny=-297.362	Nx(FF)= -248.750 Ny(FF)=-248.750 Nx(MF)= -444.411 Ny(MF)=-444.411
Nx/Ny=1 $\Delta T = -110^{\circ}C$	Nx=-305.874 Ny=-305.874	Nx=-293.699 Ny=-293.699	Nx=-296.435 Ny=-296.435	Nx(FF)=- 247.522 Ny(FF)=-247.522 Nx(MF)= -445.483 Ny(MF)=-445.483

Table 7.21. Effect of stacking sequences with thermal changes to failure loads for different 8 layered E-glass/epoxy laminated composite.

Stacking Sequences & Thermal Changes	**TENSILE FAILURE LOADS (kN/m)**			
	Tsai-Hill	**Tsai-Wu**	**Hoffman**	**Hashin-Rotem**
$[\pm 27.3/\pm 27.3]_S$ $\Delta T = 0^\circ C$	Nx=300.890 Ny=300.890	Nx=463.194 Ny=463.194	Nx=470.003 Ny=470.003	Nx(FF)=563.649 Ny(FF)=563.649 Nx(MF)=309.582 Ny(MF)= 309.582
$[\pm 27.3/\pm 27.3]_S$ $\Delta T = -110^\circ C$	Nx=296.342 Ny=296.342	Nx=459.472 Ny=459.472	Nx=466.263 Ny=466.263	Nx(FF)=569.788 Ny(FF)=569.788 Nx(MF)=302.191 Ny(MF)=302.191
$[\pm 72.9/\pm 72.9]_S$ $\Delta T = 0^\circ C$	Nx=286.854 Ny=286.854	Nx=440.815 Ny=440.815	Nx=447.007 Ny=447.007	Nx(FF)=599.798 Ny(FF)=599.798 Nx(MF)=289.016 Ny(MF)= 289.016
$[\pm 72.9/\pm 72.9]_S$ $\Delta T = -110^\circ C$	Nx=285.221 Ny=285.221	Nx=439.130 Ny=439.130	Nx=445.301 Ny=445.301	Nx(FF)=602.192 Ny(FF)=602.192 Nx(MF)=286.793 Ny(MF)= 286.793
$[0/90/0/90]_S$ $\Delta T = 0^\circ C$	Nx=339.059 Ny=339.059	Nx=500.054 Ny=500.054	Nx=507.303 Ny=507.303	Nx(FF)=492.399 Ny(FF)=492.399 Nx(MF)=377.941 Ny(MF)= 377.941
$[0/90/0/90]_S$ $\Delta T = -110^\circ C$	Nx=326.127 Ny=326.127	Nx=496.799 Ny=496.799	Nx=504.286 Ny=504.286	Nx(FF)=507.523 Ny(FF)=507.523 Nx(MF)=352.235 Ny(MF)= 352.235
$[\pm 45/\pm 45]_S$ $\Delta T = 0^\circ C$	Nx=339.059 Ny=339.059	Nx=500.054 Ny=500.054	Nx=507.303 Ny=507.303	Nx(FF)=492.399 Ny(FF)=492.399 Nx(MF)=377.941 Ny(MF)= 377.941
$[\pm 45/\pm 45]_S$ $\Delta T = -110^\circ C$	Nx=326.127 Ny=326.127	Nx=496.799 Ny=496.799	Nx=504.286 Ny=504.286	Nx(FF)=507.523 Ny(FF)=507.523 Nx(MF)=352.235 Ny(MF)= 352.235
$[0/45/0/45]_S$ $\Delta T = 0^\circ C$	Nx=293.090 Ny=293.090	Nx=451.180 Ny=451.180	Nx=457.667 Ny=457.667	Nx(FF)=583.071 Ny(FF)=583.071 Nx(MF)=297.603 Ny(MF)= 297.603
$[0/45/0/45]_S$ $\Delta T = -110^\circ C$	Nx=289.996 Ny=289.996	Nx=448.274 Ny=448.274	Nx=454.733 Ny=454.733	Nx(FF)=587.448 Ny(FF)=587.448 Nx(MF)=293.239 Ny(MF)= 293.239

Table 7.22. Tensile failure loads for $[\pm 32/\pm 32]_S$ 8 layered carbon/epoxy laminated composite.

Loading Cases	TENSILE LIMITS (kN/m)			
	Tsai-Hill	**Tsai-Wu**	**Hoffman**	**Hashin-Rotem**
Nx/Ny=1	Nx=151.995 Ny=151.995	Nx=155.204 Ny=155.204	Nx=147.782 Ny=147.782	Nx(FF)=1097.073 Ny(FF)=1097.073 Nx(MF)=153.147 Ny(MF)=153.147
Nx/Ny=2	Nx=585.660 Ny=292.830	Nx=672.925 Ny=336.462	Nx=569.832 Ny=284.916	Nx(FF)= 1275.762 Ny(FF)=637.881 Nx(MF)= 653.742 Ny(MF)=326.871
Nx/Ny=3	Nx=1201.892 Ny=400.630	Nx=1216.099 Ny=405.366	Nx=1221.399 Ny=407.133	Nx(FF)= 1349.004 Ny(FF)=449.668 Nx(MF)= 2650.503 Ny(MF)=883.501
Nx/Ny=5	Nx=581.464 Ny=116.293	Nx=904.200 Ny=180.840	Nx=1041.270 Ny=208.254	Nx(FF)= 1413.94 Ny(FF)=282.788 Nx(MF)= 641.655 Ny(MF)=128.331
Nx/Ny=10	Nx=377.539 Ny=37.754	Nx=701.888 Ny=70.188	Nx=798.970 Ny=79.897	Nx(FF)=1466.900 Ny(FF)=146.690 Nx(MF)=392.140 Ny(MF)=39.214
Nx/Ny=100	Nx=284.017 Ny=2.840	Nx=576.693 Ny=5.767	Nx=644.000 Ny=6.440	Nx(FF)=1518.100 Ny(FF)=15.181 Nx(MF)=289.900 Ny(MF)=2.899
Nx/Ny=1/2	Nx=60.228 Ny=120.457	Nx=59.353 Ny=118.706	Nx=57.977 Ny=115.954	Nx(FF)= 857.003 Ny(FF)=1714.005 Nx(MF)= 60.314 Ny(MF)= 120.627
Nx/Ny=1/3	Nx=37.522 Ny=112.567	Nx=36.650 Ny=109.951	Nx=36.013 Ny=108.040	Nx(FF)=7036.333 Ny(FF)=2110.900 Nx(MF)=37.547 Ny(MF)=112.637
Nx/Ny=1/5	Nx= 21.388 Ny=106.940	Nx=20.760 Ny=103.798	Nx=20.483 Ny=102.414	Nx(FF)= 517.362 Ny(FF)=2586.811 Nx(MF)= 21.393 Ny(MF)= 106.965
Nx/Ny=1/10	Nx=10.307 Ny=103.065	Nx=9.960 Ny=99.605	Nx=9.855 Ny=98.550	Nx(FF)=311.566 Ny(FF)=3115.663 Nx(MF)=10.307 Ny(MF)=103.071
Nx/Ny=1/100	Nx=0.998 Ny=99.804	Nx=0.961 Ny=96.103	Nx=0.953 Ny=95.304	Nx(FF)=38.182 Ny(FF)=3818.204 Nx(MF)=0.998 Ny(MF)=99.799
Nx=Ny=Nxy	Nx=141.408 Ny=141.408	Nx=134.337 Ny=134.337	Nx=150.952 Ny=150.952	Nx(FF)=473.638 Ny(FF)=473.638 Nx(MF)=165.797 Ny(MF)=165.797

Table 7.23. Effect of thermal changes to tensile failure loads for $[\pm 32/\pm 32]_S$ 8 layered carbon/ epoxy laminated composite.

Loading Cases	**TENSILE LIMITS (kN/m)**			
	Tsai-Hill	**Tsai-Wu**	**Hoffman**	**Hashin-Rotem**
Nx/Ny=1 $\Delta T = 0^{\circ}C$	Nx=151.995 Ny=151.995	Nx=155.204 Ny=155.204	Nx=147.782 Ny=147.782	Nx(FF)=1097.073 Ny(FF)=1097.073 Nx(MF)=153.147 Ny(MF)=153.147
Nx/Ny=1 $\Delta T = -10^{\circ}C$	Nx=149.316 Ny=149.316	Nx=152.773 Ny=152.773	Nx=145.414 Ny=145.414	Nx(FF)=1097.868 Ny(FF)= 1097.868 Nx(MF)=150.407 Ny(MF)= 150.407
Nx/Ny=1 $\Delta T = -20^{\circ}C$	Nx=146.607 Ny=146.607	Nx=150.301 Ny=150.301	Nx=143.012 Ny=143.012	Nx(FF)=1098.662 Ny(FF)= 1098.662 Nx(MF)=147.638 Ny(MF)= 147.638
Nx/Ny=1 $\Delta T = -30^{\circ}C$	Nx=143.868 Ny=143.868	Nx=147.789 Ny=147.789	Nx=140.575 Ny=140.575	Nx(FF)=1099.457 Ny(FF)= 1099.457 Nx(MF)=144.840 Ny(MF)=144.840
Nx/Ny=1 $\Delta T = -50^{\circ}C$	Nx=138.302 Ny=138.302	Nx=142.641 Ny=142.641	Nx=135.595 Ny=135.595	Nx(FF)=1101.045 Ny(FF)=1101.045 Nx(MF)=139.162 Ny(MF)=139.162
Nx/Ny=1 $\Delta T = -70^{\circ}C$	Nx=132.618 Ny=132.618	Nx=137.322 Ny=137.322	Nx=130.470 Ny=130.470	Nx(FF)=1102.634 Ny(FF)=1102.634 Nx(MF)=133.370 Ny(MF)=133.370
Nx/Ny=1 $\Delta T = -90^{\circ}C$	Nx=126.815 Ny=126.815	Nx=131.828 Ny=131.828	Nx=125.194 Ny=125.194	Nx(FF)=1104.223 Ny(FF)=1104.223 Nx(MF)=127.466 Ny(MF)=127.466
Nx/Ny=1 $\Delta T = -110^{\circ}C$	Nx=120.891 Ny=120.891	Nx=126.152 Ny=126.152	Nx=119.763 Ny=119.763	Nx(FF)=1105.811 Ny(FF)=1105.811 Nx(MF)=121.447 Ny(MF)=121.447

Table 7.24. Compression failure loads for $[\pm 32/\pm 32]_S$ 8 layered carbon/epoxy laminated composite.

Loading Cases	COMPRESSION LIMITS (kN/m)			
	Tsai-Hill	**Tsai-Wu**	**Hoffman**	**Hashin-Rotem**
Nx/Ny=1	Nx=-151.995 Ny=-151.995	Nx=-468.487 Ny=-468.487	Nx=-406.816 Ny=-406.816	Nx(FF)=-914.228 Ny(FF)=- 914.228 Nx(MF)=-332.912 Ny(MF)=- 332.912
Nx/Ny=2	Nx=-584.760 Ny=-292.380	Nx=-1889.158 Ny=-944.579	Nx=-1252.834 Ny=-626.417	Nx(FF)=- 1063.136 Ny(FF)=-531.568 Nx(MF)=- 1912.34 Ny(MF)=-956.170
Nx/Ny=3	Nx=-1201.893 Ny=-400.631	Nx=-1017.417 Ny=-339.139	Nx=-1021.125 Ny=-340.375	Nx(FF)=- 1124.169 Ny(FF)=-374.723 Nx(MF)=- 2652.861 Ny(MF)=-884.287
Nx/Ny=5	Nx=-581.465 Ny=-116.293	Nx=-462.885 Ny=-92.577	Nx=-496.33 Ny=-99.266	Nx(FF)=- 1178.285 Ny(FF)=-235.657 Nx(MF)=- 980.75 Ny(MF)=-196.150
Nx/Ny=10	Nx=-377.540 Ny=-37.754	Nx=-317.510 Ny=-31.751	Nx=-335.980 Ny=-33.598	Nx(FF)=-1222.420 Ny(FF)=-122.242 Nx(MF)=-659.710 Ny(MF)=-65.971
Nx/Ny=100	Nx=-284.000 Ny=-2.840	Nx=-246.200 Ny=-2.462	Nx=-258.800 Ny=-2.588	Nx(FF)=-1265.100 Ny(FF)=-12.651 Nx(MF)=-509.100 Ny(MF)=-5.091
Nx/Ny=1/2	Nx=-60.2285 Ny=-120.457	Nx=-171.351 Ny=-342.702	Nx=-160.3605 Ny=-320.721	Nx(FF)=- 714.169 Ny(FF)=-1428.338 Nx(MF)=- 124.883 Ny(MF)=-249.766
Nx/Ny=1/3	Nx=-37.522 Ny=-112.567	Nx=-104.505 Ny=-313.516	Nx=-99.489 Ny=-298.468	Nx(FF)=- 585.947 Ny(FF)=-1757.841 Nx(MF)=-76.844 Ny(MF)=-230.531
Nx/Ny=1/5	Nx=-21.388 Ny=-106.940	Nx=-58.661 Ny=-293.305	Nx=-56.505 Ny=-282.523	Nx(FF)=- 431.135 Ny(FF)=-2155.676 Nx(MF)=- 43.429 Ny(MF)=-217.145
Nx/Ny=1/10	Nx=-10.307 Ny=-103.065	Nx=-27.968 Ny=-279.684	Nx=-27.153 Ny=-271.525	Nx(FF)=-259.639 Ny(FF)=-2596.386 Nx(MF)=-20.808 Ny(MF)=-208.079
Nx/Ny=1/100	Nx=-0.998 Ny=-99.804	Nx=-2.684 Ny=-268.408	Nx=-2.623 Ny=-262.266	Nx(FF)=-31.818 Ny(FF)=- 3181.837 Nx(MF)=-2.005 Ny(MF)=-200.541
Nx=Ny=Nxy	Nx=-157.210 Ny=-157.210	Nx=-418.018 Ny=-418.018	Nx=-327.799 Ny=-327.799	Nx(FF)=- 394.698 Ny(FF)=- 394.698 Nx(MF)=- 320.061 Ny(MF)=- 320.061

Table 7.25. Effect of thermal changes to compression failure loads for 8 layered $[\pm 32/\pm 32]_S$ carbon/epoxy laminated composite.

Loading Cases	**COMPRESSION LIMITS (kN/m)**			
	Tsai-Hill	**Tsai-Wu**	**Hoffman**	**Hashin-Rotem**
Nx/Ny=1 $\Delta T = 0^{\circ}C$	Nx=-151.995 Ny=-151.995	Nx=-468.487 Ny=-468.487	Nx=-406.816 Ny=-406.816	Nx(FF)=-914.228 Ny(FF)=- 914.228 Nx(MF)=-332.912 Ny(MF)=- 332.912
Nx/Ny=1 $\Delta T = -10^{\circ}C$	Nx=-154.646 Ny=-154.646	Nx=-468.047 Ny=-468.047	Nx=-406.585 Ny=-406.585	Nx(FF)= -913.434 Ny(FF)= -913.434 Nx(MF)= -332.276 Ny(MF)= -332.276
Nx/Ny=1 $\Delta T = -20^{\circ}C$	Nx=-157.266 Ny=-157.266	Nx=-467.567 Ny=-467.567	Nx=-406.320 Ny=-406.320	Nx(FF)=- 912.639 Ny(FF)=- 912.639 Nx(MF)=- 331.621 Ny(MF)=- 331.621
Nx/Ny=1 $\Delta T = -30^{\circ}C$	Nx=-159.858 Ny=-159.858	Nx=-467.047 Ny=-467.047	Nx=-406.020 Ny=-406.020	Nx(FF)=- 911.845 Ny(FF)=- 911.845 Nx(MF)=- 330.948 Ny(MF)=- 330.948
Nx/Ny=1 $\Delta T = -50^{\circ}C$	Nx=-164.952 Ny=-164.952	Nx=-465.881 Ny=-465.881	Nx=-405.315 Ny=-405.315	Nx(FF)=- 910.256 Ny(FF)=- 910.256 Nx(MF)=- 329.548 Ny(MF)=- 329.548
Nx/Ny=1 $\Delta T = -70^{\circ}C$	Nx=-169.928 Ny=-169.928	Nx=-464.546 Ny=-464.546	Nx=-404.464 Ny=-404.464	Nx(FF)=- 908.667 Ny(FF)=- 908.667 Nx(MF)=- 328.076 Ny(MF)=- 328.076
Nx/Ny=1 $\Delta T = -90^{\circ}C$	Nx=-174.784 Ny=-174.784	Nx=-463.035 Ny=-463.035	Nx=-403.463 Ny=-403.463	Nx(FF)=- 907.078 Ny(FF)=- 907.078 Nx(MF)=- 326.532 Ny(MF)=- 326.532
Nx/Ny=1 $\Delta T = -110^{\circ}C$	Nx=-179.520 Ny=-179.520	Nx=-461.342 Ny=-461.342	Nx=-402.307 Ny=-402.307	Nx(FF)=- 905.490 Ny(FF)=- 905.490 Nx(MF)=- 324.916 Ny(MF)=- 324.916

Table 7.26. Effect of stacking sequences with thermal changes to tensile failure loads for different 8 layered carbon/epoxy laminated composite (N_x/N_y=1).

Stacking Sequences & Thermal Changes	**TENSILE FAILURE LOADS (kN/m)**			
	Tsai-Hill	**Tsai-Wu**	**Hoffman**	**Hashin-Rotem**
$[\pm 32/\pm 32]_S$ $\Delta T = 0^\circ C$	Nx=151.995 Ny=151.995	Nx=155.204 Ny=155.204	Nx=147.782 Ny=147.782	Nx(FF)=1097.073 Ny(FF)=1097.073 Nx(MF)=153.147 Ny(MF)=153.147
$[\pm 32/\pm 32]_S$ $\Delta T = -110^\circ C$	Nx=120.891 Ny=120.891	Nx=126.152 Ny=126.152	Nx=119.763 Ny=119.763	Nx(FF)=1105.811 Ny(FF)=1105.811 Nx(MF)=121.447 Ny(MF)=121.447
$[90/90/90/90]_S$ $\Delta T = 0^\circ C$	Nx=60.000 Ny=60.000	Nx=61.166 Ny=61.166	Nx=60.289 Ny=60.289	Nx(FF)=1800.000 Ny(FF)= 1800.000 Nx(MF)=60.000 Ny(MF)= 60.000
$[90/90/90/90]_S$ $\Delta T = -110^\circ C$	Nx=60.000 Ny=60.000	Nx=61.166 Ny=61.166	Nx=60.289 Ny=60.289	Nx(FF)=1800.000 Ny(FF)= 1800.000 Nx(MF)=60.000 Ny(MF)= 60.000
$[0/90/0/90]_S$ $\Delta T = 0^\circ C$	Nx=671.366 Ny=671.366	Nx=742.152 Ny=742.152	Nx=625.771 Ny=625.771	Nx(FF)= 929.211 Ny(FF)= 929.211 Nx(MF)= 954.317 Ny(MF)= 954.317
$[0/90/0/90]_S$ $\Delta T = -110^\circ C$	Nx=491.484 Ny=491.484	Nx=606.284 Ny=606.284	Nx=472.393 Ny=472.393	Nx(FF)= 940.035 Ny(FF)= 940.035 Nx(MF)= 620.811 Ny(MF)= 620.811
$[\pm 45/\pm 45]_S$ $\Delta T = 0^\circ C$	Nx=671.366 Ny=671.366	Nx=742.152 Ny=742.152	Nx=625.771 Ny=625.771	Nx(FF)= 929.211 Ny(FF)= 929.211 Nx(MF)= 954.317 Ny(MF)= 954.317
$[\pm 45/\pm 45]_S$ $\Delta T = -110^\circ C$	Nx=491.484 Ny=491.484	Nx=606.284 Ny=606.284	Nx=472.394 Ny=472.394	Nx(FF)= 940.035 Ny(FF)= 940.035 Nx(MF)= 620.811 Ny(MF)= 620.811
$[0/45/0/45]_S$ $\Delta T = 0^\circ C$	Nx=85.624 Ny=85.624	Nx=87.236 Ny=87.236	Nx=85.041 Ny=85.041	Nx(FF)= 1365.448 Ny(FF)= 1365.448 Nx(MF)= 85.705 Ny(MF)= 85.705
$[0/45/0/45]_S$ $\Delta T = -110^\circ C$	Nx=76.604 Ny=76.604	Nx=78.600 Ny=78.600	Nx=76.679 Ny=76.679	Nx(FF)= 1370.850 Ny(FF)= 1370.850 Nx(MF)= 76.647 Ny(MF)= 76.647

Table 7.27. Effect of number of layers to tensile failure loads for optimized E-glass/ epoxy and carbon/epoxy laminated composites (Nx/Ny=1)

Stacking Sequences & Material	**TENSILE FAILURE LOADS (kN/m)**			
	Tsai-Hill	**Tsai-Wu**	**Hoffman**	**Hashin-Rotem**
[±27.3] $_S$ (4 layered EGlass/Epoxy)	Nx=150.663 Ny=150.663	Nx=231.766 Ny=231.766	Nx=235.171 Ny=235.171	Nx(FF)= 281.518 Ny(FF)= 281.518 Nx(MF)= 154.791 Ny(MF)= 154.791
[±27.3/±27.3] $_S$ (8 layered EGlass/Epoxy)	Nx=300.890 Ny=300.890	Nx=463.194 Ny=463.194	Nx=470.003 Ny=470.003	Nx(FF)=563.649 Ny(FF)=563.649 Nx(MF)=309.582 Ny(MF)= 309.582
[±27.3/±27.3/±27.3] $_S$ (12 layered EGlass/Epoxy)	Nx=451.988 Ny=451.988	Nx=695.298 Ny=695.298	Nx=705.514 Ny=705.514	Nx(FF)=844.553 Ny(FF)=844.553 Nx(MF)=464.373 Ny(MF)=464.373
[±27.3/±27.3/±27.3/±27.3] $_S$ (16 layered EGlass/Epoxy)	Nx=602.650 Ny=602.650	Nx=927.064 Ny=927.064	Nx=940.685 Ny=940.685	Nx(FF)=1126.071 Ny(FF)=1126.071 Nx(MF)=619.164 Ny(MF)=619.164
[±32] $_S$ (4 layered carbon/epoxy)	Nx=75.998 Ny=75.998	Nx=77.602 Ny=77.602	Nx=73.891 Ny=73.891	Nx(FF)=548.537 Ny(FF)=548.537 Nx(MF)=76.574 Ny(MF)=76.574
[±32/±32] $_S$ (8 layered carbon/epoxy)	Nx=151.995 Ny=151.995	Nx=155.204 Ny=155.204	Nx=147.782 Ny=147.782	Nx(FF)=1097.073 Ny(FF)=1097.073 Nx(MF)=153.147 Ny(MF)=153.147
[±32/±32/±32] $_S$ (12 layered carbon/epoxy)	Nx=227.993 Ny=227.993	Nx=232.807 Ny=232.807	Nx=221.674 Ny=221.674	Nx(FF)=1645.610 Ny(FF)=1645.610 Nx(MF)=229.722 Ny(MF)=229.722
[±32/±32/±32/±32] $_S$ (16 layered carbon/epoxy)	Nx=303.991 Ny=303.991	Nx=310.409 Ny=310.409	Nx=295.565 Ny=295.565	Nx(FF)=2194.146 Ny(FF)=2194.146 Nx(MF)=306.295 Ny(MF)=306.295

The thermal tests have also been performed for different E-glass/epoxy composites with the stacking sequences [27/-27/-27/27], [0/0/0/0], [45/-45/-45/45], and [0/90/90/0] in order to compare theoretical and experimental values of CTEs. According to results given in Table 7.28, for the [27/-27/-27/27], [0/0/0/0], and [45/-45/-45/45] composites, theoretical results are good agreement with the experimental data. However, results for [0/90/90/0] composite, theoretical prediction overestimates the experimental data. In

order to find reasons of differences between theoretical and experimental CTE data for [0/90/90/0] composite, I have calculated fiber volume fractions and densities and results are given in Table 7.29. As it is seen from the table, the values for fiber volume fraction and density are not so much differ. In this case, I can interpret why dramatic differences between theoretical and experimental results occurs as follows: In order to find CTE values, DMA works in tensile mode. Since 90^o fibers prevent expansion, it can not be measured the data accurately. If we compare the CTE values for [27/-27/-27/27] (optimized stacking sequences) with conventional designs in Table 7.28, the minimum value as expected is reached by optimum design.

Table 7.28. Comparison of the theoretical and experimental coefficient of thermal expansions (CTEs) for optimized and conventional stacking sequences.

Fiber Orientation	**Theoretical CTE** $(10^{-6}/^{\circ}C)$	**Experimental CTE** $(10^{-6}/^{\circ}C)$	**Error (%)**
[27/-27/-27/27]	8.61	9.64	12
[0/0/0/0]	10.02	12.57	25
[45/-45/-45/45]	16.83	14.15	19
[0/90/90/0]	16.83	9.0	87

Table 7.29. Differences in fiber volume fraction V_f and density of the composite for optimized and conventional stacking sequences.

Stacking Sequence	V_f	**Standard Deviation**	**Density** (g/cm^3)	**Standard Deviation**
[0/0/0/0]	0.43	0.0188	1.64	0.0885
[0/90/90/0]	0.44	0.0101	1.49	0.0611
[27/-27/-27/27]	0.43	0.0162	1.40	0.0584
[45/-45/-45/45]	0.45	0.0221	1.49	0.0768

CHAPTER 8

COMPARISON OF THE STOCHASTIC OPTIMIZATION TECHNIQUES IN THE COMPOSITES

8.1. The Problem Definitions

In this chapter, design and optimization of dimensionally stable symmetric-balance $(\pm\theta_1/\pm\theta_2)_s$ eight-layered carbon/epoxy laminated composite plate satisfying the conditions low CTE in longitudinal and high elastic moduli in longitudinal and/or transverse directions. have been considered . The design is consist of three main parts: mechanical analysis, optimization and stress analysis.

In the first part, simplified micromechanics expressions are used to predict the stiffness and thermal expansion coefficients of a lamina using constituent material properties. The classical lamination theory is utilized to determine the effective elastic modulus and the effective thermal expansion coefficients.

In optimization part, the problems (see Table 8.1) are formulated as multi-objective optimization problems and solved using GA. Then, an alternative single-objective formulations are utilized for verification of the multi-objective approach. The stochastic search methods GA, GPSA and SA have been used to solve single-objective optimization problems. The effective elastic moduli and the thermal expansion coefficient have been defined as fitness functions of the optimization problems. The fiber orientation angles θ_1 and θ_2 are selected as design variables and the limiting values are $-90 \le \theta_1, \theta_2 \le 90$ in the continous domain. The fiber volume fraction and thickness of each layer are assumed as 0.50 and $150.10^{-6} m$, respectively. The solvers *ga, patternsearch, simulannealbnd* and *gamultiobj* of MATLAB *Optimization Toolbox* and *Symbolic Math Toolbox* are used to obtain Pareto-optimal and best designs for 12 different model problems.

After completing the design process, stress distributions through the thickness have been investigated for the optimized composites subjected to the hygral, thermal and mechanical loadings.

.In this chapter, three main problems (1a, 2a, 3a) are considered defining in-plane designs and optimization of thin plate composites. The optimization problems are firstly formulated based on multi-objective approach. An alternative single-objective formulations including the nonlinear constraints are utilized for verification of the multi-objective optimizition. Multi-objective optimization problems (1a, 2a, 3a) aim to minimize the CTE while simultaneously maximizing the elastic moduli. In the single-objective representation of the problems (1b-d, 2b-d, 3b-d), CTE obtained from the multi-objective formulations are used to define the nonlinear constraints of the single optimization problems. This proposed approach is quite recommended since it is possible to obtain relatively small feasible solution space and it clarifies definition of the front. Details of these model problems with different loading cases (Le Rich & Gaudin, 1998) optimization types, objective functions, constraints and bound are presented in Table 8.1.

In the last part, optimized composites, obtained from multi-objective design, have been considered for stress analysis. Stress distributions through the thickness of the composites subjected to the mechanical , thermal and hygral loadings have been calculated and shown graphically in Figures 8.2-8.5

Comparison studies for optimization of laminated composites are very few in literature and therefore, the present study fills a gap in composite design. Both of multi-objective and single-objective approaches have been considered to verify the study mathematically. However, in literature, either single-objective or multi-objective aproach have been used for composite design and optimization.

Table 8.1. Model problems

Problems	Loadings	Optimization Types	Objective Functions	Constraints& Bound
1a	LC1	Multi-objective GA	E_x, α_x (for Multi-obj.)	B1
1b		Single-objective GA	E_x (for Single-obj.)	C1
1c		Single-objective GPSA		
1d		Single-objective SA		
2a	LC1	Multi-objective GA	E_x, E_y, α_x (for Multi-obj.)	B1
2b		Single-objective GA	E_x (for Single-obj.)	C2
2c		Single-objective GPSA		
2d		Single-objective SA		
3a	LC2	Multi-objective GA	E_x, α_x (for Multi-obj.)	B1
3b		Single-objective GA	E_x (for Single-obj.)	C3
3c		Single-objective GPSA		
3d		Single-objective SA		

where

Loading Cases	**LC1:** $F_x = 20kN, F_y = 20kN, F_{xy} = 0, \Delta T = -150^\circ C, \Delta C = 0\%$
	LC2: $F_x = 50kN,\ F_y = 1kN,\ F_{xy} = 0,\ \Delta T = -150^\circ C, \Delta C = 2\%$
Constraints	**C1:** $-90^\circ \le \theta_1 \le 90^\circ, -90^\circ \le \theta_2 \le 90^\circ, \alpha_x \le -2.63.10^{-6}/^\circ C$
	C2: $-90^\circ \le \theta_1 \le 90^\circ, -90^\circ \le \theta_2 \le 90^\circ, \alpha_x \le -2.31.10^{-6}/^\circ C, E_y \ge 9.7GPa$
	C3: $-90^\circ \le \theta_1 \le 90^\circ, -90^\circ \le \theta_2 \le 90^\circ, \alpha_x \le -3.21.10^{-6}/^\circ C$
Bound	**B1:** $-90^\circ \le \theta_1 \le 90^\circ, -90^\circ \le \theta_2 \le 90^\circ$

8.2. Results and Discussion

In this section, results of laminated composite optimal design studies based on the multi and single-objective optimizations are presented for coefficient of thermal expansion and elastic moduli. If the fiber orientation angles are selected as 0° for all lamina, as expected, E_x becomes maximum ($E_x = 277.3GPa$). However, this design is not suitable for minimum coefficient of thermal expansion ($\alpha_x = -1.0.10^{-6}/^{\circ}C$). Similarly, if all the fibers have a 32° orientation, the CTE becomes minimum ($\alpha_x = -5.24.10^{-6}/^{\circ}C$), but this is again not an appropriate design for E_x of the composite ($E_x = 40.8GPa$). Regarding this fact, the model problems have been optimized for the purpose of minimizing the CTE while maximizing the elastic moduli, simultaneously. More reliable solutions and the corresponding CMEs for multi-objective optimization of the model problems (1a and 3a) are given in Table 8.2. The set of (Pareto-optimal) solutions have been obtained when the maximum number of generations has reached to 51. For practical engineering use, only one of these solutions is to be chosen. For example, if one assumes $E_x \geq 188GPa$ and $\alpha_x \leq -2.63.10^{-6}/^{\circ}C$, design 5 is to be an appropriate solution and therefore the stacking sequence becomes $[\pm 13.8/\mp 18.5]_s$. Distribution of set of solutions are also given in Figure 8.1. Pareto-optimal design for model problem 2a is listed in Table 8.3. In model problem 2a, design 8 is to be chosen with the assumptions $E_x \geq 180GPa$, $E_y \geq 9.5GPa$, $\alpha_x \leq -2.30.10^{-6}/^{\circ}C$ and therefore, the corresponding stacking sequence for the composite becomes $[\pm 5.7/\pm 25.5]_s$.

Distributions of Pareto optimal solution of problem 2a are illustrated in Figures 8.2-8.4 in the objective functions spaces, $E_x - \alpha_x$, $E_y - \alpha_x$, $E_x - E_y$, respectively. The Pareto-optimal curves enable us to perform trade-off studies. It is noted that design problems 1a-3a have been previously solved by Aydin and Artem (2009).

After obtaining the multi-objective GA results, we have performed single-objective optimization methods such as GA, GPSA and SA. Single-objective GA results are given in Figures 8.5-8.7 for problems 1b, 2b and 3b, respectively. Evolutions of the fitness function value for those problems are illustrated in Figures 8.5a, 8.6a, and 8.7a.

It is observed from the figures, this value converges after 4 generations as a result of relatively small feasible solution space obtained from the multi-objective solutions. Average distances between individuals for each generation are given in Figures 8.5b, 8.6b, and 8.7b. The fitness functions final values for problems 1b-3b has been supported by 9, 6 and 13 individuals, respectively and given in Figures 8.5c, 8.6c, and 8.7c.

Table 8.2. Pareto-optimal designs for the model problems 1a and 3a and the corresponding CMEs (Source: Aydin & Artem, 2009)

Design	E_x (GPa)	α_x (10^{-6}/^{O}C)	β_x (10^{-6}/%M)	θ_1 (Deg)	θ_2 (Deg)
1	115.9	-3.66	-58.8	25.9	-19
2	127.6	-3.49	-54.1	24.6	-18
3	152.7	-3.21	-46.1	20	-18
4	169.4	-2.89	-37.3	14.9	-20.5
5	188.0	-2.63	-29.9	13.8	-18.5
6	194.2	-2.44	-24.7	20.6	-10.2
7	206.9	-2.16	-17.0	4.7	-21.6
8	222.1	-1.99	-12.2	19.5	-2.6
9	239.9	-1.80	-6.8	8.1	-13.7

GPSA iteration steps for problems 1c-3c are illustrated in Figures 8.8-8.10, respectively. As it is seen from the figures, the optimum results are obtained after 4 iterations and decreasing mesh sizes are observed. In SA method (Figure 8.11), relatively much more iteration is obtained for the solution compared with GA and GPSA. Table 8.3 gives a comparison of the results obtained from multi-objective GA, single-objective GA, GPSA and SA. In model problems 1a -1d, maximum E_x value is obtained from single-objective GPSA and maximum E_y from multi-objective GA. Single-objective SA algorithm has produced minimum CTE after 1486 iterations. For all model problems, it is seen that similar results have been obtained in both multi and single-objective approaches for E_x, E_y, α_x and β_x with different stacking sequences.

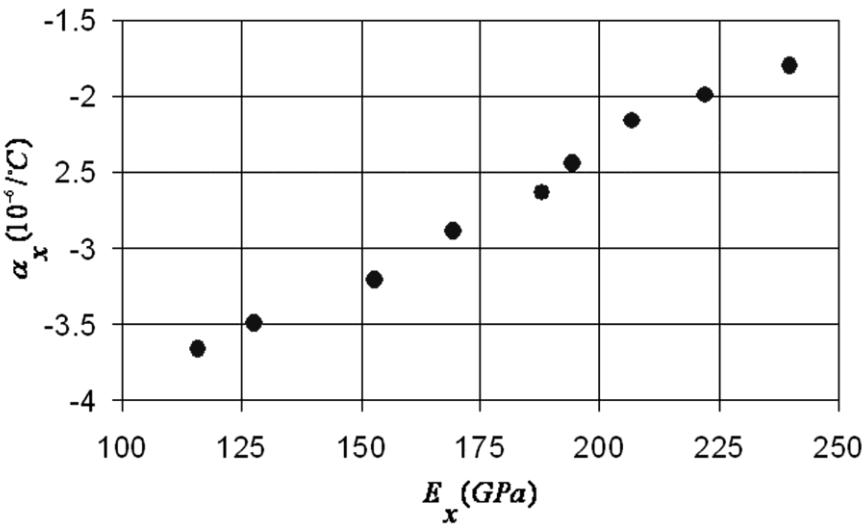

Figure 8.1. Pareto-optimal designs for maximum E_x and minimum α_x for model problems 1a and 3a (Source: Aydin & Artem, 2009a)

Table 8.3. Pareto optimal designs of the model problem 2a and the corresponding CMEs (Source: Aydin & Artem, 2009a)

Design	E_x (GPa)	E_y (GPa)	α_x (10^{-6}/°C)	β_x (10^{-6}/%M)	θ_1 (Deg)	θ_2 (Deg)
1	149. 5	9.1	-2. 90	-36. 3	13	26.5
2	159. 5	16.9	-1. 90	-9.7	1.2	34.7
3	159. 8	13.0	-2. 21	-18. 3	6.5	31.2
4	161. 3	7.4	-3. 00	-40. 5	15.5	21.2
5	170. 2	8.4	-2. 69	-31. 8	11.6	23.7
6	172. 4	11.8	-2. 20	-17. 9	3.9	29.2
7	181. 9	8. 0	-2. 57	-28. 4	10.9	22.1
8	184. 1	9. 7	-2. 31	-21. 0	5.7	25.5
9	190. 2	7. 2	-2. 60	-29. 2	13.7	18.3
10	193. 2	8. 5	-2. 34	-21. 8	7.4	22.7
11	202. 6	9. 0	-2. 15	-16. 5	1.2	23.3
12	217. 8	8. 1	-2. 04	-13. 4	2.5	20.3
13	234. 0	7. 6	-1. 85	-8. 1	2.1	17.4
14	245. 9	7. 4	-1. 67	-3. 3	0.3	15.2

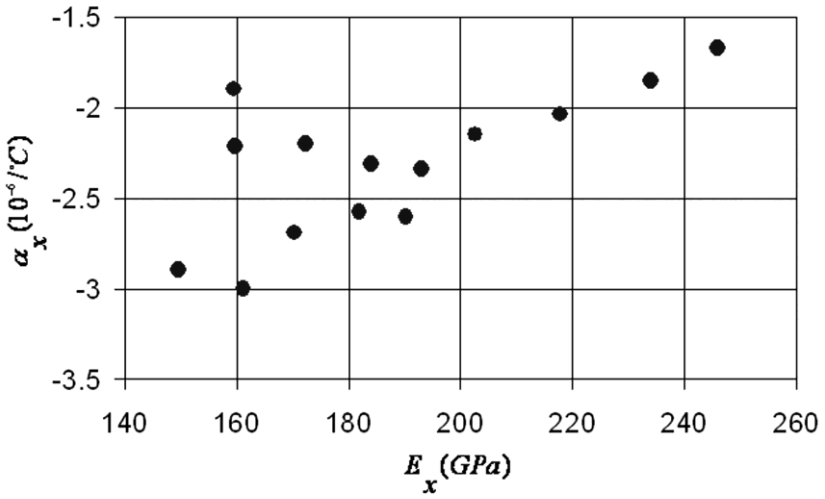

Figure 8.2. Pareto-optimal designs for maximum E_x and minimum α_x for model problem problem 2a (Source: Aydin & Artem, 2009a)

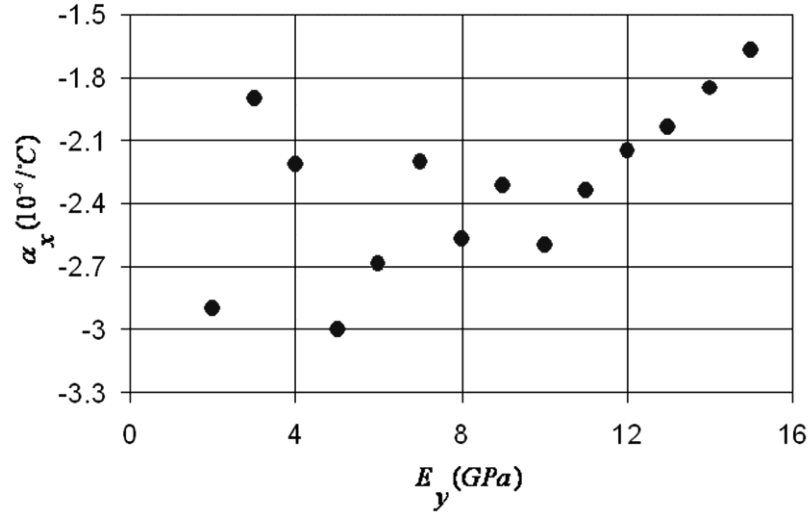

Figure 8.3. Pareto-optimal designs for maximum E_y and minimum α_x for model problem 2a (Source: Aydin & Artem, 2009a)

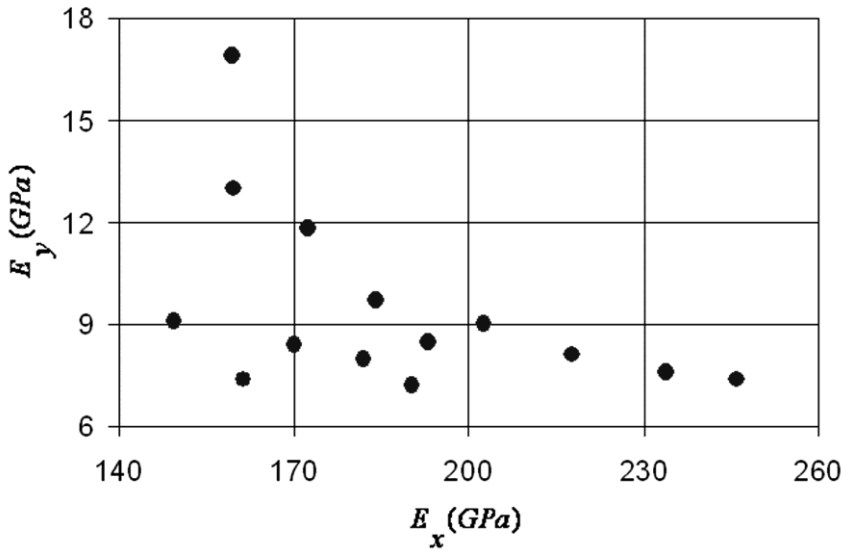

Figure 8.4. Pareto-optimal designs for maximum E_x and maximum E_y for model problem 2a (Source: Aydin & Artem, 2009a)

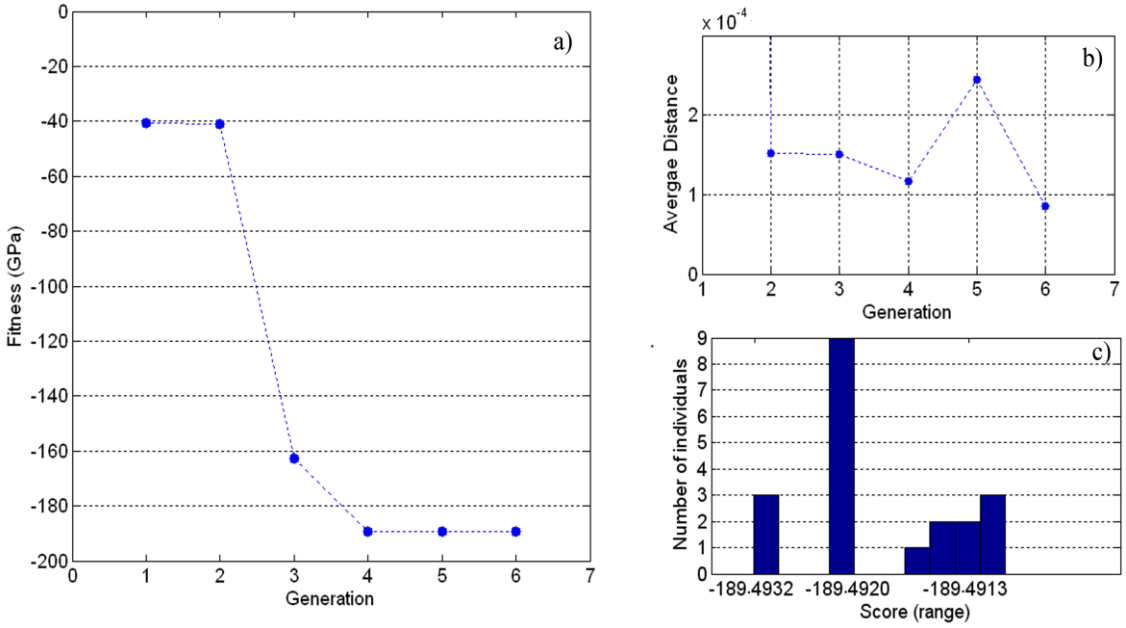

Figure 8.5. Single-objective GA results for problem 1b; (a) evolution of the fitness function, (b) average distance between individuals, (c) histogram for individuals

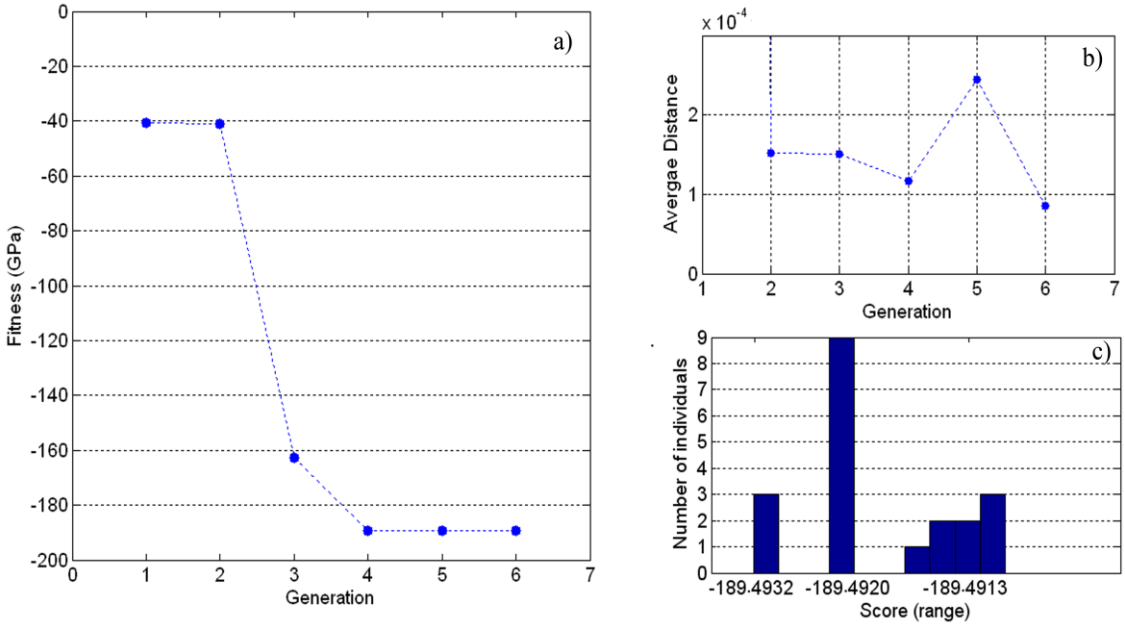

Figure 8.6. Single-objective GA results for problem 2b; (a) evolution of the fitness function, (b) average distance between individuals, (c) histogram for individuals.

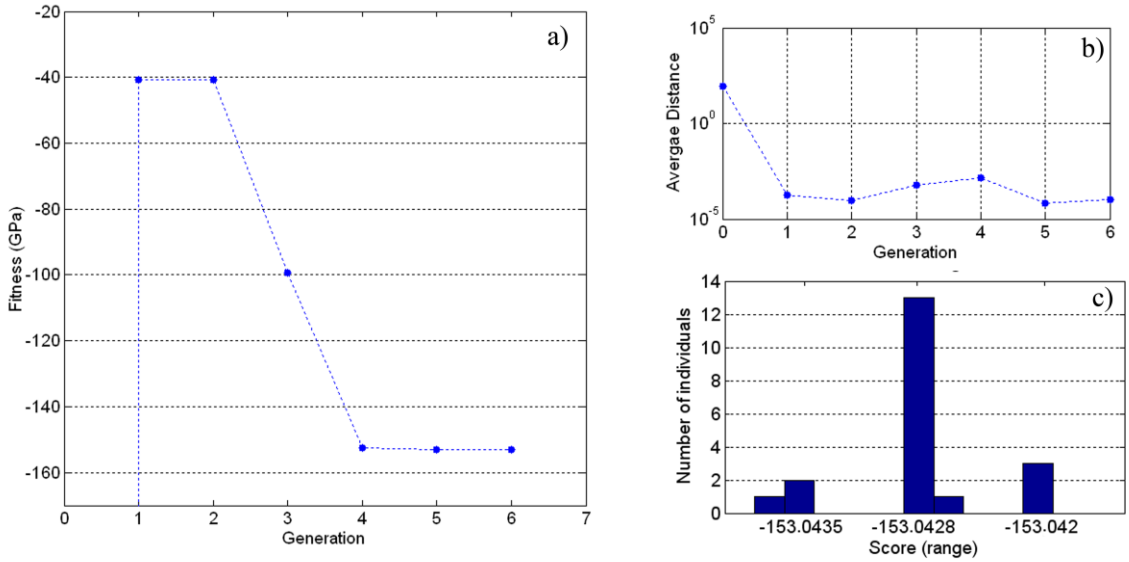

Figure 8.7. Single-objective GA results for problem 3b; (a) evolution of the fitness function, (b) average distance between individuals, (c) histogram for individuals.

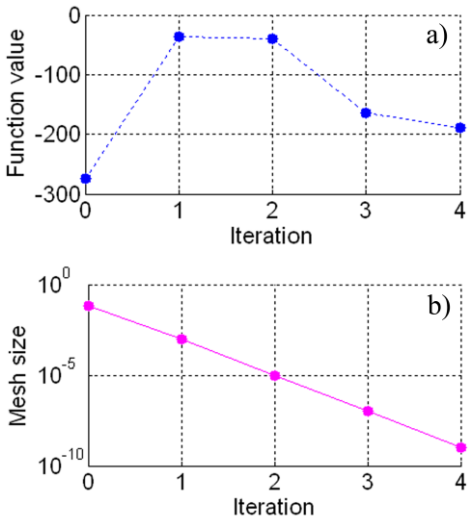

Figure 8.8. Single-objective GPSA results for problem 1c; (a) iteration steps for fitness function value, (b) variation of mesh size

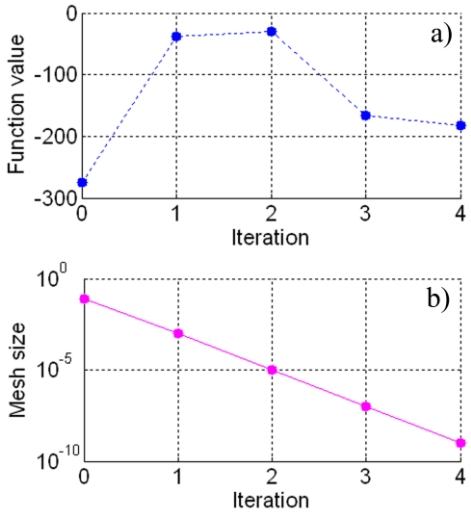

Figure 8.9. Single-objective GPSA results for problem 2c; (a) iteration steps for fitness function value, (b) variation of mesh size

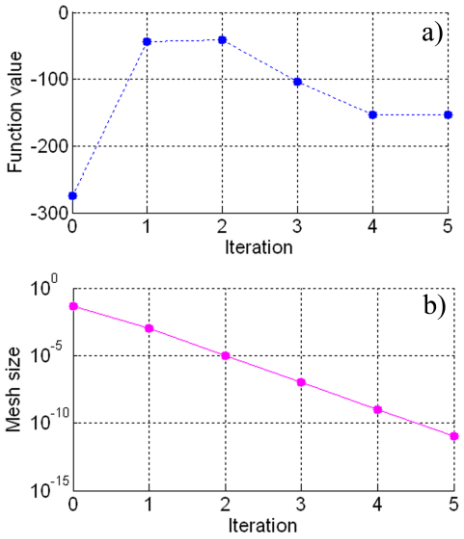

Figure 8.10. Single-objective GPSA results for problem 3c; (a) iteration steps for fitness function value, (b) variation of mesh size

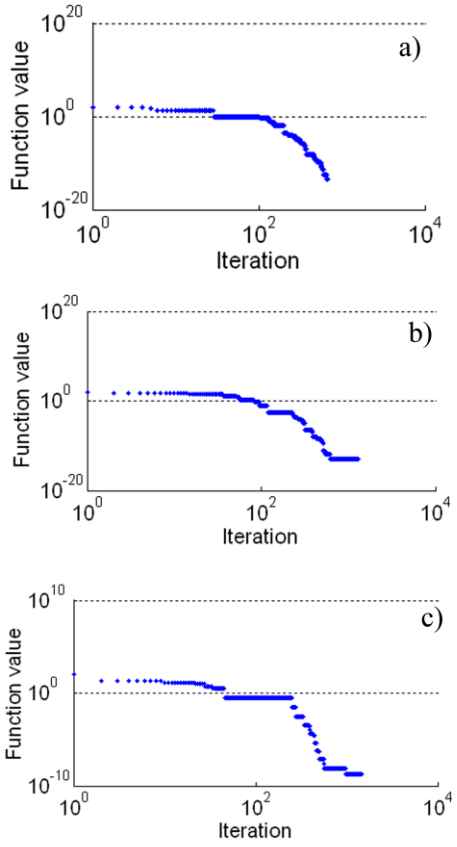

Figure 8.11. Single-objective SA algorithm iteration steps for (a) problem 1d, (b) problem 2d, (c) problem 3d.

Table 8.4. Comparison of the results obtained from multi-objective GA, single-objective GA, GPSA and SA.

Problem	Optimization Type	E_x (GPa)	E_y (GPa)	α_x (10^{-6}/^{O}C)	β_x (10^{-6}/%M)	Stacking Sequence
1a	Multi-objective GA	187.90	7.3	-2.63	-29.88	$(\pm 13.8/\mp 18.5)_s$
1b	Single-objective GA	188.93	7.1	-2.64	-30.25	$(\pm 16.1)_{2s}$
1c	Single-objective GPSA	189.54	7.1	-2.63	-29.99	$(\mp 16/\pm 16.1)_s$
1d	Single-objective SA	188.26	7.1	-2.65	-30.43	$(\pm 17/\mp 15.3)_s$
2a	Multi-objective GA	184.22	9.6	-2.31	-20.96	$(\pm 5.7/\pm 25.5)_s$
2b	Single-objective GA	183.48	9.7	-2.31	-21.10	$(\mp 5.8/\pm 25.6)_s$
2c	Single-objective GPSA	183.48	9.7	-2.31	-21.20	$(\mp 25.6/\mp 5.8)_s$
2d	Single-objective SA	182.00	9.8	-2.32	-21.38	$(\pm 6/\pm 25.8)_s$
3a	Multi-objective GA	152.77	7.2	-3.21	-46.08	$(\pm 20/\mp 18)_s$
3b	Single-objective GA	152.66	7.1	-3.22	-46.38	$(\mp 19.3/\mp 18.7)_s$
3c	Single-objective GPSA	152.65	7.1	-3.22	-46.41	$(\mp 18.9/\pm 19.1)_s$
3d	Single-objective SA	151.01	7.2	-3.23	-46.66	$(\mp 17.8/\pm 20.5)_s$

8.3. Stress Analysis

Investigation of stresses for optimized problems under combined loading gives some additional information about composite design. This type of information provides production of safer structures (Hyer, 1998). For this purpose, the through the thickness normal and shear stress distributions of the optimized (using multi-objective approach) composite plate under the mechanical, thermal and hygral loads are presented in Figures 8.12-8.15 for model problems 1a-3a. In Figure 8.12 it can be observed that maximum normal stresses occur in ply numbers 3-6 and shear stress in 4 and 5 when the composite subjected to mechanical load. Applying only thermal load, relatively lower stress values are obtained for both normal and shear stresses. Combination of thermal and mechanical loading leads to decrease the effect of mechanical load and therefore this produces lower values of normal and shear stresses at the plies where the maximum

stresses occur. As it is seen from Figure 8.13, stress distributions for model problem 2a show similar behavior to 1a. Effects of loadings on stress distributions are also presented for model problem 3a in Figures 8.14, 8.15. It can be seen from Figure 8.14, mechanical load is significantly effective compared to hygral and thermal loads for normal stress σ_x.However, for σ_y thermal load dominates to the others. It would be so due to relatively low mechanical load along y direction. It can be concluded from Figure 8.14 that it is advantageous to absorb moisture. Unfortunately moisture degrades the strength of laminates (Hyer, 1998). Therefore, it is not really an advantage to use the stress relieving tendencies of moisture absorption. The maximum values of normal stresses occur in the interior plies of the composite subjected to both mechanical and thermal loads (Figure 8.15). However, negative values for thermal stresses leads to relatively low stresses in the exterior plies. Another observation is that for Figure 8.15, shear stress distribution is more complicated compared to the normal stress distributions.

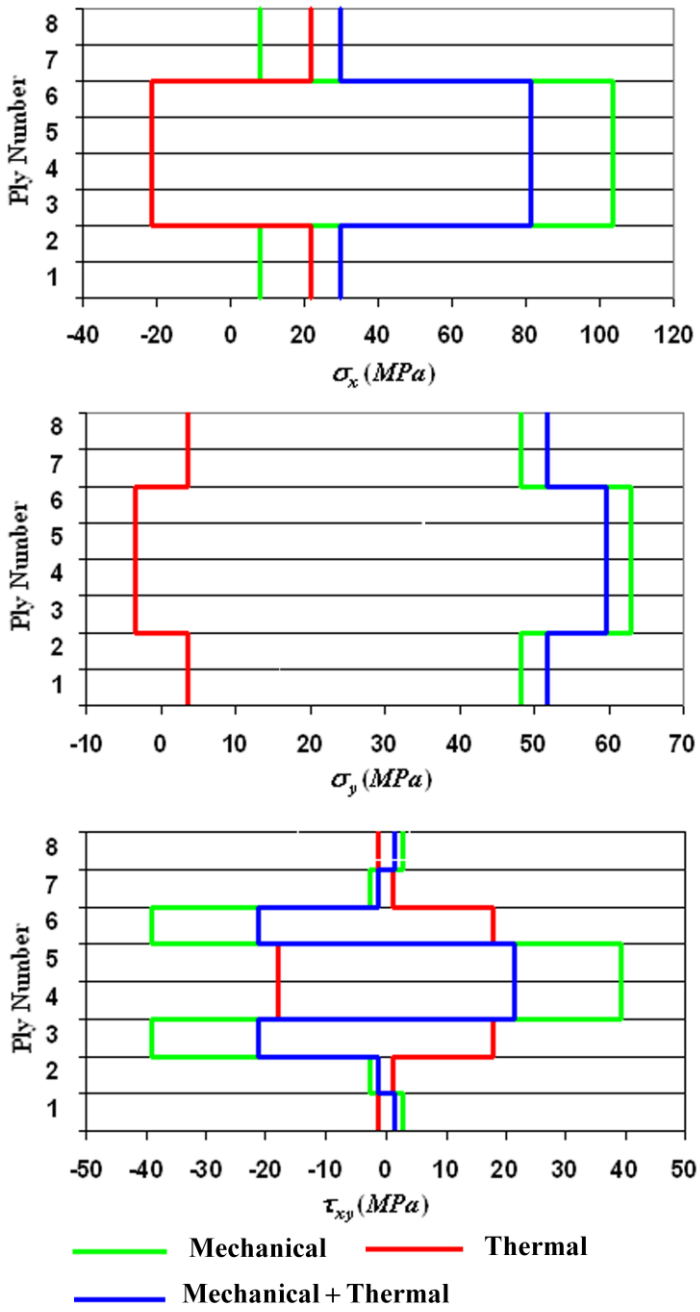

Figure 8.12. Stress distributions of the composite subjected to combination of mechanical and thermal loads for model problem1a ($N_x = 20\,kN/m$, $N_y = 20\,kN/m$, $N_{xy} = 0\,kN/m$ $\Delta T = -150^{\circ}C$)

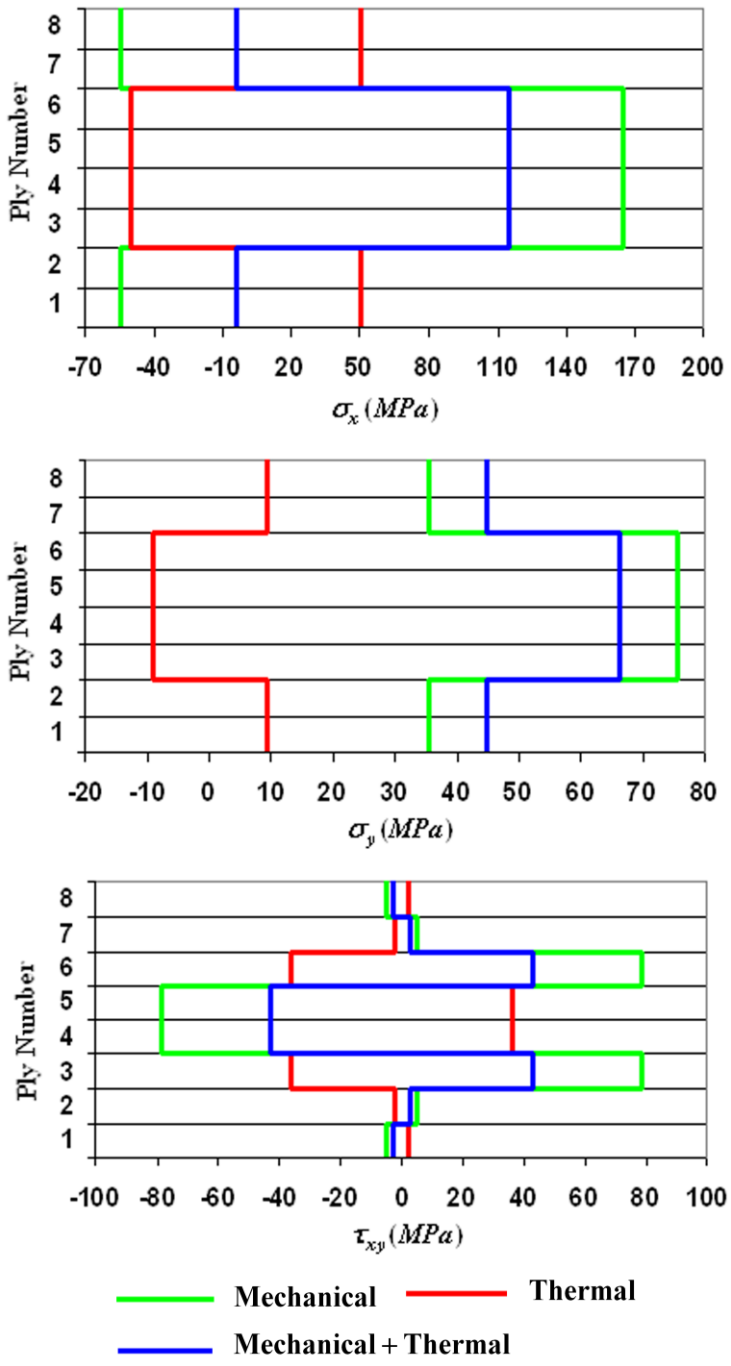

Figure 8.13. Stress distributions of the composite subjected to combination of mechanical and thermal loads for model problem 2a ($N_x = 20\,kN/m$, $N_y = 20\,kN/m$, $N_{xy} = 0\,kN/m$ $\Delta T = -150^\circ C$)

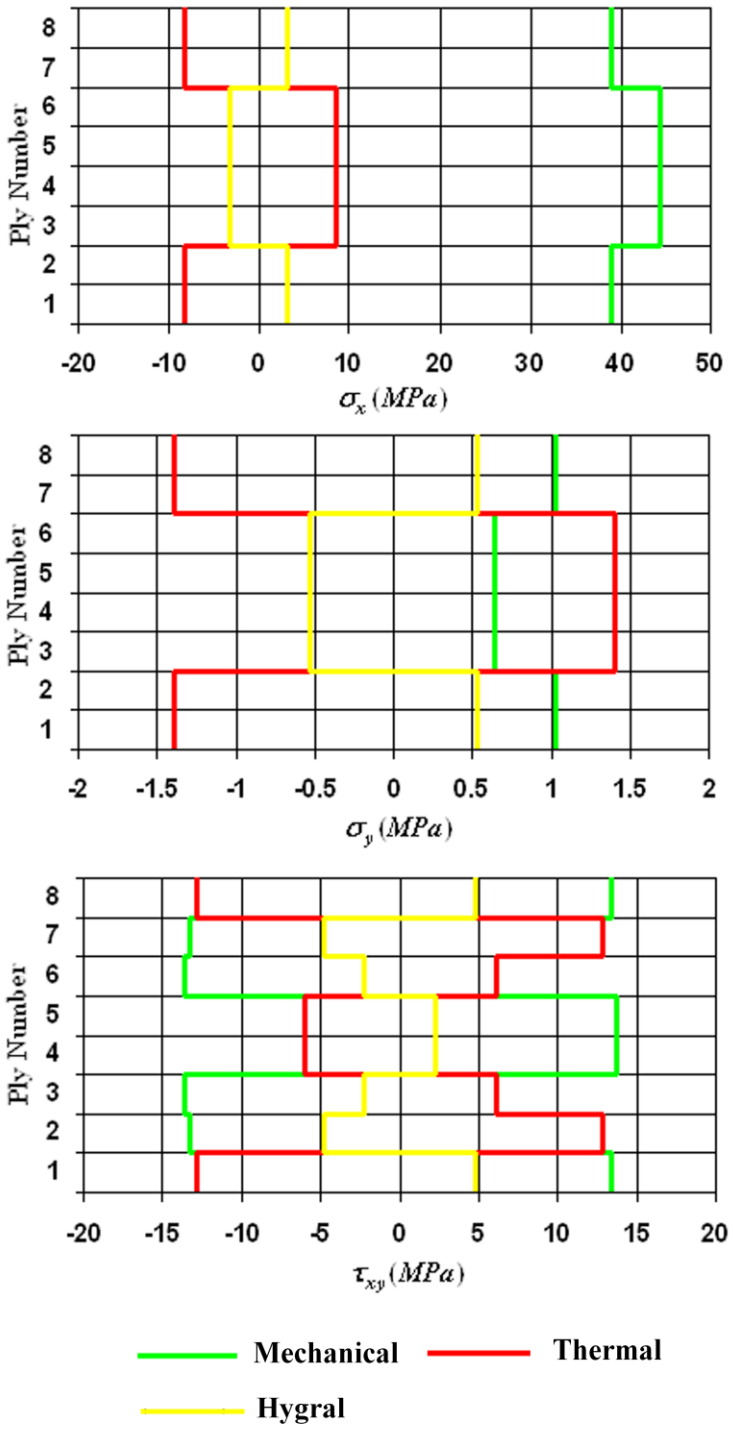

Figure 8.14. Stress distributions of the composite subjected to mechanical, thermal and hygral loads for problem 3a ($N_x = 50kN/m$, $N_y = 1kN/m$, $N_{xy} = 0$, $\Delta T = -150^{\circ}C$, $\Delta M = 2\%$)

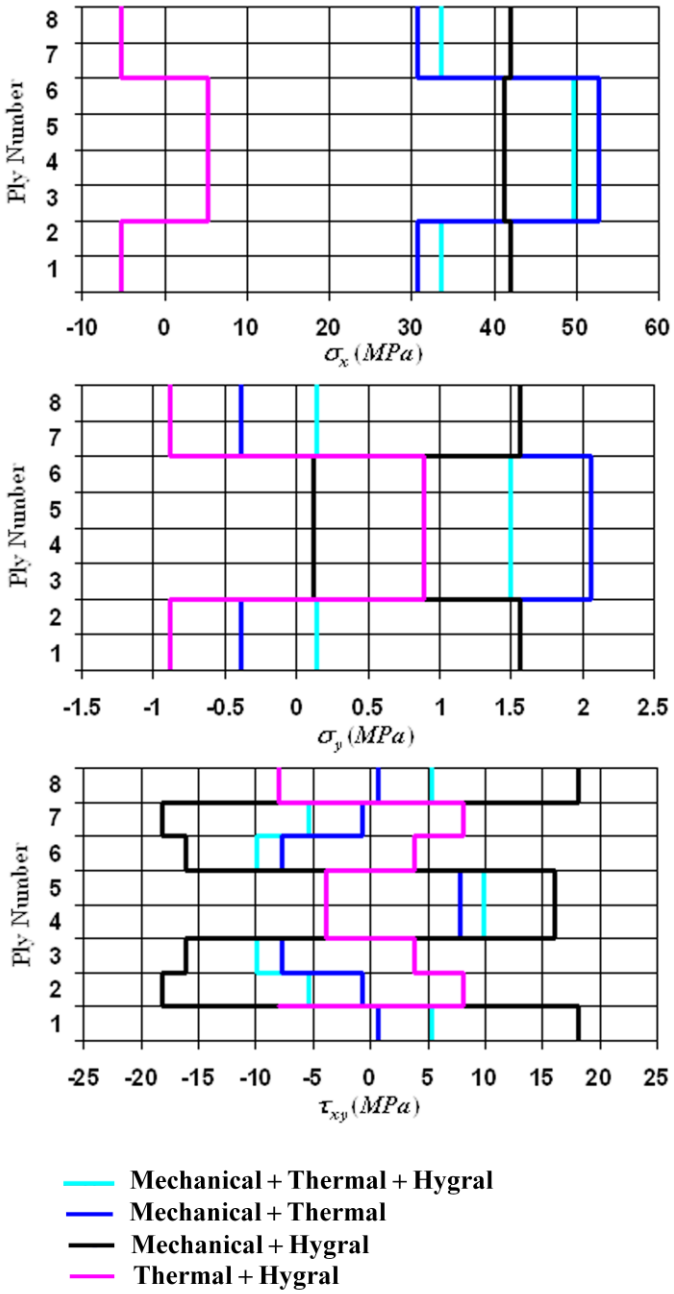

Figure 8.15. Stress distributions of the composite subjected to combination of mechanical, thermal and hygral loads for problem 3a ($N_x = 50kN/m$, $N_y = 1kN/m, N_{xy} = 0$, $\Delta T = -150^\circ C$, $\Delta M = 2\%$)

CHAPTER 9

CONCLUSION

This thesis has presented a study of design of dimensionally stable laminated composite by stochastic optimization methods. The composite is subjected to hygrothermomechanical loading. In the development of dimensionally stable laminated composite plates, satisfying the conditions lower weight, lower coefficient of thermal and moisture expansion, higher elastic moduli, effect of environmental conditions such as moisture and temperature has to be considered for a wide range of space applications. Fiber-reinforced polymer composite materials can satisfy these requirements with an appropriate stacking sequence. In order to design optimum laminated composite materials with such a stacking sequence, it is necessary to adapt some of the optimization methods to composite design problems.

In this thesis, stacking sequences design and optimization of 4, 8, 12 and 16 layered carbon/epoxy and E-glass/epoxy laminated composites satisfying the conditions low coefficients of thermal and moisture expansion with high elastic moduli have been performed. Totally 140 (128+12) optimization problems have been solved by using stochastic search techniques GA, GPSA and SA. Therefore, alternative dimensionally stable composite materials have been developed for space applications.

MATLAB Optimization Toolbox solvers *gamultiobj, ga, patternsearch* and *simulannealbnd* have been incorporated to optimization of 8 layered $[\pm\theta_1/\pm\theta_2]_s$ carbon/epoxy composite. It is shown how the commercial product MATLAB can be adapted to the composite design and optimization problems. All the solvers carried out in the present study have produced almost the same results with different stacking sequences. Even if the number of iterations of the algorithms GA, GPSA and SA are quite different, the CPU times are approximately the same.

Two different approaches, single-objective and multi-objective optimization formulation, have been utilized for mathematical verification of some model problems appeared in Chapter 8. Since the constraints used in single-objective approach significantly narrows the search space, I get the results with fewer number of iterations.

The effect of number of plies to stacking sequences design for the carbon/epoxy

and E-glass/epoxy laminated composites have been investigated for low CTE and high stiffness. It can be concluded that carbon/epoxy and E-glass/epoxy have different optimum fiber orientation angles 32 and 27.3, respectively and it is independent of number of layers of the composites.

Effects of combination of mechanical, thermal and hygral loads to normal and shear stress distributions of the optimized carbon/epoxy laminated composite have been investigated and can be summarized as: mechanical load is significantly effective compared to hygral and thermal loads for normal stress σ_x. However, for σ_y thermal load dominates to the others. Applying only thermal load, relatively lower stress values are obtained for both normal and shear stresses. Combination of thermal and mechanical loading leads to decrease the effect of mechanical load and therefore this produces lower values of normal and shear stresses at the plies where the maximum stresses occur.

Comparison of failure loads of optimized carbon/epoxy and E-glass/epoxy laminated composites by using failure theories Tsai-Hill, Tsai-Wu, Hoffman and Hashin-Rotem including thermal and moisture effects have been performed. It can be concluded form this part that (i) Tsai-Hill failure criterion overestimates the failure loads among the others for loading ratios in the interval [1,100], (ii) compression limits are smaller than tensile limits based on Tsai-Wu, Hoffman and Hashin-Rotem theories. (iii) the magnitude of failure loads decreases with increasing thermal changes, (iv) addition of shear load to optimized composites have decreased the failure load moderately, (v) after thermal change, minimum increase occurs in the case of anti-optimum stacking sequences.

Resulting fiber orientation angels automatically minimize the coefficient of moisture expansion (CME) and this gives an important advantage for the materials used in satellite structures. Therefore, it is sufficient to minimize the CTE only and not necessary to solve a new optimization problem in order to minimize the CME of the laminated composites.

Since the analysis and optimum design of composite structures require the determination of the basic properties of the lamina for use as an input data, the E-glass/epoxy composite is tested experimentally and the minimum CTE value is reached by [27/-27/-27/27] stacking sequence. The same stacking sequence was previously obtained by optimization process.

REFERENCES

Apalak, M. K., Yildirim, M., & Ekici, R. (2008). Layer optimization for maximum fundamental frequency of laminated composite plates for different edge conditions. *Composite Science and Technology*, *68*, 537–550.

Aydin, L.,& Artem, H.S. (2009a, June).Multi-objective genetic algorithm optimization of the composite laminates as a satellite structure material for coefficient of thermal expansion and elastic modulus. *Proceedings of 4th International Conference on Recent Advances in Space Technologies*, Istanbul, TURKEY, 14-119.

Aydin, L., & Artem, H.S. (2009b, August). Multi-objective optimization of fiber reinforced composite laminates for stiffness and thermal expansion coefficient using genetic algorithm. *Proceedings of the 5th Ankara International Aerospace Conference*, METU, Ankara, TURKEY, 1-9.

Aydin, L., & Artem, H.S. (2010, October). Single and multi-objective genetic algorithm optimizations of the laminated composites used in satellite structures. *Proceedings of the International Symposium of Mechanism and Machine Science*, Izmir Institute of Technology, Izmir, TURKEY, 219-226.

Bruyneel, M., (2006). A general and effective approach for the optimal design of fiber reinforced composite structures. *Composites Science and Technology*, *66*(10), 1303-1314.

Cho, M., & Rhee, S.Y. (2004). Optimization of laminates with free edges under bounded uncertainty subject to extension, bending and twisting. *International Journal of Solids and Structures, 41*, 227–245.

Choo, V.K.S. (1990). *Fundamentals of Composite Materials*. Knowen Academic Press.

Costa, L., Fernandes, L., Figueiredo, L., Judice, J., Leal, R., & Oliveira, P. (2004). Multiple and single objective approach to laminate optimization with genetic algorithms. *Structural and Multidisciplinary Optimization*, *27*, 55-65.

Daniel, I. M., & Ishai O. (1994). *Engineering mechanics of composite materials*.Oxford, England: Oxford University Press.

Deb, K. (2001). *Multi-objective optimization using evolutionary algorithms*. John Wiley & Sons, Inc.

Deng, S., Pai, P.F., Lai, C.C., & Wu, P. S. (2005). A solution to the stacking sequence of a composite laminate plate with constant thickness using simulated annealing algorithms. *International Journal of Advance Manufacturing Technology*, *26*, 499-504.

Di, M., Gherlone, M., & Lomario, D. (2003). Multiconstraint optimization of laminated and sandwich plates using evolutionary algorithms and higher order plate theories. *Composite Structure, 59,* 149-154.

Diaconu, C. G., & Sekine, H. (2003). Flexural characteristics and layup optimization of laminated composite plates under hygrothermal conditions using lamination parameters. *Journal of Thermal Stresses, 26,* 905–922.

Erdal, O., & Sonmez, F. O. (2005). Optimum design of composite laminates for maximum buckling load capacity using simulated annealing. *Composite Structure, 71,* 42-52.

Farshi, B., Herasati, S. (2006). Optimum weight design of fiber composite plates in flexure based on a two level strategy. *Composite Structures, 73,* 495–504.

Fares, M.E., Youssif Y. G.,& Hafiz, M.A. (2005). Multi-objective design and control optimization for minimum thermal post buckling dynamic response and maximum buckling temperature of composite laminates. *Structural and Multidisciplinary Optimization, 30,* 89-100.

Genetic Algorithm and Direct Search Toolbox™ User's Guide 2004–2008 by The MathWorks, Inc.

Ghiasi, H., Pasini, D., & Lessard, L. (2009). Optimum stacking sequence design of composite materials Part I: Constant stiffness design.*Composite Structure, 90*(1), 1-11.

Ghiasi, H., Fayazbakhsh, K., Pasini, D., & Lessard, L. (2010). Optimum stacking sequence design of composite materials Part II: Variable stiffness design. *Composite Structure, 93*(1), 1-13.

Gurdal, Z., Haftka, R.T., & Hajela, P. (1999). *Design and optimization of laminated composite materials*. John Wiley & Sons, Inc.

Hasancebi, O., Carbas, S., Dogan, E., Erdal, F., & Saka, M. P. (2010). Comparison of non-deterministic search techniques in the optimum design of real size steel frames. *Computer and Structure, 88,* 1033-1044.

Hufenbach, W., Gude, M., Kroll, L., Sokolowski, A., & Werdermann, B. (2001). Adjustment of residual stresses in unsymmetric fiber-reinforced composites using genetic algorithms. *Mechanics of Composite Material, 37*(1), 216-222.

Hyer, M. W. (1998). *Stress analysis of fiber reinforced composite materials*. McGraw-Hill .

Kameyama, M., & Fukunaga, H. (2007). Optimum design of composite plate wings for aeroelastic characteristics using lamination parameters. *Computers and Structures, 85,* 213-224.

Karakaya, S., & Soykasap, O. (2009). Buckling optimization of laminated composite plates using genetic algorithm and generalized pattern search algorithm. *Structural and Multidisciplinary Optimization, 39*, 477-486.

Kaw, A. K. (2006). *Mechanics of composite materials* (2nd ed.). CRC Press Taylor & Francis Group .

Khalil, M., Bakhiet, E., & El-Zoghby, A. (2001). Optimum design of laminated composites subjected to hygrothermal residual stresses. *Proceedings of the Institution of Mechanical Engineers, 215*, 175-186.

Kollar, L. P., & Springer G. S. (2003). *Mechanics of composite structure*. Cambridge University Press .

Le Rich, R., & Gaudin J. (1998). Design of dimensionally stable composites by evolutionary optimization. *Composite Structure, 41*, 97-111.

Mallick, P. K. (2007). *Fiber-reinforced composites : materials, manufacturing, and design*. Taylor & Francis Group, LLC.

Mangalgiri, P.,D.(1999). Composite materials for aerospace applications. *Buletin of*

Manoharan, S., & Shanmuganathan, S. (1999). A comparison of search mechanisms for structural optimization. *Computers & Structures, 73*, 363-372.

Narita, Y., Robinson, P. (2006). Maximizing the fundamental frequency of laminated cylindrical panels using layerwise optimization. *International Journal of Mechanical Sciences, 48*, 1516–1524.

Narita, Y. (2003). Layerwise optimization for the maximum fundamental frequency of laminated composite plates. *Journal of Sound and Vibration, 263*, 1005–1016.

Nicosia, G., & Stracquadanio, G. (2008). Generalized pattern search algorithm for peptide structure prediction. *Biophysical Journal, 95*(10), 4988-4999.

Pelletier, J. L., & Vel, S. S. (2006). Multi-objective optimization of fiber reinforced composite laminates for strength, stiffness and minimal mass. *Composite Structure, 84*, 2065-2080.

Park, C. H., Lee, W., Han, W. S., & Vautrin, A. (2008). Improved genetic algorithm for multidisciplinary optimizationof composite laminates. *Computers and Structure, 86*, 19-24.

Rao, S. S. (2009). *Engineering optimization*: *Theory and practice* (4th ed.). John Wiley & Sons, Inc.

Sairajan, K. K., Nair, P. S. (2011). Design of low mass dimensionally stable composite base structure for a spacecraft. *Composites Part B Engineering, 42*, 280-288.

Spallino, R., & Rizzo, S. (2002). Multi-objective discrete optimization of laminated structures. *Mechanics Research Communication*, *29*, 17–25.

Spallino, R., & Thierauf, G. (2000). Thermal buckling optimization of composite laminates by evolution strategies. *Computers and Structures*, *78*, 691-697.

Spall J. C. (2003). *Introduction to stochastic search and optimization: estimation, simulation, and control*. John Wiley & Sons, Inc.

Sivanandam, S. N., & Deepa, S. N. (2008). *Introduction to genetic algorithms*. Springer-Verlag: Berlin Heidelberg.

The Mathworks, Inc, MATLAB Optimization Toolbox in version R2008b.

The Mathworks, Inc, MATLAB Genetic Algorithm and Direct Search Toolbox in version R2008b.

The Mathworks, Inc, MATLAB Symbolic Math Toolbox in version R2008b.

Torczon, V. (1997). On the convergence of pattern search algorithms. *Siam Journal Optimization*, *7*, 1–8.

Wolff E. G. (2004). *Introduction to the dimensional stability of composite materials*. DEStech Publications.

APPENDIX A

MATLAB COMPUTER PROGRAM

In this part, the computer program calculating the physical properties of the composites; elastic moduli E_x, E_y; shear modulus G_{xy}; and midplane strains $\varepsilon_x^0, \varepsilon_y^0, \varepsilon_{xy}^0$ in symbolic form is given. After obtaining the expressions for physical properties, they can be utilized in optimization toolbox.

```
clear all
clc
syms th1
thetad_half=[th1 -th1];% ply angles in degrees
thetad=[thetad_half fliplr(thetad_half)]
thetadt=thetad*pi/180
Nplies = 4;
h_ply  =150e-6;
%%%%%%%%%%%%%%%%%%%%%%%%%%%%%%%%%%%%%%%%%%%%%%%%%%%%%%%%%%%%%%%%
h      = Nplies * h;
for i = 1:Nplies;
  zbar(i) = - (h +h)/2 + i*h_ply;
end;
%%%%%%%%%%%%%%%%%%%%%%%%%%%%%%%%%%%%%%%%%%%%%%%%%%%%%%%%%%%%%%%%
Vf=0.50;%Volume fraction
E1f=550.2*10^9;%pascal
E2f=9.52*10^9;%pascal
Em=4.34*10^9;%pascal
Gm=1.59*10^9;
G12f=6.90*10^9;
v12f=0.20;%poisson ratio
vm=0.37; %matrix poisson ratio
Alpha1f=-1.35*10^-6;%
Alpha_m=43.92*10^-6;%matrix thermal coefficient
Beta1m=2000*10^-6;%matrix moisture coefficient(1/%M biriminde)
Beta2m=2000*10^-6;
E1=Vf*E1f+(1-Vf)*Em
E2=Em/(1-(Vf)^0.5*(1-Em/E2f))
G12=Gm/(1-(Vf)^0.5*(1-Gm/G12f))
v12=Vf*v12f+(1-Vf)*vm
nu21 = v12 * E2 / E1 ;
denom = 1 - v12 * nu21 ;
Q11 = E1 / denom       ;
Q12 = v12 * E2 / denom ;
```

```
Q22 = E2 / denom        ;
Q66 = G12;
Alpha1=(Vf*Alpha1f*E1f+(1-Vf)*Alpha_m*Em)/E1%Longitudinal thermal coeff.
Alpha2=Alpha2f*Vf^0.5+(1-Vf^0.5)*(1+Vf*vm*E1f/E1)*Alpha_m
Beta1=(1-Vf)*Beta1m*Em/E1%Longitudinal moisture coefficient
Beta2=Beta1m*(1-Vf^0.5)*(1+(Vf^0.5*(1-Vf^0.5)*Em)/(Vf^0.5*E2+(1-Vf^0.5)*Em))
%%%%%%%%%%%%%%%%%%%%%%%%%%%%%%%%%%%%%%%%%%%%%%
Nx=20000/0.3;%N/m
Ny=20000/0.3;%N/m
Nxy=0;
Mx=0;%Moment resultants
My=0;
Mxy=0;
DELTA_T=-150;%
DELTA_M=0;
Nx_Ny_Nxy_vector=[Nx;Ny;Nxy];%Mechanical loads in vector form
Mx_My_Mxy_vector=[Mx;My;Mxy];%Moment resultants in vector form
%Curvature_vector=[Kappax;Kappay;Kappaxy]
Curvature_vector=[0;0;0];
Q = [ Q11 Q12 0; Q12 Q22 0; 0 0 Q66];
A = zeros(3,3);
B = zeros(3,3);
D = zeros(3,3);
NT=0;
NT_Thermal_expansion=0;
NM=0;
NM_Moisture_expansion=0;

for i = 1:Nplies;
  theta  = thetadt(i);
  m = cos(theta) ;
  n = sin(theta) ;
  T = [ m^2 n^2 2*m*n; n^2 m^2 -2*m*n; -m*n m*n (m^2 - n^2)];
  Qbar = inv(T) * Q * (inv(T))' ;
   A = A + Qbar * h_ply-h;
  B = B + Qbar * h_ply -h* zbar(i);
  D = D + Qbar * (h_ply-h * zbar(i)^2  + h_ply^3 / 12);

%%%%%%%%%%%%%%%%%%%%%%%%%%%%%%%%%%%%%%%%%%%%%%
      NT=NT+DELTA_T*(Qbar *[(cos(thetadt(i)))^2*Alpha1+...
      (sin(thetadt(i)))^2*Alpha2;...
      (sin(thetadt(i)))^2*Alpha1+...
      (cos(thetadt(i) ))^2*Alpha2;2*cos(thetadt(i))*...
      sin(thetadt(i) )*Alpha1-2*cos(thetadt(i))*...
      sin(thetadt(i))*Alpha2]*h_ply);

%%%%%%%%%%%%%%%%%%%%%%%%%%%%%%%%%%%%%%%%%%%%%%
   NT_Thermal_expansion=NT_Thermal_expansion+(Qbar *[(cos(thetadt(i)
))^2*Alpha1+...
      (sin(thetadt(i) ))^2*Alpha2;...
```

```
      (sin(thetadt(i) ))^2*Alpha1+...
      (cos(thetadt(i) ))^2*Alpha2;2*cos(thetadt(i) )*...
      sin(thetadt(i) )*Alpha1-2*cos(thetadt(i))*...
      sin(thetadt(i) )*Alpha2]*h_ply);
  MT=0;
%%%%%%%%%%%%%%%%%%%%%%%%%%%%%%%%%%%%%%%%%%%
%%%%%%%%%%%%%%%%%%%%%%%%%%%%%%%%%%%%%%%%%%%
   NM=NM+DELTA_M*(Qbar *[(cos(thetadt(i)))^2*Beta1+...
      (sin(thetadt(i)))^2*Beta2;...
      (sin(thetadt(i)))^2*Beta1+...
      (cos(thetadt(i) ))^2*Beta2;2*cos(thetadt(i))*...
      sin(thetadt(i) )*Beta1-2*cos(thetadt(i))*...
      sin(thetadt(i))*Beta2]*h_ply);

%%%%%%%%%%%%%%%%%%%%%%%%%%%%%%%%%%%%%%%%%%%
%%%%%%%%%%%%%%%%%%%%%%%%%%%%%%%%
  NM_Moisture_expansion=NM_Moisture_expansion+(Qbar
*[(cos(thetadt(i)))^2*Beta1+...
      (sin(thetadt(i)))^2*Beta2;...
      (sin(thetadt(i)))^2*Beta1+...
      (cos(thetadt(i) ))^2*Beta2;2*cos(thetadt(i))*...
      sin(thetadt(i) )*Beta1-2*cos(thetadt(i))*...
      sin(thetadt(i))*Beta2]*h_ply);
  %Aþaðýdaki yapý moisture Moment resultants
  MM=0;

%%%%%%%%%%%%%%%%%%%%%%%%%%%%%%%%%%%%%%%%%%%
%%%%%%%%%%%%%%%%%%%%%%%%%%%%%%%%%%%%%%%%%%%
end

A_inverse=inv(A)
format long
Strain_zero_vector=(inv(A)*(NT+NM+Nx_Ny_Nxy_vector))%(
Curvature_zero_vector=inv(D)*(MT+MM+Mx_My_Mxy_vector)%(
alpha_vector=inv(A)*NTThermal_expansion
Beta_vector=inv(A)*NM_Moisture_expansionHH=h_ply*Nplies;
Exeff=(A(1,1)*A(2,2)-A(1,2)^2)/(A(2,2)*HH)
Eyeff=(A(1,1)*A(2,2)-A(1,2)^2)/(A(1,1)*HH)
Gxyeff=A(3,3)/HH
```

VITA

Levent AYDIN
10-11-1978, Denizli/TURKEY

EXPERIENCES

2004-2011: Research Assistant in Department. of Mechanical Engineering,
İzmir Institute of Technology

EDUCATION

Ph.D. (2005-2011) : Mechanical Engineering, İzmir Institute of Technology
M.Sc. (2002-2005) : Mechanical Engineering, İzmir Institute of Technology
P.S. (2001-2002) : Preparation School (English), İzmir Institute of Technology
B.Sc (1997-2001) : Mechanical Engineering, Celal Bayar University

ACHIEVEMENTS

Ph.D. with High Honor Degree
M.Sc. with High Honor Degree
Biography in the 2010 Edition of Who's Who in the World

ACADEMIC FIELDS OF INTERESTS

Advanced Engineering Mathematics
Special Functions, Elliptic Functions, Elliptic Integrals, Integral Transform Methods, Analytical Solutions of PDEs and ODEs, Numerical Solutions of Singular Integral Eqs.
Fracture Mechanics - Solid Mechanics
Stress Intensity Factor Approach, Axisymmetric Cracks in Hollow Cylinders Dynamic Buckling, Vibration of Nonuniform Rods
Mechanics of Composites and Optimization
Stress and Failure Analysis of Fiber Reinforced Polymer Composites; Satellite Structure Material Improvement Using Stochastic Optimization Methods;Genetic Algorithm, Generalized Pattern Search and Simulated Annealing Optimization of Composites
The Mathematical Softwares: Matlab, Mathematica and Maple for Engineering

SCI EXPANDED JOURNAL PAPERS

- **Aydin L, Artem HS,** *Effects of Different Failure Theroies on Dimensionally Stable Composite Structures* (In Preperation)
- **Aydin L, Artem HS,** *Comparison of Stochastic Search Optimization Algorithms for the Laminated Composites under Mechanical and Hygrothermal loadings* JOURNAL OF REINFORCED PLASTICS AND COMPOSITES
- **Yardimoglu B, Aydin L,** *Analytical Solution of Longitudinal Vibration of nonuniform rods*, SHOCK AND VIBRATION- Volume: 18 Issue: 4 Pages 555-562, 2011
- **Artem HS, Aydin L,** *Exact solution and analysis of a dynamic buckling problem having the elliptic type loading* APPLIED MATHEMATICS AND MECHANICS- Volume: 31 Issue: 10 Pages 1317-1324, 2010
- **Aydin L, Artem HSA,** *Axisymmetric crack problem of thick-walled cylinder with loadings on crack surfaces* , ENGINEERING FRACTURE MECHANICS Volume: 75 Issue: 6 Pages: 1294-1309 , 2008